Physical fisheries' impacts on seabed habitats (JAMBAY WP2)

Ole R. Eigaard, Barry O'Neill, Asbjørn Christensen, Mikael van Deurs, and Grete E. Dinesen (eds.)

DTU Aqua Report no. 446-2024

Physical fisheries' impacts on seabed habitats (JAMBAY WP2)

Ole R. Eigaard, Barry O'Neill, Asbjørn Christensen, Mikael van Deurs, and Grete E. Dinesen (eds.)

with contributions from:
Ole R. Eigaard, Barry O'Neill, Asbjørn Christensen, Mikael van Deurs, Josefine Egekvist, Nurul Huda, Ole Henriksen, Henrik Mosegaard, Jeppe Olsen, Karin J. van der Reijden, Jonathan Stounberg, Marie Villefrance, and Grete E. Dinesen

Colophon

Preface

The project "Mapping of seabed habitats and impacts of beam trawling and other demersal fisheries for spatial ecosystem-based management of the Jammer Bay (JAMBAY)" (Grant Agreement No 33113-B-23-189) was funded by the European Maritime and Fisheries Fund (EMFF) and the Ministry of Food, Agriculture and Fisheries of Denmark.

This Work Package 2 Report is the last of four detailed work package reports. This report presents the results of "Physical fisheries' impacts on seabed habitats (JAMBAY WP2)". These results are summarised in the Executive Report of the JAMBAY project, where also the detailed results of Work Package 5 are presented (DTU Aqua Report no. 445-2024).

This project had a short timeframe to conduct its work, given the magnitude and complexity of the work involved. It started in March 2023 and ended in December 2023. The initial application was accepted and awarded 12 million Danish kr., and in September was expanded to include additional work and an added 14 million Danish kr., to a total of 26 million Danish kr. More than 100 scientists and consultants from several research institutes and private companies were directly involved. Furthermore, the project indirectly involved several stakeholders.

The data collected, newly developed methods and models generated during this project have been reported upon. Part of the work has been disseminated nationally and internationally, but further work is needed to integrate the data and information across the professional fields. Follow up projects have been initiated towards this end. The outputs will inform and provide the opportunity for cross-sectorial, ecosystem-based management.

Kongens Lyngby, March 2024

Grete Elisabeth Dinesen
Senior Consultant

Contents

English summary

There are two overarching objectives in WP2 in JAMBAY; the first is to analyse and map the activities and ecosystem pressures of the different fisheries in the case study area, and the second is to analyse the connectivity and recruitment dynamics of selected fish and invertebrate species in the case study area and the surrounding waters.

In **Task 2.1** fishing pressure data of swept area ratio (SAR), landed catch, fuel-use intensity, and sediment mobilisation were estimated for individual grid cells of 0.001 degrees longitude and latitude (approx. 60x100 meter). This was made possible through the development of a polygon-based approach to the calculations of haul-based swept areas for individual vessels and a hierarchical use of information in Black Box (BB), Automated Information System (AIS), and Vessel Monitoring by Satellite (VMS) monitoring data. The refinement and application of these state-of-the-art methodologies to Danish fisheries monitoring data enabled the estimation of fishing pressure data in an unprecedented quality and resolution, which is more than 1000 times higher than other publicly available SAR maps and data that are currently used for impact and trade off assessments. For the foreign fleet, AIS data were combined with information on gear type and vessel size in the EU vessel register to provide the SAR, fuel-use, and sediment mobilization estimates per grid cell. Because we did not have access to logbook data for the foreign vessels, landings weight and value per grid cell could not be estimated, and the estimates of SAR, fuel-use, and sediment-mobilisation are substantially more uncertain than the estimates for the Danish fleet.

The maps of the gridded fishing pressure from 2015-2022 show that the JAMBAY case study area is intensively fished with mobile bottom-contacting gears, where larger areas of the deeper, more offshore parts of the case study area are fished more than 10 times annually. In the shallower fishing grounds, closer to shore, the fishing intensity is lower, but also here there are hot spot areas that are fished more than 10 times a year, and a large proportion of the seafloor is fished between 5 and 10 times a year. Another clear outcome of mapping the SAR estimates by fleet and gear type is that the DK fleet and the foreign fleet are largely complementary in their choice of fishing grounds. Whereas the Danish fleet is responsible for the largest fishing pressure on the sandy sediments (Danish seines) and soft sediments (otter trawlers), the international fleet (e.g., beam trawlers) exerts the largest pressure on the coarser sediments. The spatial distribution of landed catch, fuel-use intensity, and sediment mobilisation closely follows the distribution of fishing intensity, with the highest values per grid cell being found in the grid cells that also have the highest intensity of fishing. There are some deviations between the maps of the different pressures, which are brought about by the price-difference of the species, the difference in the engine-power requirements of the gear types, and the differences in sediment silt-fractions of the habitat types.

In **Task 2.2** the aim was to get a better understanding of the interaction of towed fishing gears with boulders. This will help fishers choose what gears can be used on given fishing grounds and will help fisheries managers protect seabed habitats and features. We focused on estimating the snagging probability of different demersal trawls and boulders and carried out a scaled model flume tank study (i) to identify which gears are more likely to snag on boulders, (ii) to evaluate at which part of a given gear snagging is more likely to occur, and (iii) to determine if

there are any characteristic features of a boulder that increases the likelihood of snagging. A central outcome of the study is that tickler chain beam trawls had the highest snagging probability across boulder shapes and sizes, indicating that this gear type is the most restricted in terms of fishable substrate composition. It was expected that Danish seines would be the most snagging gear type and that tickler chain beam trawls would be better at passing coarse substrate types than both otter trawls and the seines. An explanation might be that high snagging risk in a seabed habitat does not per se prevent beam trawling as these vessel types generally have high engine power and likely can move and turn over boulders when snagging does occur. The study also demonstrated that the use of chain mats instead of tickler chains substantially reduced the snagging probability of the beam trawls. Even so, our modelling-based results indicate that tickler chain beam trawlers are more restricted in their choice of fishing grounds than generally perceived.

In **Task 2.3,** a high-resolution hydrographic dataset covering the Jammer Bay and surrounding basins was established to assess hydrographic control of biological processes in the Jammer Bay area. Interfaces to Python and Lagrangian simulation software was developed to enable cross-disciplinary analyses within the project. Biological modules describing plaice larvae and early life stages of habitat-forming invertebrates were added.

The connectivity for hydrographic plaice habitats in the Jammer Bay and surrounding basins was assessed by considering drift from known spawning grounds and settlement at coastal nurseries with suitable habitat conditions. The investigations indicated that the recruitment potential has increased slightly in the period 2014-2022, but spatial and temporal fluctuations in recruitment contributions also increased over the period, lowering the stability of the recruitment potential. The connectivity for representative habitat-forming invertebrates in the Jammer Bay and surrounding basins was assessed. A representative set of four species with contrasting traits was considered. The species with longer pelagic duration of early life stages indicate a slight increase in recruitment potential, but also larger spatial and temporal fluctuations, as was found for plaice larvae. Species with shorter pelagic duration of early life stages did not exhibit similar noticeable increase.

Details of settling plaice larval development and the low scope for escape behaviour of the metamorphosing post-larvae together with stage duration define the vulnerability of this recruitment period to mobile bottom-contacting fishing gear. Studies of gear impact on plaice larvae and small juveniles was not found in the literature, but judged from field biology and experimental studies of predator-prey interactions, vulnerability peaks at a larval length of 12-15 mm and exponentially declines until the juvenile has reached about 25 mm. An index for disturbance of plaice recruitment by mobile bottom-contacting gear was defined and assessed for the Jammer Bay. The index described a spatio-temporal overlap between Danish/anchor seine fishery and plaice post-larval nurseries, where the relative trend in this index is less sensitive to the current absence of impact quantification studies. The index showed an unfortunate coincidence with peak fishing effort and arrival of newly settled larvae, which stresses the importance of future impact quantification studies.

The primary aim of **Task 2.4** was to understand the "source-sink dynamics" of sandeel larvae and the connectivity between habitats from the Jammer Bay to the north-eastern North Sea and western Skagerrak. The project successfully developed a protocol for measuring sandeel larvae

using image processing tools and created two valuable datasets for larvae abundances and lengths. The work involved meticulous remeasurement and recalibration of larvae samples to address initial measurement inconsistencies, ensuring data accuracy. Challenges in completing larval drift and statistical modelling analyses were faced due to time and data readiness constraints. Nonetheless, the project offers significant insights into sandeel recruitment patterns from hatching to settlement and is crucial for effective fisheries management and conservation in marine environments.

Dansk resume

Der er to overordnede mål i WP2 i JAMBAY; den første er at analysere og kortlægge aktiviteterne og økosystem presfaktorer fra de forskellige fiskerier i casestudieområdet, og det andet er at analysere forbindelses- og rekrutteringsdynamikken for udvalgte fisk og hvirvelløse arter i casestudieområdet og de omkringliggende farvande.

I **Task 2.1** blev der beregnet en række forskellige data for fiskeritryk i form af berørt havbundsareal (Swept Area Ratio, SAR), landet fangst og værdi, brændstofforbrug, og sedimentmobilisering, som blev estimeret for individuelle gitterceller i en rumlig skala på 0,001 x 0,001 længde- og breddegrad (ca. 60x100 meter). Dette blev muliggjort gennem udviklingen af en ny polygonbaseret tilgang til beregning og aggregering af trawlspor for individuelle fartøjer og en hierarkisk brug af informationen i Black Box, AIS og VMS overvågningsdata. Denne metodeudvikling gjorde det muligt at estimere og kortlægge data for fisketrykket i en hidtil uset kvalitet og opløsning, som er mere end 1000 gange højere end andre offentligt tilgængelige kort og data, der aktuelt bruges til vurderinger af fiskeripåvirkning. For den udenlandske flåde blev AIS-data kombineret med oplysninger om redskabstype og fartøjsstørrelse i EU's fartøjsregister til estimering af SAR-værdier, brændstofforbrug og sedimentmobilisering pr. gittercelle. Da vi ikke havde adgang til logbogsdata for de udenlandske skibe, kunne landingsvægt og -værdi pr. gittercelle ikke beregnes, og desuden er estimaterne for SAR, brændstofforbrug og sedimentmobilisering væsentligt mere usikre end estimaterne for den danske flåde.

Kortene over fisketrykket fra 2015-2022 viser, at der er et intensivt fiskeri med bundslæbende redskaber i det meste af JAMBAY-casestudieområdet (Figur 1), hvor større områder af de dybere dele af casestudieområdet fiskes mere end 10 gange årligt. På de mere lavvandede fiskepladser, tættere på kysten, er fiskeintensiteten lavere, men også her er der hot spot områder, der fiskes mere end 10 gange om året, og en stor del af havbunden fiskes mellem 5 og 10 gange om året. Et andet tydeligt resultat af kortlægningen af SAR-estimaterne per flåde og redskabstype er, at den danske flåde og den udenlandske flåde i høj grad er komplementære i deres valg af fiskepladser (Figur 1), og at den danske flåde er ansvarlig for det største fiskeritryk på sandede sedimenter (snurrevod) og bløde sedimenter (bundtrawlere), og at det for de grovere sedimenter hovedsageligt er den internationale flåde (bomtrawlere), der udøver det største tryk. Den rumlige fordeling af landet fangst, brændstofforbrug og sedimentmobilisering følger nøje fordelingen af fiskeriintensitet, hvor de højeste værdier pr. gittercelle findes i de gitterceller, der også har den højeste fiskeriintensitet. Der er nogle afvigelser mellem kortene over de forskellige mål for fiskeritryk tryk, som er forårsaget af arternes prisforskel, forskellen i fartøjstypernes motorkraft og forskelle i sediment-kornstørrelserne af habitattyperne.

Hovedmålet i **Task 2.2** var at forbedre vidensgrundlaget og forståelsen af de fysiske interaktioner mellem bundslæbende fiskeredskaber og kampesten. En øget forståelse af dette samspil vil både hjælpe fiskerne med at vælge, hvilke redskaber der kan bruges på bestemte fiskepladser og hjælpe fiskeriforvaltere med at beskytte havbundens levesteder og funktioner mod fiskeripåvirkninger. Vi fokuserede på at estimere sandsynligheden for, at forskellige typer af bundslæbende redskaber hænger fast i forskellige størrelser og former af kampesten, og udførte analyse baseret på nedskalerede modeller af redskaber og kampesten i prøvetanken i Hirtshals.

Formålene var (i) at identificere, hvilke redskaber der er mere tilbøjelige til at hænge fast i kampesten, (ii) at vurdere hvilken del af et givet redskab, der mest tilbøjelig til at hænge fast, og (iii) at afgøre, om der er nogle karakteristiske træk ved en kampesten, der øger sandsynligheden for at redskaber hænger fast.

Et centralt resultat fra undersøgelsen er, at bomtrawl med traditionelle 'tickler chains' havde den højeste sandsynlighed for at hænge fast på kampesten af forskellige former og størrelser, hvilket indikerer, at denne redskabstype er den mest begrænsede med hensyn til hvilken type af havbund den kan anvendes på. Det var forventet, at snurrevod ville være det mest bundtypebegrænsede redskab, og at bomtrawl bedre ville passere grove substrattyper end både bundtrawl og snurrevod. En forklaring kan være, at høj risiko for at hænge fast i bunden ikke i sig selv forhindrer bomtrawling, da disse fartøjstyper generelt har høj motorkraft og sandsynligvis kan flytte og vende kampesten, når redskabet hænger fast. Desuden viste forsøget at brugen af kædemåtter i stedet for 'tickler chains' væsentligt reducerede risikoen for at hænge fast. Alligevel indikerer vores modelleringsbaserede resultater, at traditionelle bomtrawlere med 'tickler chains' er mere begrænsede i deres valg af fiskepladser, end det generelt opfattes.

I **Task 2.3** blev der udviklet et hydrografisk datasæt i høj opløsning, der dækker Jammerbugten og de omkringliggende bassiner, med det formål at vurdere hvorledes de hydrografiske forhold påvirker de biologiske processer i Jammerbugt-området. Der blev udviklet ny software i grænsefladen mellem Python og Lagrangian simuleringsværktøjer for at muliggøre tværfaglige analyser inden for projektet og en række biologiske moduler, der beskriver udviklingen af rødspættelarver og tidlige livsstadier for habitatdannende hvirvelløse dyr, blev tilføjet.

Forbindelsen mellem rødspættehabitater i Jammerbugten og de omkringliggende bassiner blev analyseret gennem hydrografisk baseret modellering af drift fra kendte gydepladser og kystnære opvækstområder med passende habitatforhold. Analysen indikerede at rekrutteringspotentialet er steget en smule i perioden 2014-2022, men rumlige og tidsmæssige udsving i rekrutteringsbidragene er også steget over perioden, hvilket sænker stabiliteten af rekrutteringspotentialet. Forbindelsen mellem habitatdannende hvirvelløse dyr i Jammerbugt og de omkringliggende bassiner blev også undersøgt. Et repræsentativt sæt af fire arter med kontrasterende egenskaber blev analyseret. For arterne med længere pelagisk varighed af tidlige livsstadier indikerede analyserne en lille stigning i rekrutteringspotentiale over perioden, men også større rumlige og tidsmæssige udsving, som det blev fundet for rødspættelarver. Arter med kortere pelagisk varighed af tidlige livsstadier udviste ikke en tilsvarende stigning.

De begrænsede muligheder for flugtadfærd hos rødspætternes metamorfoserende post-larver, sammen med stadiets varighed, definerer denne rekrutteringsperiodes sårbarhed overfor bundslæbende fiskeredskaber. Studier af redskabspåvirkning på rødspættelarver, post-larver og små juvenile er ikke fundet i litteraturen, men vurderet ud fra feltbiologi og eksperimentelle undersøgelser af rovdyrs og byttedyrs interaktioner, er der en sårbarhedstop ved en larvelængde på 12-15 mm, som aftager eksponentielt indtil de juvenile fisk, har nået ca. 25 mm. Et indeks for forstyrrelse af rekruttering af rødspætter med bundslæbende redskaber blev defineret og estimeret for Jammerbugt. Indekset beskriver de spatio-temporale overlap mellem snurrevodsfiskeriet og opvækstområderne for post-larvestadiet. Indekset viste et rumligt og tidsligt sammenfald mellem de højeste fiskeriindsatser og de nyligt bundfældede larver, hvilket understreger vigtigheden af fremtidige undersøgelser, der kan kvantificere effekten på larverne.

Det primære formål med **Task 2.4** var at forstå spredningsdynamikken af tobislarver og forbindelsen mellem habitater i Jammerbugt og den nordøstlige Nordsø og det Vestlige Skagerrak. Projektet udviklede med succes en protokol til måling af tobislarver ved hjælp af billedbehandlingsværktøjer og skabte to værdifulde datasæt for larvernes forekomst og længde. Arbejdet involverede omhyggelig genmåling og genkalibrering af larveprøver for at afhjælpe indledende måle-inkonsistens, hvilket sikrede datanøjagtighed. Den udviklede metode og protokol har givet væsentlige nye indsigter i rekrutteringsmønstre for tobis, fra klækning til bosættelse, og forbedrer grundlaget for en fremtidig bæredygtig forvaltning af fiskeri og havmiljøer.

1.   Introduction to WP2

There were two overarching objectives in WP2 in JAMBAY; the first was to analyse and map the activities and ecosystem pressures of the different fisheries in the case study area, and the second was to analyse the connectivity and recruitment dynamics of selected fish and invertebrate species in the case study area and the surrounding waters.

In Task 2.1 we apply state of the art methodology for processing fisheries monitoring data to provide spatial and temporal high-resolution fishing pressure data for the Jammer Bay case study area. The main outputs are grid-cell based swept area ratio (SAR) estimates and maps for all Danish and international fisheries with mobile bottom-contacting gears (beam trawl, otter trawl, Danish seine, fly-shooter) in the case study area, which will form the basis of calculating different benthic state indicators (in WP3) as well as complementary indicators of sediment mobilization and fuel-use related CO_2 emissions for each fishery in WP2. Additionally, landings weight and monetary value has been assigned to each grid cell by gear type and target species, which has enabled analyses of impact (in WP3) and resource harvest (in WP4), as well as spatial ecosystem-based trade-off analyses (in WP5) for each grid cell and seabed habitat type. The fishing pressure data will also be correlated with data from GEUS' sediment analyses of grains size composition and carbon content (WP1), including total carbon (TC), total sulphur (TS) and total organic carbon (TOC) to inform about potential emissions from the sediment.

In Task 2.2 we investigated the snagging potential (i.e., reef damage and loss) of i), otter trawls, ii), beam trawls and iii), Danish seines. These three gear types are commonly applied by fisheries in the Jammer Bay, on boulders and rocky reefs. A down-sized scale version of each gear and a variety of shapes and sizes of boulders (at the same scale as the gears) will be deployed in a flume tank to investigate the interaction between gears and boulders. Video recordings will be made of the experimental runs and high resolution (100 Hz) measurements will be taken of the tension forces in the towing wires/ropes.

In Task 2.3 an agent-based modelling framework will be used to simulate the dispersal of larvae of fish and habitat-forming invertebrates in the Jammer Bay. The recruitment potential of plaice and the dispersal potential of invertebrate larvae with different biological traits and life-cycles will be assessed based on a suite of hydrographic variables, such as current, temperature, light conditions, seabed shear stress and plankton. The analyses will include the effect of fishing pressure (from Task 2.1) on dispersal and recruitment dynamics, and the connectivity with the Skagerrak and Kattegat.

In Task 2.4 the focus is on analysing the source-sink dynamics of sandeel recruitment to seabed habitats. Sandbanks form essential habitats in large areas of the central Jammer Bay. The sandeel resource on the sandeel banks in the waters off the coast, stretching from Hanstholm to Skagen, is highly variable in size with major influence on fisheries opportunities, in particular for the smaller fishing boats. It is currently not known if the large amounts of sandeel found in some years in this area are produced locally or established by larvae drifting in from neighbouring areas, or by juveniles actively aggregating here because of rich feeding opportunities. A previous project has studied the connectivity between sandeel banks in the North Sea using samples of

sandeel larvae in combination with drift-modelling and statistical analysis. However, the complexity of the hydrography in the North-Eastern corner of the North Sea and its connectivity with Skagerrak has not yet been resolved because of limitations in the available oceanographic data used for the drift modelling. The new, high-quality oceanographic data acquired in the Jammer Bay project will solve this issue. We will apply the new data to model and report upon the source-sink dynamics of sandeel recruitment in the Jammer Bay and the connectivity with the adjacent North-Eastern North Sea and Western Skagerrak by expanding on the above-mentioned North Sea connectivity study.

2. Fisheries footprints on seabed habitats (Task 2.1)

Ole Ritzau Eigaard, Jeppe Olsen, Karin J. van der Reijden, Jonathan Stounberg, Grete E. Dinesen, Josefine Egekvist

2.1 Introduction and aim

The main objectives were to produce outputs of high-resolution grid-cell based swept area ratio (SAR) estimates for all Danish and international fisheries with mobile bottom-contacting gears (beam trawl, otter trawl, Danish seine, fly-shooter) in the case study area. Additionally, landings weight and monetary value will be assigned to each grid cell by gear type and target species, and grid cell sediment mobilization and fuel-use related CO_2 emissions will be calculated for each fishery. This fishing pressure data will then be used to map and analyse the impacts of all individual mobile bottom-contacting gear types on the seabed habitats in the subsequent work packages of the JAMBAY project. This includes the calculation of different benthic state indicators and analyses of impact (in WP3) and resource harvest (in WP4), as well as spatial ecosystem-based trade-off analyses (in WP5) for each grid cell and seabed habitat type. The fishing pressure data will also be correlated with data from GEUS' sediment analyses of grains size composition and carbon content (WP1), including total carbon (TC), total sulphur (TS) and total organic carbon (TOC) to inform about potential emission from the sediment.

2.2 Materials and methods

The focus area for the analyses and data are the ICES statistical rectangles covering the Jammer Bay (Fig. 2.1). This area is dominated by sandy sediments with a central southwest – northeast band of coarser sediment patches.
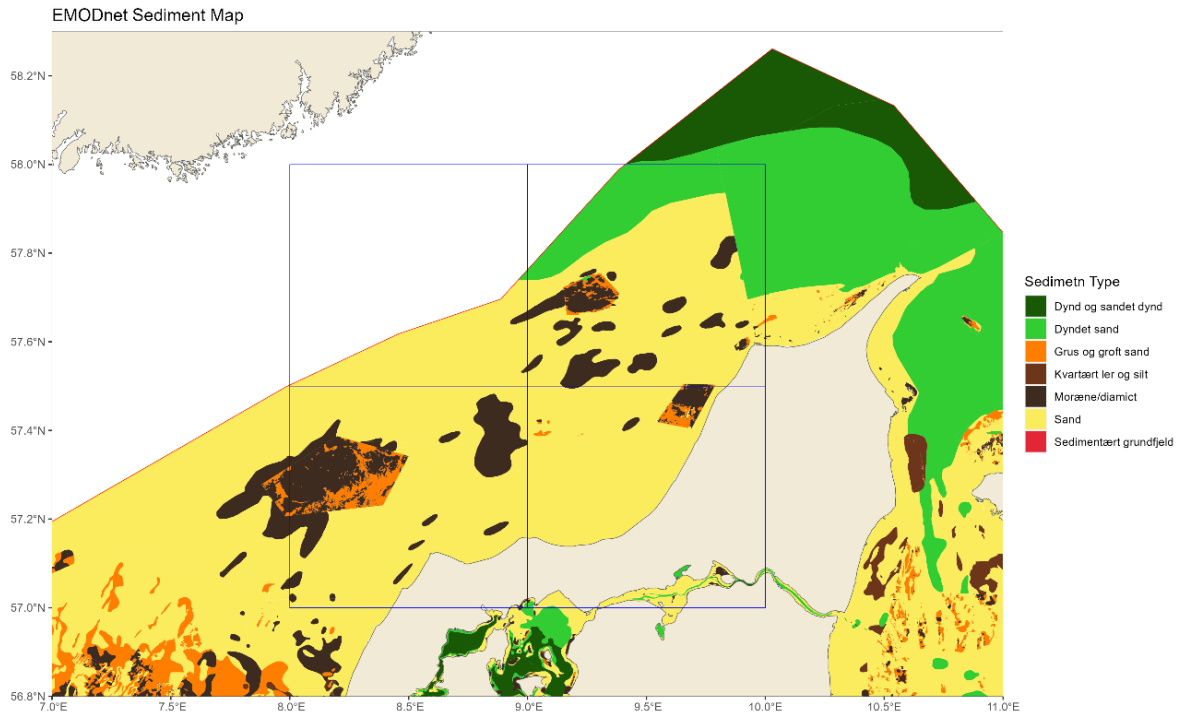
Figure 2.1. Distribution of sediment within the DK EEZ part of the JAMBAY case study area.

Swept area ratios and catch proportions

For the Danish fleet, data from AIS and VMS monitoring of fishing vessels were combined with logbook information to model SAR values for grid cells of 0.001 x 0.001 degrees latitude and longitude (approx. 60 x 100 m) from 2010 to 2022 based on methodology developed by Bastardie et al. (2010), Hintzen et al. (2010) and Eigaard et al. (2016, 2017). For the foreign fleet, AIS data was combined with information on gear type and vessel size (length and engine power) in the EU vessel register to provide equivalent SAR estimates. Both procedures (DK vessels and foreign vessels, respectively) are detailed below, together with the steps taken to couple landing weights and values to each fishing trip, polygon, and grid cell (only possible for the Danish vessels).

For each vessel in the Danish fishing fleet, the following procedure was carried out:

- VMS, AIS, and BB data were aligned. If there were gaps in data of a vessel that only has VMS information, a non-linear interpolation based on heading between pings was made. Hereafter sailing/fishing/non-harbor points were determined by overlapping the points with polygons of the Danish harbors (obtained from the Danish Fisheries Agency) and the sequence of points going in and out of the harbor polygon were then assigned a unique trip id.
- Fishing operations for the individual trips were identified primarily from speed filters, where the ranges of minimum and maximum speeds were determined by expert judgment in collaboration with the ices group "Working Group Spatial Fisheries Data" (WGSFD). If there were more than 10 min between points of fishing these were designated separate fishing operations.
- The fishing operations identified from the speed information in the positions data from BB, AIS and VMS were combined with data in the sales notes and logbook data.

- The sales notes and logbook data were combined by landing date, so that the amounts and values for each species were coupled to a reported fishing trip. Weight and value for total catch, and for cod and plaice were assigned to each trip by species and gear type. In the more recent years, where data from electronic logbooks were available for a larger proportion of the vessels, the catch proportions were assigned at the level of individual hauls. For the earlier years this was done at the trip level. It was only possible to assign catch proportions to grid cells for the Danish fleet as logbooks for international vessels were not available to the project.
- The fishing operation was turned into the actual polygon of contact between gear and seabed substrate for the fishing event, by first turning continuous points into lines, and then assigning a width to the lines by coupling the gear type and vessel size information with the standard workflow and parameters developed by ICES-WGSFD2, which is available on "https://github.com/ices-tools-dev/sfdSAR". For Danish Seines and fly-shooters, the fishing polygon was made by identifying the standard shape of the fishing operation in the positional data of the vessel activity (McLaverty et al. 2023).

For foreign vessels the following procedure was carried out:
- AIS data of the vessels that were active in the case study area and period was downloaded from Søfartsstyrelsen (https://www.soefartsstyrelsen.dk/)
- Individual vessel information (vessel size, engine size and primary gear type) wa extracted from the EU-fleet register.
- Positions data and vessel information was combined by the EU-vessel Id, and the primary gear was assumed to be used throughout the fishing operations of the year.
- Fishing operations were identified by speed filter, based on the primary gear from the EU-fleet registry.
- The fishing operation was turned into the actual polygon for the fishing event by first turning continuous points into lines, and then assigning a width to the lines by coupling the gear type and vessel size information using the workflow and parameters from ICES-WGSFD on "https://github.com/ices-tools-dev/sfdSAR".

After completion of the above steps for the Danish and foreign vessels and trips, respectively, the resulting trip-based polygons of gear-seabed contact and associated landings within the case study area were overlaid with each other and subsequently gridded into cells of 0.001° longitude and latitude. In the four ICES rectangles that cover the Jammer Bay and constitute the JAMBAY case study area this amounts to 1.254.802 grid cells of approx. 60 x 100 m.

Fuel use intensity
The high-resolution fishing pressure data was applied by vessel and gear type to model fuel use intensity (fuel use per kg landed) and CO2 emission following the methodology described in Bastardie et al. (2022). Trip-based logbook records of gears used were coupled with the individual vessel geo-positioning data (VMS, AIS, BB data), which enabled estimation of the trip duration in hours for each trip of each recorded vessel. Fuel consumption per hour was modelled based on the engine power (kW) recorded in the fleet register, which was used as the primary explanatory factor for a maximum fuel consumption rate factor (f_{max}, in litre fuel per hour) (following Bastardie et al. 2013).

$$f_{max} = 3.976 + 0.236 \quad \times \quad kW$$

The speed of the vessel strongly influences the actual fuel use (e.g., Ronen 1982) and therefore, the vessel speeds recorded in AIS, VMS, and BB data were used to decrease the theoretical maximal fuel consumption f_{max} during the steaming phase by a cubic factor (see Ronen 1982), i.e., fuel consumption rate (L per hour) at a given speed for a given vessel was estimated as the ratio of maximum fuel consumption rate factor f_{rate} (in L per hour) over the cube of the maximal observed speed s_{max} of this vessel.

$$f_{rate} = \begin{cases} f_{max} \times 0.9, & when \ towing \\ \frac{f_{max}}{s_{max^3}} \times s^3, & when \ steaming \ or \ not \ towing \end{cases}$$

This corrective decrease in fuel consumption rate along with lower speed was, however, not applied during the fishing phases of vessels using towed gear, where the decrease in speed is more the result of the resistance of the gear being dragged than a decrease in the use of the engine power. To account for this effect, we assumed 90% of the developed maximal engine load during towing phases, as referred by Coello et al. (2015). As a rule of thumb, trawl designers are used to scaling the size of trawls to the performance of the engine, which has been confirmed by examining flow meter data of individual trips using trawl (Ole R. Eigaard, pers. comm.). Finally, using spatial BB, AIS, and VMS data linked to the national logbook and vessel register (DK) and EU vessel register (foreign vessels) allows for an estimated fuel use in a given location (e.g., c-square, grid cell) on a trip basis for each vessel.

Sediment mobilization

We used the annual swept area (m^2) to determine the total amount of sediment mobilized in each grid cell. In this, we combined métier-specific estimates of the hydrodynamic drag generated by the entire gear with silt fraction estimates based on the prevailing habitat type, in line with equation 12 in Rijnsdorp et al. (2021). The benthic Broad Habitat Types (BHTs), as defined under the Marine Strategy Framework Directive (MSFD) and obtained from the EMODnet seabed habitats portal (version 2021: https://emodnet.ec.europa.eu/en/seabed-habitats), were reclassified into the categories "sand", "mud", and "gravel". All MSFD habitats mentioning "coarse" and "rock" seabed were classified as "gravel". All MSFD habitats that solely comprised "mud" at the seabed were classified as "mud". All other habitats were classified as "sand". The following silt fractions were assigned to the three habitat classes: Gravel: 0.05; Sand: 0.175; Mud: 0.55.

The métier-specific estimates of hydrodynamic drag were derived from several sources. For the beam trawlers, we applied the fleet-estimate for the large vessels (>221 kW) using traditional tickler chain or chain mat gears from Rijnsdorp et al. (2021). For otter trawls, the values from van der Reijden et al. (in prep) were used. This study computes component-specific estimates of the hydrodynamic drag for three Danish otter trawl fisheries, based on detailed information on the individual component dimensions and exact gear configuration. From the component-specific hydrodynamic drag estimates, we determined the amount of sediment mobilized per square meter of seabed swept for the three silt fractions. We then multiplied the component-specific mobilization estimates with the contribution of the component-specific footprint in relation to the total footprint to achieve a métier-specific estimate of mobilization per square meter swept seabed. For Danish anchor seines (SDN_DMF) and Scottish seines (SSC_DMF), we adjusted the

functions used by van der Reijden et al. (in prep) that determine the hydrodynamic drag of the sweeps and the ground gear in the otter trawls. We changed parameters of component dimensions according to literature values (Eigaard et al. 2015; O'Neill and Summerbell 2016; Noack et al. 2019; O'Neill and Noack 2021) and determined the métier-specific estimates by applying the Danish seine gear footprint proportions from Noack et al. (2019).

Fishing intensity and sediment carbon
Data from GEUS' sediment analyses of grain size composition and carbon content in samples from the JAMBAY case study area (including sediment content of total carbon [TC], total sulphur [TS], and total organic carbon [TOC]), were modelled across a high-resolution fishing intensity gradient to correlate disturbance from fisheries with mobile bottom-contacting gears with carbon content and potential emission from the sediment. Generalized Linear modelling will be applied to matching data points of carbon and sulphur content and fishing pressure values as well as other environmental variables such as depth and bed sheer stress. The fishing pressure values are calculated as circular SARs (50 m radius) around the sediment sample positions.

2.3   Results

Swept area ratios and catch proportions
The Jambay case study area is intensively fished with mobile bottom-contacting gears (Fig. 2.2). When pooling all the gears together the average annual SAR-values from the period 2015-2022 showed that larger areas of the deeper, more offshore parts of the case study area were fished with frequencies that exceed 10 times annually. In the shallower fishing grounds, closer to shore, the fishing intensity was lower, but also here there were hot spot areas that were fished more than 10 times a year, and a large proportion of the seafloor was fished between 5 and 10 times a year.
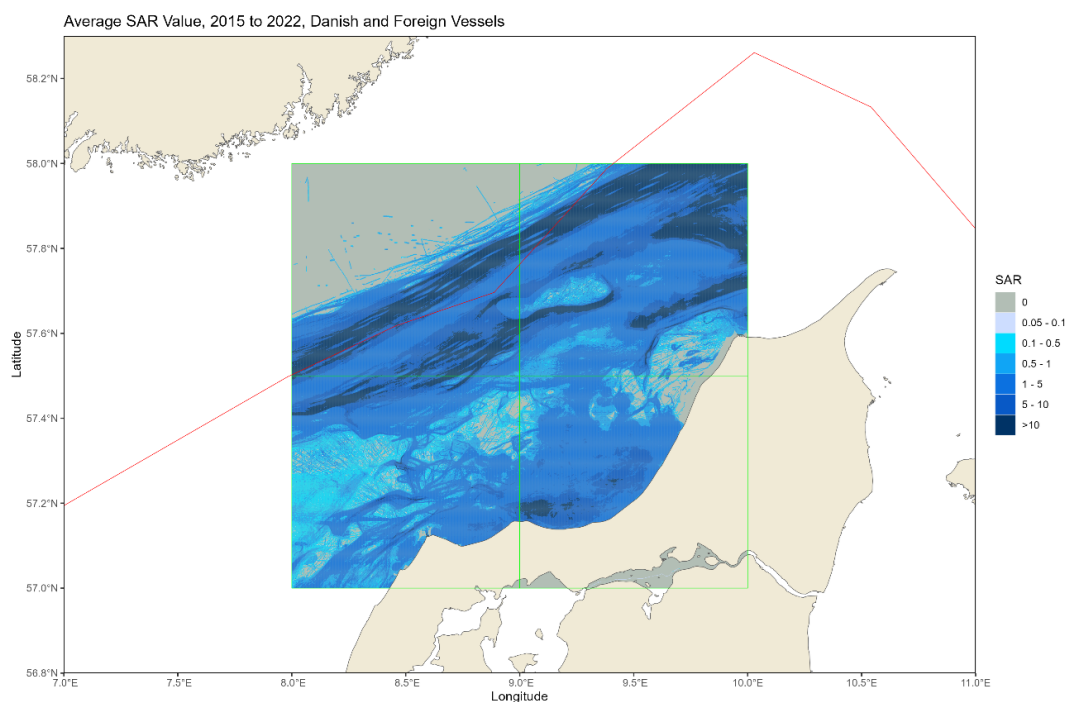
Figure 2.2. SAR values (annual average from 2015-2022 in grid cells of 0.001°) for all gears and DK and foreign fisheries combined, within the JAMBAY case study area.

When splitting the fishing effort into the contributions from Danish and foreign vessels, respectively (Fig. 2.3), it is evident that the Danish fleet by far exerts the largest pressure on the seafloor in the case study area, and more so in the coastal than in the more offshore areas.
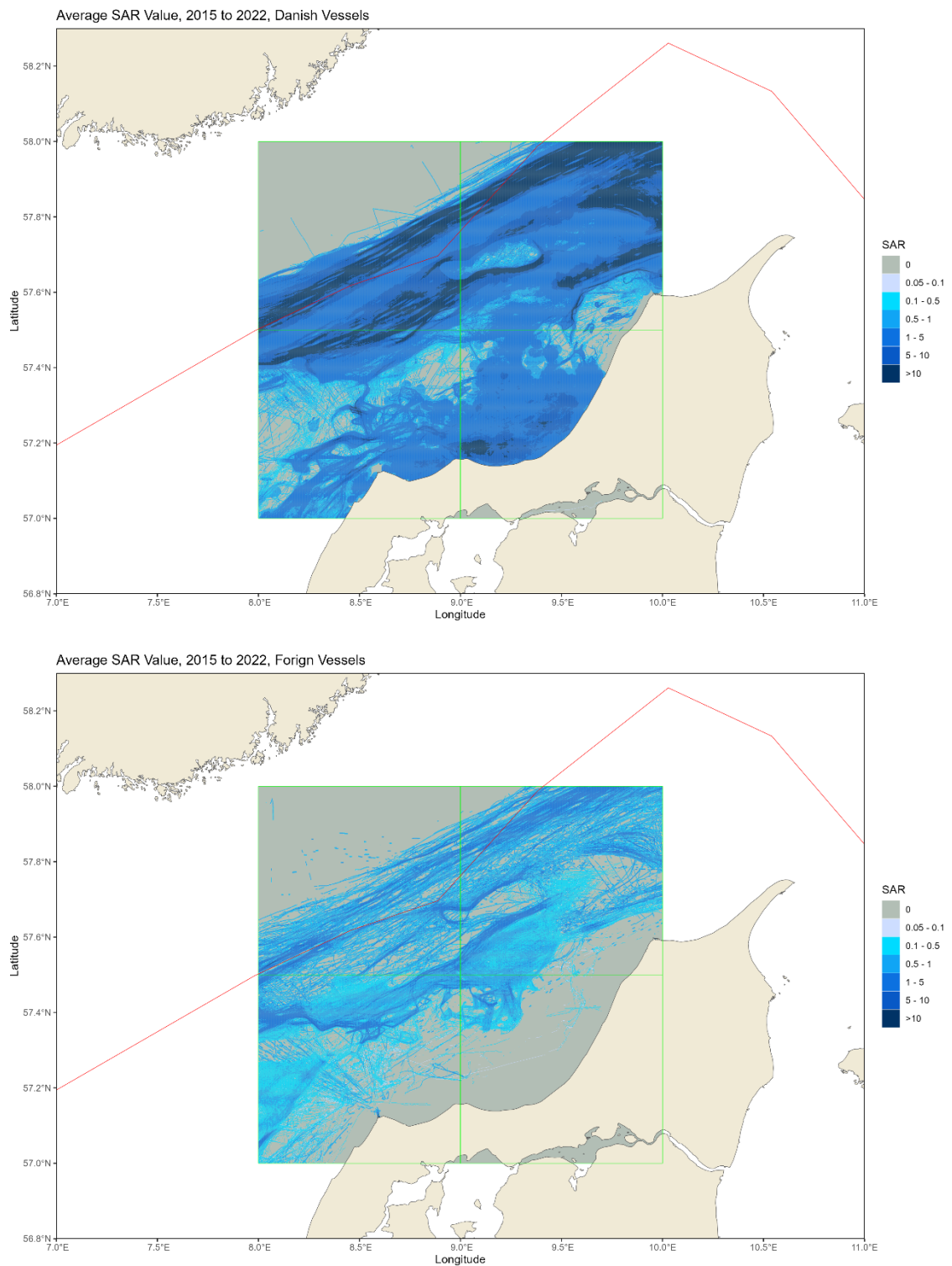
Figure 2.3. SAR values (annual average from 2015-2022 in grid cells of 0.001°) for all gears, and DK (top) and foreign fisheries (bottom) separated, within the JAMBAY case study area.

When splitting the effort into the three overarching gear types a pattern emerges (Fig. 2.4), where the otter trawlers dominate the deeper, soft-sediment offshore areas, the Danish seiners dominate the shallower and more coastal areas with sandy sediments, and both these gears are absent in the central band of the case study area, which is dominated by coarser substrates such as boulders, limestone patches and stone reefs, where the beam trawlers dominate.

Bottom Trawl - Average SAR Value, 2015 to 2022, Danish and Foreign Vessels

Danish Seine - Average SAR Value, 2015 to 2022, Danish and Foreign Vessels
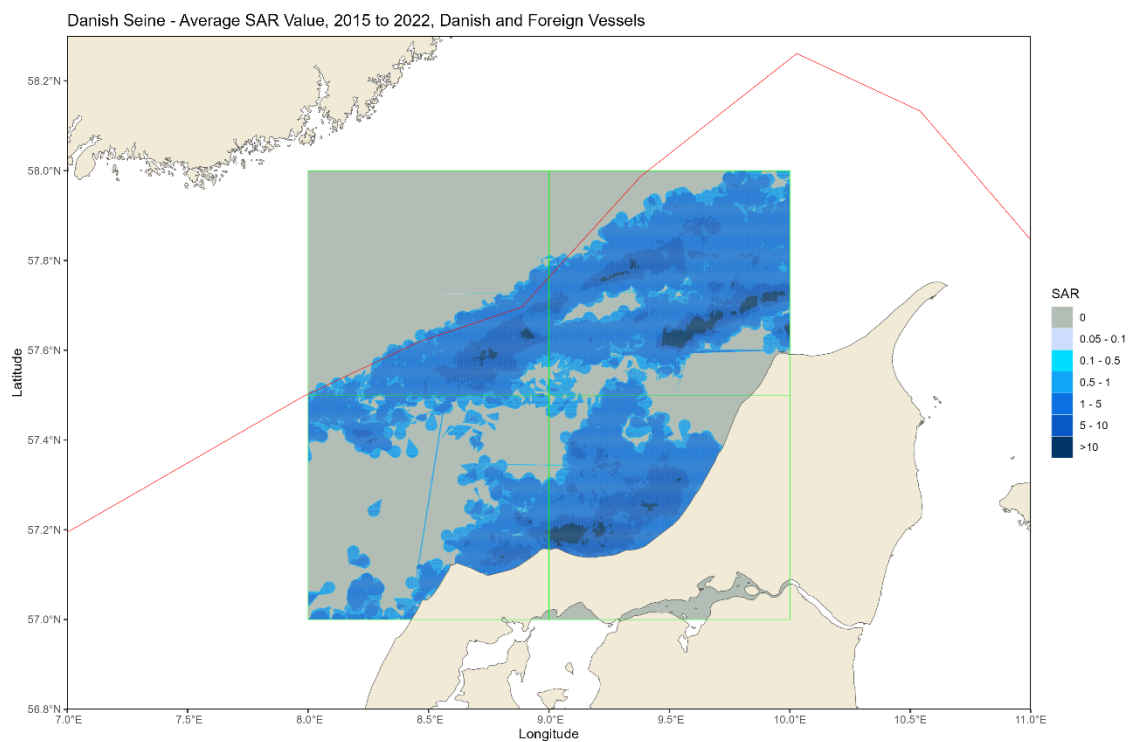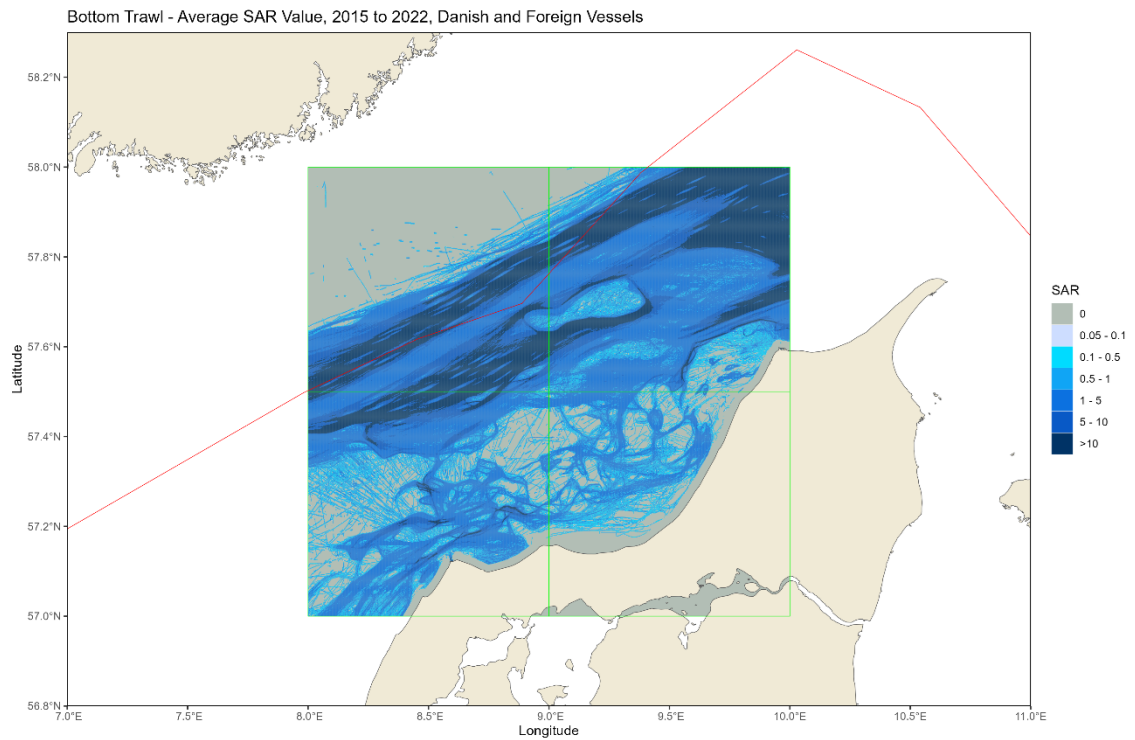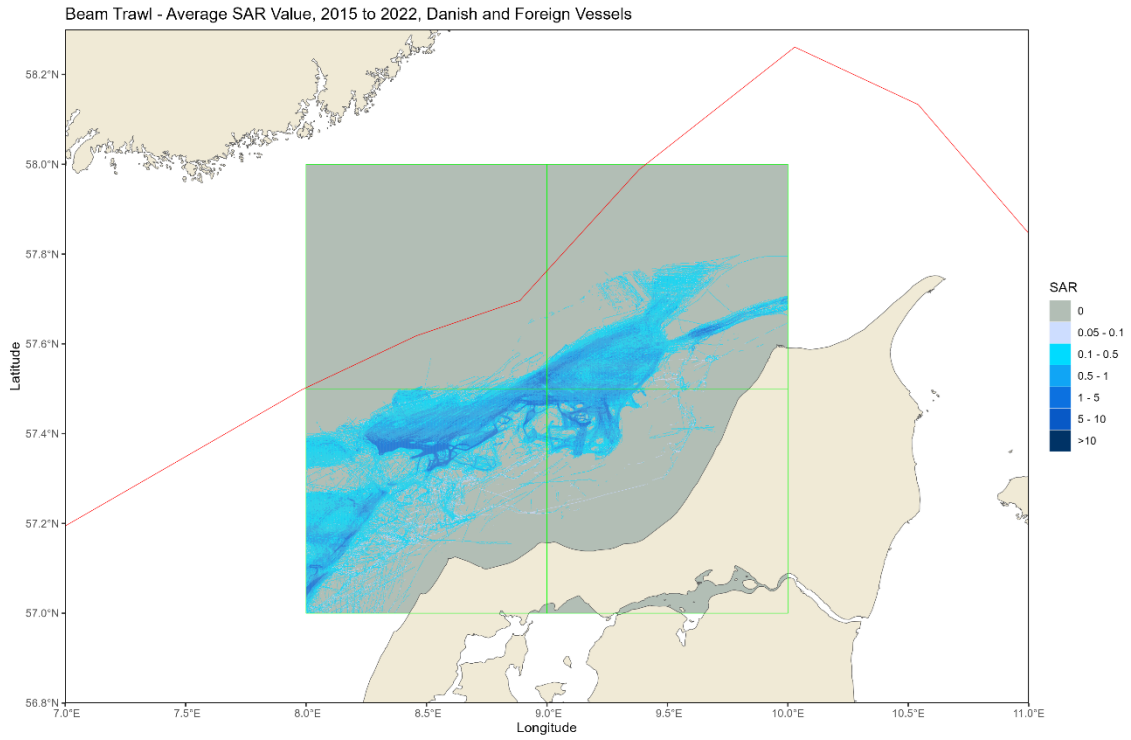
Figure 2.4. SAR values (annual average 2015-2022 in grid cells of 0.001°) for three gear groups (top: Otter trawl, center: Danish seines, and bottom: Beam trawls), DK and foreign fisheries combined.

The spatial distribution of landing values across grid cells from the Danish fleet (Fig. 2.5) closely follows the distribution of fishing intensity (SAR) with the highest values per grid cell being found in the grid cells that also have the highest intensity of fishing. There are some deviations between the two maps (Figs. 2.5 and 2.3), which are brought about by the price-difference of the species.
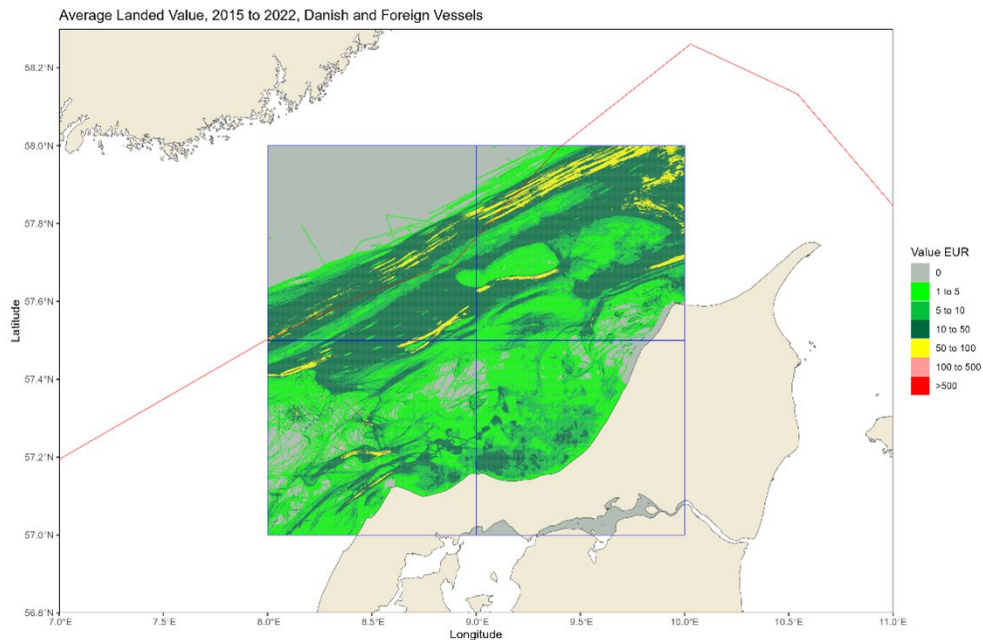
Figure 2.5. Catch proportions (total landings value) from logbook and landings data for all gears combined for the Danish fleet (annual average from 2015-2022 in grid cells of 0.001°), within the JAMBAY case study area.

Fuel use intensity

The spatial distribution of total (Danish and foreign fleet) fuel use intensity across grid cells (Fig. 2.6) closely follows the distribution of fishing intensity (SAR) with the highest values per grid cell being found in the grid cells that also have the highest intensity of fishing. There are some deviations between the two maps (Figs. 2.6 and 2.3), which are brought about by the difference in the engine-power requirement of the gear types.
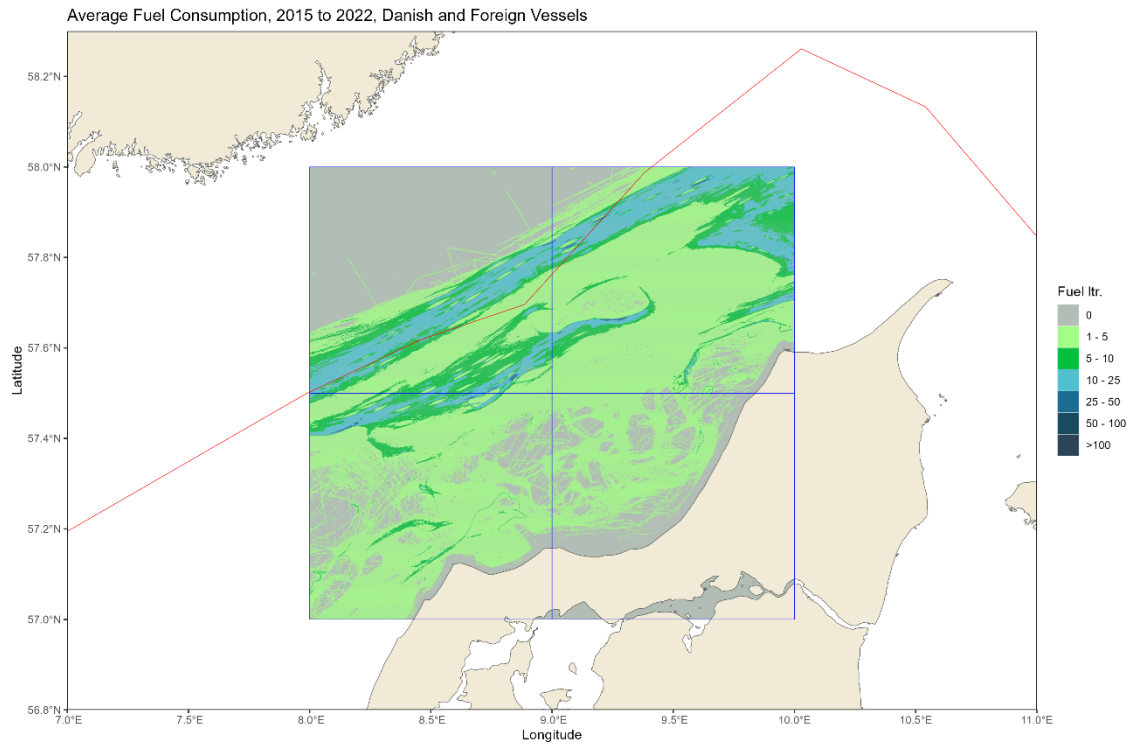
Figure 2.6: Fuel-use intensity estimates for all gears combined for both the Danish and foreign fleet (annual average from 2015-2022 in grid cells of 0.001°), within the JAMBAY case study area.

Sediment mobilization

The spatial distribution of total (Danish and foreign fleet) sediment mobilization across grid cells (Fig. 2.7) largely follows the distribution of fishing intensity (SAR) with the highest values per grid cell generally being found in the grid cells that also have the highest intensity of fishing. There are, however, some deviations between the two maps (Figs. 2.7 and 2.3), which are brought about by the differences in sediment silt-fractions of the habitat types and the different penetration-depths and drags of the gears.
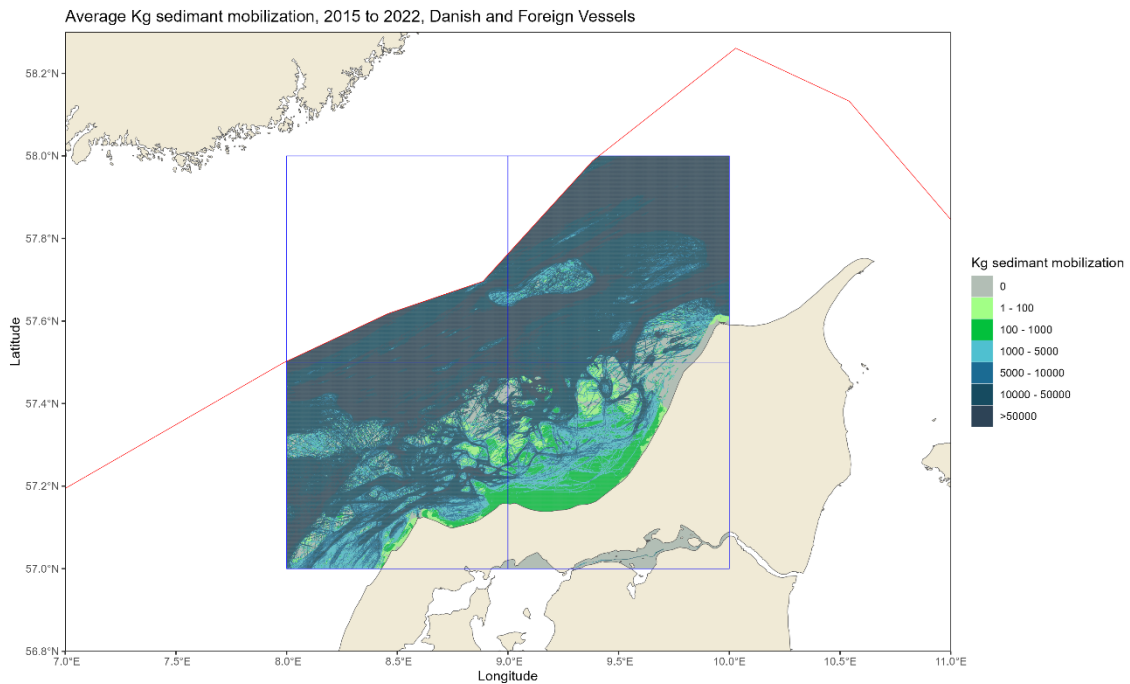
Figure 2.7. Sediment mobilization estimates for all gears combined for both the Danish and foreign fleet (annual average from 2015-2022 in grid cells of 0.001°), within the JAMBAY case study area.

Fishing intensity and sediment carbon

In total 131 sediment samples were collected by GEUS and DTU Aqua in the JAMBAY case study area. These samples are being worked up in the laboratory at GEUS and currently 69 samples have been completed. When all 131 samples have been analysed for grain size composition and content (including sediment content of total carbon [TC], total sulphur [TS], and total organic carbon [TOC]), they will be modelled across a high-resolution fishing intensity gradient to correlate mobile bottom-contacting fisheries disturbance with carbon content and potential emission from the sediment.

2.4 Discussion and perspectives

The Task 2.1 calculation and mapping of fishing pressure in the case study area, showed that the DK fleet is responsible for the largest fishing pressure on the sandy sediments (Danish seines) and the soft-sediments (otter trawlers), and that the international beam trawl fleet exerted the largest pressure on the coarser sediments.

The spatial distribution of landed catch, fuel-use intensity, and sediment mobilisation generally followed the distribution of fishing intensity, with the highest values per grid cell being found in the grid cells that also had the highest fishing intensity (i.e., highest SAR estimates). There were, however, some deviations between the maps of the different pressures, which were brought about by the price-difference of the species, the difference in the engine-power requirements of the gear types, the differences in sediment silt-fractions of the habitat types, and the different penetration-depths and drags of the gears. The largest deviations between SAR values and the fuel-use intensity and sediment mobilisation estimates were seen for the more coastal areas, where the Danish seine fishery had high SAR values, but relatively low values of fuel use and sediment release because of low engine-power requirements, shallow penetration depth, and sandy sediment requirement of this gear type.

The fishing pressure data of swept area ratio (SAR), landed catch, fuel-use intensity, and sediment mobilisation were estimated for individual grid cells of 0.001 degrees longitude and latitude (approx. 60x100 meter). This was made possible through the development of a polygon-based approach to the calculations of haul-based swept area calculations for individual vessels and a hierarchical use of information in BB, AIS, and VMS monitoring data. The refinement and application of these state-of-the-art methodologies to Danish fisheries monitoring data has enabled the estimation of fishing pressure data in an unprecedented quality and resolution, which is more than 1000 times higher than other publicly available SAR maps and data that are currently used for impact and trade off assessments. It is well established that grid cell size plays a crucial role in the accuracy and reliability of fishing pressure and impact assessments so that uncertainty increases with increasing grid cell size (e.g., Amoroso et al. 2018) and consequently the resolution in the pressure data achieved here adds certainty to the estimates. However, there are still some caveats in the available data and the deployed methodology that can be improved in subsequent stages:

Speed filtering
The current approach for separating the individual positional observations (AIS, VMS, and BB data) into fishing or non-fishing vessel activity is based on typical speed ranges of each fishery (defined by gear type and target species group) and this approach carries a risk of positions falsely being assigned as fishing activity because the vessels slow down for other reasons than trawling (e.g., harbours, waterways, and shallow waters) and enter the speed range that is automatically defined as 'fishing' in the R-based work-flow.

Gridded approach and MSFD
In most gridded approaches to the estimation of D6C2 in an assessed area, including our approach, it is assumed that in a grid cell with an annual SAR value of 1 or above, the full grid cell area is swept by a fishing gear. This can potentially result in an overestimation of the total area fished, because trawl tracks are often placed on top of each other over time. There are also different ways of calculating the proportion of each grid cell that is swept by a fishing gear, based on the SAR values. When estimating the proportion swept across periods with multiple fishing events in the same grid cell, there are several approaches, which differ in their assumptions about the distribution of the individual trawl tracks inside the grid cell during the assessed period. For multi-year periods, we have deployed the 'maximum annual proportion' approach, where it is assumed that all trawl tracks of the assessed period are confined to an area defined

by the annual maximum proportion of the period. This can potentially result in an underestimation of the total area fished). The smaller the grid cells, the smaller the uncertainty.

International fishing effort

For the foreign fleet, AIS data was combined with information on gear type and vessel size (length and engine power) in the EU vessel register to provide SAR estimates. The positions data and vessel information were combined by the EU-vessel Id, and the primary gear is assumed to be used throughout the fishing operations of the year. This approach with a full year gear assumption, necessitated by the lack of logbook data for the foreign vessels, is much cruder than the method used for the Danish fleet, where detailed gear information was available at the individual trip level. Consequently, the SAR estimates for the foreign fishery are more uncertain than the estimates for the Danish fleet.

2.5 Acknowledgements

2.6 References

Amoroso RO, Parma AM, Pitcher CR, McConnaughey R, Jennings S. 2018. Comment on "Tracking the global footprint of fisheries". Science, 361: eaat6713,

Bastardie F, Nielsen JR, Ulrich C, Egekvist J, Degel H. 2010. Detailed mapping of fishing effort and landings by coupling fishing logbooks with satellite-recorded vessel geo-location. Fisheries Research, 106, 41–53.

Bastardie F, Hornborg S, Ziegler F, Gislason H, Eigaard OR. 2022. Reducing the Fuel Use Intensity of Fisheries: Through Efficient Fishing Techniques and Recovered Fish Stocks. Frontiers in Marine Science, 9, [817335]. https://doi.org/10.3389/fmars.2022.817335.

Eigaard OR, Bastardie F, Breen M, Dinesen GE, Hintzen NT, Laffargue P, Mortensen LO. et al. 2016. Estimating seabed pressure from demersal trawls, seines, and dredges based on gear design and dimensions. ICES Journal of Marine Science, 73, i27–i43.

Eigaard OR, Bastardie F, Hintzen NT, Buhl-Mortensen L, Buhl-Mortensen P, Catarino R, Dinesen GE. et al. 2017. The footprint of bottom trawling in European waters: distribution, intensity, and seabed integrity. ICES Journal of Marine Science, 74, 847–865.

Hintzen NT, Piet GJ, Brunel T. 2010. Improved estimation of trawling tracks using cubic Hermite spline interpolation of position registration data. Fish Research, 101, 108–115.

McLaverty C, Eigaard OR, Olsen J, Brooks ME, Petersen JK, Erichsen AC, van der Reijden K, Dinesen GE. 2023. European coastal monitoring programmes may fail to identify impacts on benthic macrofauna caused by bottom trawling. Journal of Environmental Management, 334, Article 117510. https://doi.org/10.1016/j.jenvman.2023.117510.

Noack T, Stepputtis D, Madsen N, Wieland K, Haase S, Krag LA. 2019. Gear performance and catch process of a commercial Danish anchor seine. Fisheries Research, 211, 204-211. https://doi.org/10.1016/j.fishres.2018.11.012.

O'Neill FG, Summerbell KJ. 2016. The hydrodynamic drag and the mobilisation of sediment into the water column of towed fishing gear components. Journal of Marine Systems, 164, 76–84.

O'Neill FG, Noack T. 2021. The geometry and dynamics of Danish anchor seine ropes on the seabed. ICES Journal of Marine Science, 78(1), 125-133. DOI: 10.1093/icesjms/fsaa198.

Rijnsdorp AD, Depestele J, Molenaar P, Eigaard OR, Ivanović A, O'Neill FG. 2021. Sediment mobilization by bottom trawls: a model approach applied to the Dutch North Sea beam trawl fishery. ICES Journal of Marine Science, 78(5), 1574-1586. [fsab029]. https://doi.org/10.1093/icesjms/fsab029.

Van der Reijden KJ, Eigaard OR, Bastardie F, O'Neill FG. (in prep). Gear component-specific impact assessments of three Danish otter trawl fisheries.

3. Physical seabed disturbance of mobile gear components (Task 2.2)

Nurul Huda, Ole R. Eigaard, Barry O'Neill

3.1 Introduction and aim

The characteristics of the seabed substrate define the fish and shellfish species that live there and the types of fishing gears than can be deployed for catching them. Beam trawls with chain mats or tickler chains can be deployed on almost all substrates from boulders and stones to gravel and sand, whereas Danish seiners are restricted to sandy habitats because of their relatively light gear and their specialized fishing technique. Otter trawlers and Fly-shooters are more restricted by substrate type than beam trawlers, but less restricted than Danish seiners, and typically operate on a substrate size spectrum between mud and gravel. The nature of the physical interaction between the gear and seabed structures not only defines the areas in which the different gears can be deployed, it is also central in understanding and assessing the adverse effects of fishing on the seafloor habitats. The frequency of fishing and the sensitivity of the seabed and benthic ecosystem are additional factors that together with the physical gear impact determines the ecosystem effects of bottom trawling.

From the fisheries perspective, loss of gear is the most definitive and least desired outcome of the interactions between gear and seabed. A major cause of the loss of demersal fishing gears is snagging on seabed features and obstructions (Richardson et al. 2021; Ayaz et al. 2010; Brown et al. 2005). Surveys of Australian and Indonesian fishers across all gear types revealed that gear loss occurred mostly because of snagging on an obstruction (78%), followed by gear conflicts with third parties (19%), and poor weather conditions (Richardson et al. 2018). Similarly, a survey in Canada indicated that snagging gear on rough substrate was the most important reason for loss across all gear categories, followed by seafloor type (Frenkel et al. 2023). The loss of fishing gear has immediate economic consequences for fishers. It will result in missed fishing opportunities, and the financial cost of having to replace the gear. There are ecological and environmental concerns, and Abandoned, Lost or Discarded Fishing Gear (ALDFG) can continue to fish and will degrade with time to produce microplastics. Snagging gears on seabed obstructions can also have serious safety implications, and there have been incidences where vessels have sunk, and lives lost following a snagging event.

In general, however, fishers will either avoid grounds with obstructions or choose or modify their gears to reduce the likelihood of snagging. In this study, we aim to get a better understanding of the interaction of towed fishing gears with boulders. This will help fishers choose what gears can be used on given fishing grounds and will help fisheries managers protect seabed habitats and features. We focus on estimating the snagging probability of different demersal trawls with boulders and carry out a scaled model flume tank study (i) to identify which gears are more likely to snag on boulders, (ii) to evaluate at which part of a given gear snagging is more likely to occur, and (iii) to determine if there are any characteristic features of a boulder that increases the likelihood of snagging.

3.2   Materials and methods

Experimental trials

The experimental trials were conducted in the Hirtshals Flume Tank, (length 30 m, depth 2.7 m, and width 8 m; Fig.3.1) with 1:6 scale models of four different types of towed demersal fishing gear. An otter trawl, a tickler-chain beam trawl, a chain-mat beam trawl and the ropes of a Danish seine, were modelled (Fig. 3.2).

Figure 3.1. SINTEF Flume Tank, Hirtshals.

Scale model fishing gears

The model otter trawl corresponds to a full-scale gear with a 34 m ground gear and an approximate headline height of 2.2 m and wing-end spread of 15.2 m. It is representative of the flatfish trawls used in the Jammer Bay by vessels in the size range of approx. 12 – 20 m. The model beam trawls correspond to typical 12 m tickler-chain and chain-mat beams that are used in pairs by North Sea and Skagerrak beam trawlers to fish flatfish species. The model Danish Seine ropes correspond to full scale ropes of 40 mm diameter.
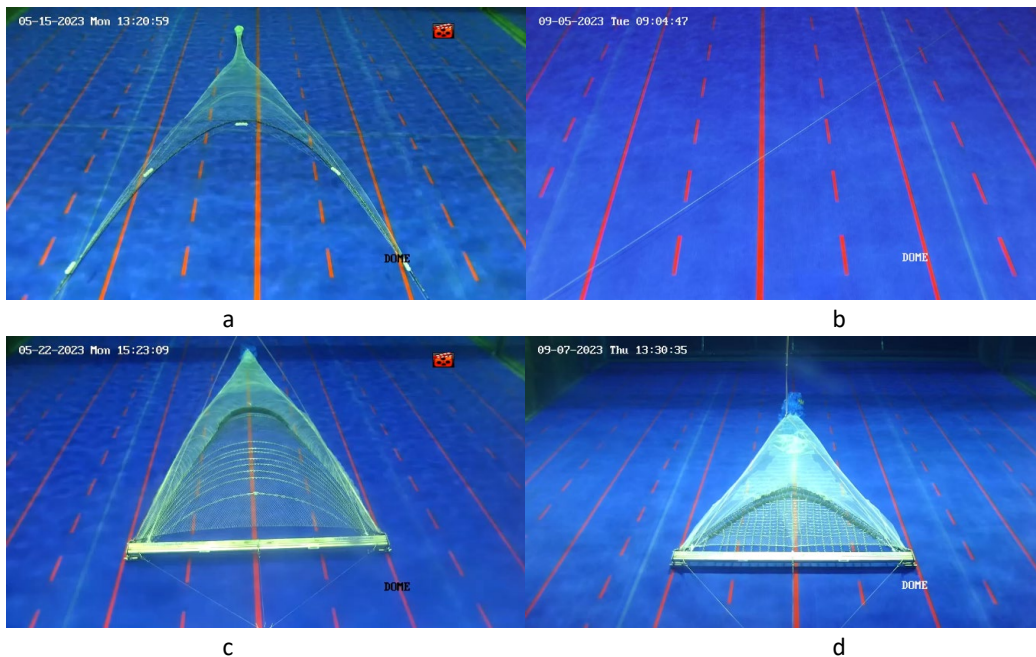
Figure 3.2. Fishing gears model scale a) Otter trawl b) Danish seine c) Beam trawl with tickler chain d) beam trawl with chain mat.
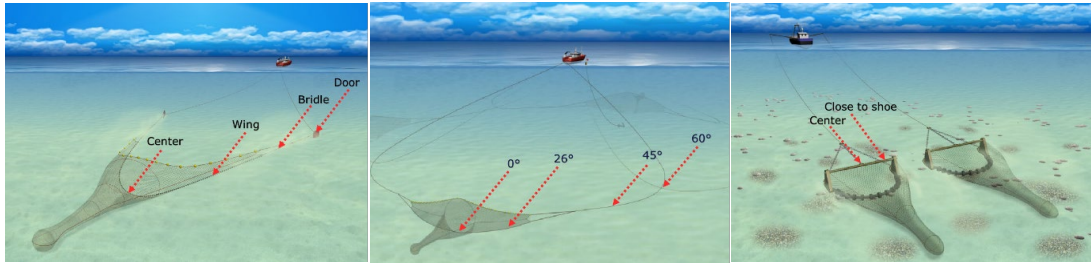
Figure 3.3. The position/components targeted on a) the otter trawl b) the Danish seine and c) a beam trawl.

Component-based approach

To get a broad appreciation of the likelihood of snagging of a particular gear, it is necessary to investigate the interaction of boulders with different parts and components of the gears. For the otter trawl, we focused on the centre of the ground gear, the wings, the bridles and sweeps and the trawl door. For the beam trawls we targeted the centre of the beam and close to the beam shoe, and subsequently, if the boulder was able to pass the beam at either of these two positions, we examined the interaction with either the tickler chains or the chain mat (Fig. 3.3). The ropes of a Danish seine account for over 95% of their swept area and here we focused on how rope at different angles of attack (30, 45, 64 and 90°) interact with the boulders.

Scale model boulders

The boulders are modelled as three-dimensional ellipsoids, and we investigated how boulder size and the slope angle at the boulder base influenced the likelihood of snagging of each of the gears. Three boulder shapes were defined according to whether their slope angle at the base was inward sloping, straight, and outward sloping. For each shape, three different full-scale heights of boulder (48, 60 and 120 cm) were examined (8, 10 and 20 cm, model scale). Consequently, a total of nine boulder models were employed (Fig. 3.4, Table 3.1). The boulders were made from polyethylene terephthalate glycol (PETG), fabricated using a 3D printer, and fitted 24 cm from the front edge of a stainless-steel plate of length 200 cm, width 125 cm, thickness 0,6 cm, and weight 120 kg.
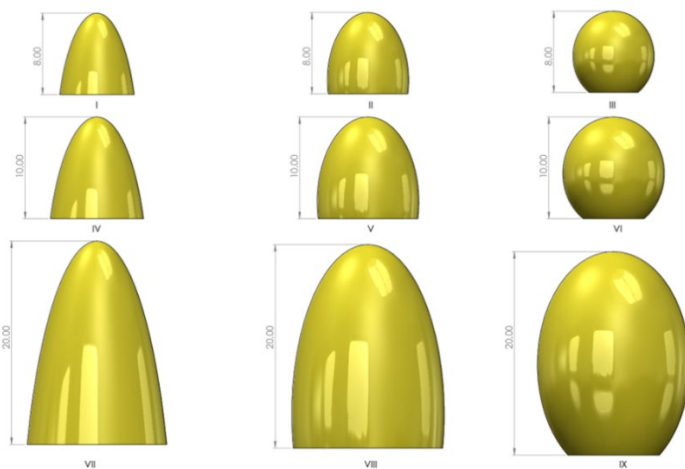
Figure 3.4. The boulder models.

Table 3.1. Boulder models.

Labels	Full Scale Height (cm)	Model Scale Height (cm)	Shapes
I	48	8	Inward Sloping
II	48	8	Straight
III	48	8	Outward Sloping
IV	60	10	Inward Sloping
V	60	10	Straight
VI	60	10	Outward Sloping
VII	120	20	Inward Sloping
VIII	120	20	Straight
IX	120	20	Outward Sloping

Experimental procedure

The boulder plate was positioned on the flume tank belt so that it was a few meters ahead of the gear and aligned with the planned collision point. The initial placement was done at a low towing speed and on a stationary belt, and the plate was held in place by a rope attached to a towing support. The flow speed and conveyer speed were then increased to 0.5 m/s and the relative alignment of boulder and gear were checked again. When the positioning was satisfactory, the plate was released, and the boulder proceeded to snag or pass under the gear (Fig. 3.5). The belt was then stopped, the water current reduced, the gear raised a few centimetres from the belt, and the plate retracted to its original position. This process was repeated six times for each boulder shape, and at each of the four otter trawl positions, the two tickler-chain and two chain-mat beam trawl positions, and the four Danish seine rope with different angles of incidence, resulting in total in 84 trials. Each trial was video-recorded, and the outcome (snagging or passing) was noted.
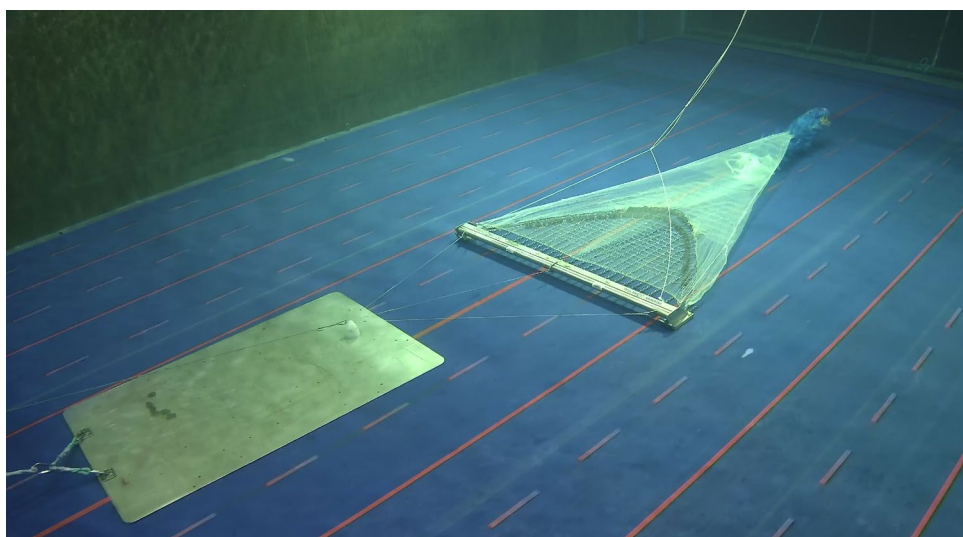
Figure 3.5. Boulder approaching the chain mat beam trawl.

3.3   Results

The results are summarized in the following tables, where a green tick signifies no snagging, an orange triangle signifies that a half or fewer of the trials snagged, a red diamond signifies that more than half snagged, and a red cross signifies that all trials snagged. In general, less snagging occurs on inward sloping boundaries; the amount of snagging for a particular component/position increases as the slope becomes more outward sloping; and more snagging occurs as the boulders got bigger.

The doors of the otter trawl passed all the boulders, regardless of size and shape, while the bridles could not pass the boulders with an outer sloping shape but mostly passed the boulders with a straight and inward sloping shape. The centre and wing of the otter trawl could not pass the boulders with straight and outer sloping shapes but could mostly pass inward-sloping boulders (Table 3.2).

Table 3.2. Interaction of otter trawl with boulders.

Boulder Height (cm)	Boulders Shape											
	Inward Sloping				Straight				Outward Sloping			
	Position				Position				Position			
	Center	Wing	Bridle	Door	Center	Wing	Bridle	Door	Center	Wing	Bridle	Door
8	△	✓	✓	✓	✗	✗	✓	✓	✗	✗	✗	✓
10	✓	✓	✓	✓	✗	✗	△	✓	✗	✗	✗	✓
20	✗	△	✗	✓	✗	✗	✗	✓	✗	✗	✗	✓

The ropes of a Danish seine passed nearly all of the largest inward sloping boulders, while they got snagged on nearly all of the straight and outward sloping ones (Table 3.3).

Table 3.3. Interaction of Danish seine with boulders.

Boulder Height (cm)	Boulders Shape											
	Inward Sloping				Straight				Outward Sloping			
	Angle				Angle				Angle			
	0	26	45	60	0	26	45	60	0	26	45	60
8	✓	✓	✓	✓	✗	✗	✗	✓	✗	✗	✗	✗
10	✓	✓	✓	✓	✗	✗	✗	✗	✗	✗	✗	✗
20	✗	✓	✗	✓	✗	✗	✗	✗	✗	✗	✗	✗

The tickler chain beam trawl was the gear that snagged the most and probably reflects the fact that if the beam passed over a boulder, there were then multiple further opportunities for snagging on each of the individual chains. Indeed, the only time it was able to pass was when its shoe interacted with inward sloping boulders (Table 3.4).

Table 3.4. Interaction of beam trawl with tickler chain with boulders.

Boulder Height (cm)	Boulders Shape					
	Inward Sloping		Straight		Outward Sloping	
	Position		Position		Position	
	Center	Shoe	Center	Shoe	Center	Shoe
8	✗	✓	✗	✗	✗	✗
10	✗	✓	✗	✗	✗	✗
20	✗	⚠	✗	✗	✗	✗

Beam trawls with a chain mat could mostly pass when hit with the inward sloping boulders in all positions, but it snagged more when hitting the boulders with a straight shape, and almost always snagged when hitting the boulders with outward sloping shapes (Table 3.5).

Table 3.5. Interaction of beam trawl with chain mat with boulders.

Boulder Height (cm)	Boulders Shape					
	Inward Sloping		Straight		Outer Sloping	
	Position		Position		Position	
	Center	Shoe	Center	Shoe	Center	Shoe
8	✓	✓	◆	✗	✗	✗
10	✓	✓	⚠	✓	◆	✗
20	✗	◆	✗	◆	✗	✗

3.4   Discussion and perspectives

The gear-specific borders between fishable and non-fishable substrates are far from clear-cut, and the objective of Task 2.2 has been to examine how the different gear types and components interact with boulders and stones. We focused on estimating the snagging probability of different bottom-contacting gears with boulders and carried out a scaled model flume tank study to (i), identify which gears are more likely to snag on boulders, (ii), to evaluate at which part of a given gear snagging is more likely to occur, and (iii), to determine if there are any characteristic features of a boulder that increases the likelihood of snagging.

Apart from the tickler chain beam trawl, all gears were generally able to pass the inward sloping boulders at the small and medium size, but not the largest boulders. The tickler chain beam trawl was the gear that snagged the most and probably reflects the fact that if the beam passed over a boulder, there were then multiple further opportunities for snagging on each of the individual chains. None of the gears significantly outperformed the others in passing the straight and inward sloping boulders, but for these two boulder shapes, the tickler chain beam trawl and the Danish seine snagged at practically all combinations of gear-components, and boulder-sizes, whereas both the chain mat beam trawl and the otter trawl passed for several combinations of gear-components and boulder-sizes.

The doors of the otter trawls can pass all the boulders, regardless of size and shape, while the bridles and centre and wing of the ground gear can mostly pass inward-sloping boulders (small

and medium-sized), but not boulders with straight and outer sloping shapes. The ropes of a Danish seine pass nearly all the largest inward sloping boulders, at all angles, while they get snagged on nearly all the straight and outward sloping ones. For the two beam trawl types, the shoe snags less than the tickler chains and chain mats, respectively, and the chain mats snag less than the tickler chains.

The study of boulder features in relation to snagging showed that across gears, less snagging occurs on inward sloping boundaries; the amount of snagging for a particular component/position increases as the slope becomes more outward sloping and more snagging occurs as the boulders get bigger.

A central outcome and a somewhat surprising key message is that tickler chain beam trawls appear to be the most restricted gear type in terms of substrate composition as this gear type snagged the most across boulder shapes and sizes. It was expected that Danish seines would be the most restricted and that tickler chain beam trawls would be able to fish on more coarse substrate types than both otter trawls and the seines. An explanation might be that high snagging risk in a seabed habitat does not per se prevent beam trawling as these vessel types generally have high engine power and likely can move and turn over boulders when snagging does occur. Even so, our modelling-based results indicate that tickler chain beam trawlers are more restricted in their choice of fishing grounds than generally perceived.

3.5 Acknowledgements

3.6 References

Ayaz A, Ünal V, Acarli D, Altinagac U. 2010. Fishing gear losses in the Gökova Special Environmental Protection Area (SEPA), eastern Mediterranean, Turkey. Journal of Applied Ichthyology, 26(3), 416–419. https://doi.org/10.1111/j.1439-0426.2009.01386.x

Brown J, Macfadyen G, Huntington T, Magnus J, Tumilty J. 2005. Ghost fishing by lost fishing gear. Final Report to DG Fisheries and Maritime Affairs of the European Commission. Fish/2004/20. Institute for European Environmental Policy/Poseidon Aquatic Resource Management Ltd Joint Report, 151.

Frenkel C, Eadie M, Murphy A, Iacarella JC, Ban NC. 2023. Why, and where, is commercial fishing gear lost? A global review and case study of Pacific Canada. Marine Pollution Bulletin, 196. https://doi.org/10.1016/j.marpolbul.2023.115528.

Richardson K, Gunn R, Wilcox C, Hardesty BD. 2018. Understanding causes of gear loss provides a sound basis for fisheries management. Marine Policy, 96, 278–284. https://doi.org/10.1016/j.marpol.2018.02.021.

Richardson K, Hardesty BD, Vince JZ, Wilcox C. 2021. Global Causes, Drivers, and Prevention Measures for Lost Fishing Gear. Frontiers in Marine Science, 8. https://doi.org/10.3389/fmars.2021.690447.

4. Hydrographic sea-model of seabed disturbance and dispersal (Task 2.3)

Asbjørn Christensen, Henrik Mosegaard

4.1 Introduction and aim

The overall aim of this task is to assess the relation between oceanographic conditions, biodiversity and ecosystem functioning as a basis for quantifying the impacts of beam trawls and other mobile bottom-contacting gears. Since observations are only scattered (or related to the sea surface), the work will be based on an extensive data set of oceanographic conditions generated by a state-of-art operational, coupled circulation and biogeochemical model covering the study area. The data set, including a suite of hydrographic variables, such as current, temperature, light conditions, seabed shear stress and plankton, will be coupled to an agent-based modelling framework and will be used to simulate the dispersal of fish eggs and larvae as well as habitat-forming invertebrates in the Jammer Bay. This will enable us to simulate the local recruitment potential of plaice and the dispersal potential of invertebrate larvae with different biological traits. The analysis will include the effect of fishing pressure (using data established in Task 2.1) on plaice larval nurseries to assess the potential recruitment impact.

Plaice is a benthic flatfish species that in the North Sea performs migrations to time invariant spawning areas where they spawn during winter and early spring at locations influenced to some degree by environmental factors like temperature and salinity (Höffle et al. 2018). The pelagic eggs and larvae drift with ocean currents from the spawning grounds towards nursery areas along the coasts (Hufnagl et al. 2013). Early larvae are passive drifters but with increasing size they improve their swimming capacity (Silva et al. 2015). In the late larval stage (12-15 mm), buoyancy as well as asymmetry increases, and the metamorphosing plaice spends most of its time near the bottom where habitat selection may depend on depth, food availability and/or lack of predators (Wennhage and Gibson 1998). Metamorphosis imposes large demands on the metabolism of the larval stage, affecting mobility and perhaps vision and thus reactive distance although eyes are fully migrated at settling (Geffen et al. 2007). Judged from their vulnerability to *Crangon crangon* (L., 1758) predators the metamorphosed juvenile plaice may have achieved full escape capacity at the size of 25 mm (Taylor 2003), with a potential flight response of up to 20 x body lengths s^{-1} (Williams and Brown 1992). The vulnerability of the metamorphosing benthic larvae from 12 mm up to a juvenile size of 25 mm is therefore the focus in the present modelling study of recruitment impact on plaice by fishing bottom-contacting gear.

4.2 Materials and methods

4.2.1 Hydrographic data set

A hydrographic database of physical and biogeochemical variables was established by Danish Meteorological Institute (DMI), which is the regionally leading hydrographic institution and member of the Baltic Monitoring Forecasting Centre (BAL MFC) providing data to the EU Marine Copernicus service CMEMS. The data is generated by DMI rerunning the NEMO4-ERGOM model in operational setup for 2014-2022 with a high spatial resolution of 1 nm for the Skagerrak, North Sea, Kattegat, and western Baltic Sea, and up to 56 vertical layers, so that the variable

hydrodynamics in the transition zone are well described and mesoscale structures in the hydro-dynamics are well represented. The purpose of the rerun was to store extra data from the oceanographic reanalysis that is not stored in standard runs, data which is needed in JAMBAY. The temporal resolution in the database will be 1 hour for physical variables, so that direct and indirect tidal effects can be addressed. The database covers the entire water column for physical and biogeochemical variables. The biogeochemical variables are based on the latest calibration of the ERGOM model coupled to the NEMO4 model and include nutrients, oxygen concentration, Chl.a, phytoplankton groups, as well as micro- and mesozooplankton. Biogeochemical variables are stored as daily averages in the database. The physical variables from the NEMO4 model include current, salinity, temperature, water level, vertical and horizontal turbulence, and bottom shear stress.
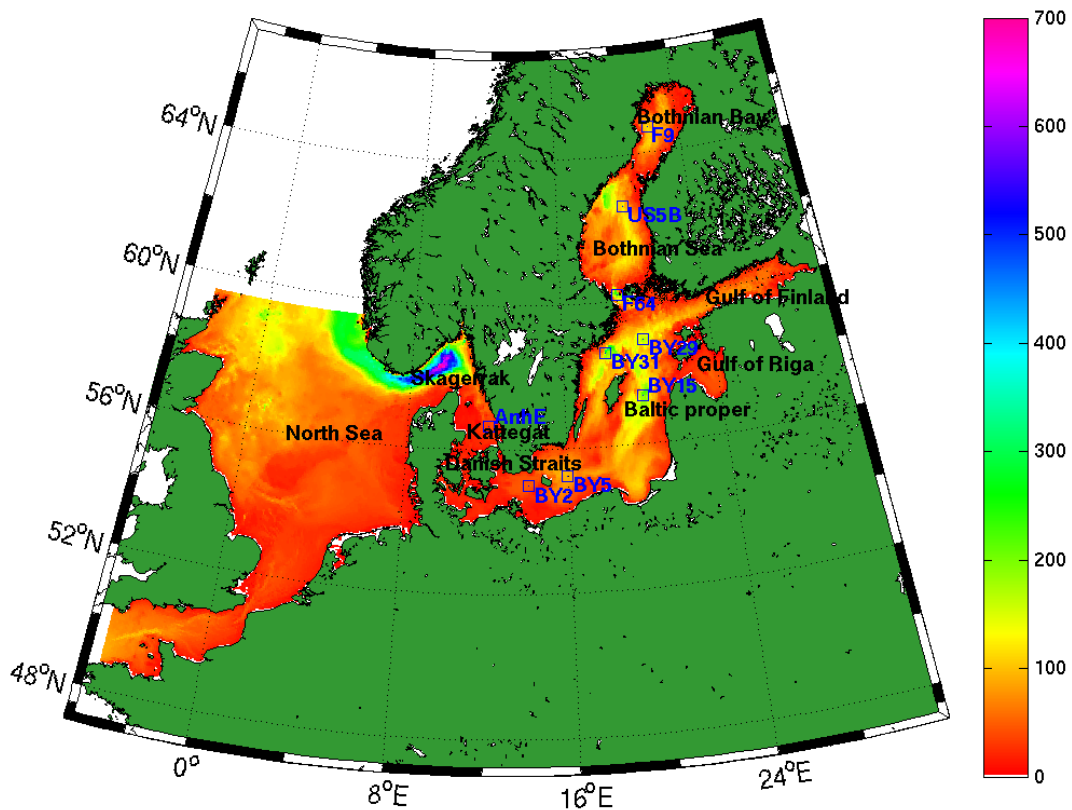
Figure 4.1. The native model domain for the NEMO4-ERGOM system covers the North Sea and Baltic Sea with open boundaries at Scotland-Norway and the English Channel (colors represent m water depth).

The model domain is shown in Fig. 4.1. The model system consists of four building blocks:

1. The 3D ocean-ice model NEMO (Nucleus for European Modelling of the Ocean), which is an open community ocean model (https://nemo-ocean.eu). In the BAL MFC model system, the NEMO version 4.0 is used in combination with the sea ice and thermodynamic model SI3. Our NEMO configuration and setup is adapted for the Baltic Sea.

2. The biogeochemical model ERGOM (Ecological Regional Ocean Model, https://ergom.net/), which is developed at IOW (Germany) to model biogeochemical cycles in the Baltic Sea. The version used in the BAL MFC model system is based on Neumann et

al. (2015). The model describes the basic nutrient and carbon cycles through 15 pelagic state variables. The sediment is not vertically resolved and consists of two organic nutrient components.

3. The wave model WAM, an open-source model developed at Hereon, Germany (https://github.com/mywave/WAM). The WAM version used in the BAL MFC model system is based on WAM version 4.6.2 and has been adapted to the Baltic Sea. The model uses 36 spectral directions and 35 different frequencies between 0.04 and 1.07 Hz.

4. The data assimilation system PDAF (Parallel Data Assimilation Framework https://pdaf.awi.de/), used with the LESTKF filter.

The NEMO and ERGOM models are run one-way and online coupled and use the PDAF system to assimilate observations into the analysis field in NEMO. The WAM model runs independently from the NEMO-ERGOM-PDAF system. Both model systems run with the same bathymetry grid based on GEBCO v2013 data (https://www.gebco.net). Both model systems are forced with the same best available atmospheric forcing dataset. Further technical details about the NEMO-ERGOM setup can be found in NEMO4-ERGOM (2023).

The hydrographic database generated by DMI was stored in NetCDF format at a Synology NAS server with 384 TB capacity, acquired for the work in JAMBAY.

4.2.2   Individual-based simulations

The connectivity investigations in the present work are based on individual-based simulations. In essence, a representative set of organisms is simulated for a period of their life cycle including available knowledge on vital biological processes. Thereby the population level dynamics can be assessed. The work is based on an existing setup of an agent-based framework (IBMlib) developed at DTU Aqua for simulating dispersal of early life stages (Christensen et al. 2018). IBMlib is designed and programmed according to modern object-oriented principles. This implies that IBMlib is not only able to represent one object type in a specific region with a specific hydrographic data set but can easily be extended to address new object types, new mechanisms coupled to new hydrographic data set. In this way IBMlib has been developed from scratch by DTU Aqua over the last 10 years with roots in biological problems, proving its worth in very diverse projects, e.g., simulating dispersal of sandeel larvae (Christensen et al. 2013), plaice larvae (Ulrich et al. 2016) and propagation risk of invasive species (Hansen and Christensen 2018), plastic pollution dispersal (Christensen et al. 2023) and across-species assessment of connectivity in the entire Atlantic ocean (Pereira Gabellini et al. 2023). IBMlib is being distributed as open source, so that everybody freely can apply, develop, or verify the code. The IBMlib design principle is shown in Fig. 4.2. The core idea is that object dynamics (e.g., biology), hydrography and scientific task are kept strictly separate according to a well-defined protocol; thereby each part can be replaced by alternatives, without having to change the rest, and each part can be developed independently from the rest. Therefore, the same setup can be applied in the present context for plaice and invertebrates, by just exchanging the biological modules and input data, as outlined in Fig. 4.2. Any hydrographic data set can be attached to IBMlib, with little effort; for the North Sea-Baltic region DTU Aqua often uses state-of-art hydrography and biogeochemistry from DMIs operational model HBM. IBMlib comes along with a database of interfaces to different hydrographic data sets, including COARDS compliant data, which encompasses e.g., CMEMS data sets.

In addition to advection by currents averaged at a 1 nm scale and possibly vertical/horizontal swimming, propagules simulated in the present work are subject to vertical/horizontal turbulence calculated from first principles in the NEMO4 setup. The effect of these sub scale eddies is represented as an overlaid vertical/horizontal random walk process with intensity set so exact subscale dispersion is reproduced without artificial particle aggregation, as outlined in Visser (1997).
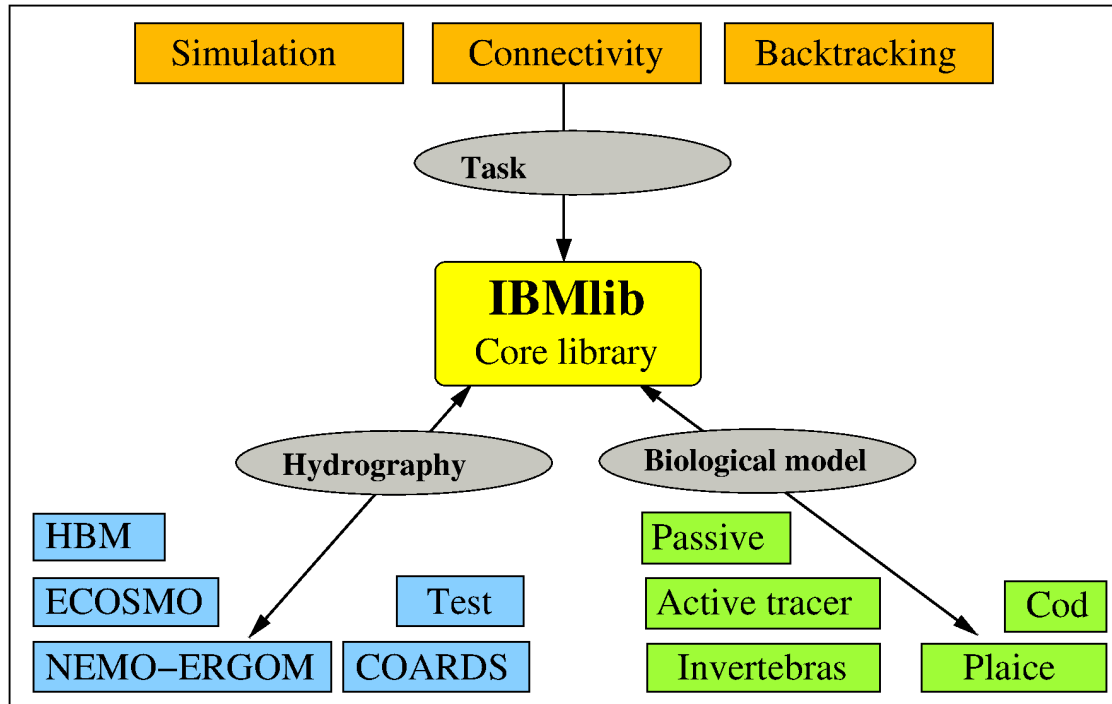
Figure 4.2. Modular design principle of IBMlib with biology, hydrography and scientific task are kept strictly separate according to a well-defined protocol.

In the present project the API (application programming interface) to the hydrographic database format provided by DMI was constructed based on existing templates. Additionally, a Python API to the dataset were constructed based on previous code to facilitate data extractions used in other WPs in JAMBAY.

Ecological connectivity is used in many different senses across ecology; we apply a tangible definition where it is the transport/migration probability between habitats. For sessile species with an early pelagic stage and fish eggs and larvae, this connectivity is mainly determined by hydrology. A connectivity simulation starts by providing a set of spawning (starting) habitats and a set of settlement (target) habitats – these sets may be coincident, depending on the biology. Then propagule is released from spawning habitats and allowed to move freely according to biological processes and prevailing water currents. At the end of the simulation, the abundance in each settlement habitat is counted. Thus, the basic output is the so-called connectivity matrix C_{ij} being the probability of being transported to habitat i, given spawning in habitat j. C is naturally bounded as $0 < C < 1$ and not a priori symmetrical. C_{ij} is in first order proportional to the area of habitat i but not j. Summing C_{ij} over i gives the survival (settling success) of propagule starting from j, whereas summing C_{ij} over j gives a receptiveness of habitat i, which is proportional to the

likelihood of settling in i, if spawning is equally distributed. The former is bound to [0,1], whereas the latter has no upper bound. A band around the diagonal C_{ii} gives the retention of habitat i.

4.2.3 Connectivity of plaice in the Jammer Bay

The IBMlib setup of for simulating plaice larvae (Ulrich et al. 2016) in relation to the EFF-funded project *MSC certification of plaice fisheries in area IIIa – basic investigations and development of a management plan* was revisited and updated with the latest biological knowledge. Maps of potential settlement areas and spawning areas were updated corresponding to the new available hydrographic database described above, in particular the improved resolution of the coastline in the study area.

Growth model

Based on the work of Bolle et al. (2000) and Hufnagl et al. (2013) a degree-day model is applied for each of the three early life stages represented explicitly in the model for plaice: egg, pelagic and demersal post-larvae. The progression of s_i at temperature T in each ontogenetic stage *i*, represented as a number between *i-1* and *i*, is simulated as the temperature divided by the stage-completion parameter in Table 1 below. The progression is described by the rate equation

$$\frac{ds_i}{dt} = \frac{T}{P_i(T)} \tag{1}$$

where i=1(egg), 2(pelagic larvae) and 3(demersal post-larvae), and $P_i(T)$ is given in Table 4.1. From this the timing of settling can be resolved. In connectivity calculations, we solve Eq. 1 for an ensemble of larvae using the actual ambient water temperature at the larvae.

Behavioural and mortality model

In addition to passive drift, propagule in all stages is subject to vertical and horizontal turbulence calculated from first principles in the NEMO4 circulation model.

Table 4.1. Stage-specific plaice mortalities from Wennhage (1999). Following Hufnagl et al. (2013) we assume demersal larvae died, if not settled at the end of the larval period. For stage-completion dynamics, each stage is completed when the time integral of the experienced temperature exceeds the limit P_i.

Stage	Horizontal	Vertical	Mortality (1/year)	Stage-completion P_i (T) [deg Celcius * days]
Egg	Passive	The literature indicates that plaice eggs have positive buoyancy, but there is no consensus on egg density; Coombs 1990 finds egg density ρ =1.02552 g cm^{-3} for the North Sea, while Petereit 2014 finds ρ =1.0136 g cm^{-3} for the Baltic. We follow Petitgas (2006) by applying Stokes terminal velocity for an egg with radius 1 mm and constant density ρ =1.020 g cm^{-3}	33.4	exp(3.95 - 0.15 T)
Pelagic larval	Passive	Passive	16.5	exp(5.00 - 0.15 T)
Demersal larval	Passive; settles if conditions are OK	Seeks toward the seabed with average velocity 4 mm s^{-1} Hufhagl (2013); Ryland (1963).	5.86	exp(3.40 - 0.15 T)

Spatial spawning time and distribution

Nielsen et al. (2004) indicates "late February and early March" for the Kattegat; Hufnagl et al. (2013) samples a longer spawning period, 15/12-15/3. We use March 1th as the centre time. In this work, we focus on plaice larvae spawned or settling in the study area. Therefore, spawning in Kattegat south-west of Skagen is not included, because previous work indicated little exchange across Skagen. We include the spawning areas indicated in Cardinale et al. (2011, their fig 2) in the Jammer Bay. In order to be able to assess the relationship between endogenous/exogenous larvae in the Skagerrak, the Dogger and German Bight areas are included, because these are advected northward by the prevailing counterclockwise circulation in the North Sea. For the spawning areas in the Skagerrak and Kattegat, the observation that the spawning areas are located in 10-40 m of water is also superimposed. Numerically, the spawning areas are generated by taking 1 x 1 nm grid cells from the hydrodynamic model into account if they lie in the areas mentioned above (the Jammer Bay, Dogger Bank and German Bight). Each cell is then scanned for water depths, and if 50% of the cell has a depth in the range 10-40 m, it is included as a spawning ground. The resulting spawning grounds are shown below in Fig. 4.3a.

Conditions for settling/requirements for nursery

There is no clear demarcation of requirements for suitability of bottom settlement habitat; Ulrich et al. (2013) states "0-3 m substratum", Nielsen et al. (2004) states "shallow water, sand/silt"; Hufnagl et al. (2013) uses 0-20 m without substrate requirements. We interpret "sand/silt" as bottom type 1, 2, 3 on GEUS' sediment map (i.e., mud, sandy mud, sand, locally with gravel and stones). In this work, numerically, settling habitats are generated in the following way: from all 1 x 1 nm grid cells that make up the numerical grid for the hydrographic model, all cells that make

up the coast are taken (Fig 4.2). Each coastal cell is now scanned for its suitability as a settling habitat to point-by-point check about depth requirements (0-10 m see Fig. 4.17) and sediment requirements (soft bottom type, GEUS type 1,2,3) is fulfilled. This is done by embedding a sub sampling grid in each coastal cell, and then using a high-resolution topography model (IOWtopo2, rev.03, https://www.io-warnemuende.de/topography-of-the-baltic-sea.html) as well as a high-resolution sediment model (GEUS 1999) to determine the area fraction of each coastal cell that is suitable for plaice fry settlement; then each coastal cell is shrunk towards the coast, corresponding to the area fraction that is suitable for recruitment, so that the coastal area that is suitable for recruitment is correct and distributed correctly within a scale of 1 nm. Thus, sub scale (<< 1 nm) effects are represented in the current model. Since even the high-resolution sediment and topography models have a finite resolution (and accuracy) and Wennhage's (1999) alleged northern micro habitats are not visible in the high-resolution models, a lower limit for the width of the coastal cells perpendicular to the coast is assumed, so far 50 m. You can thus recruit for all coastal stretches within 50 m - 1 nm from the coast (depending on bottom conditions). Fig. 4.3b shows the coastal cells, where size perpendicular to coast has been reduced proportionally reflecting the habitat quality locally as settlement ground, as described above. In simulations, settling is assumed to occur at the first instance when the propagule in a stage ready for settling enters a settling habitat in its settlement period as defined above.
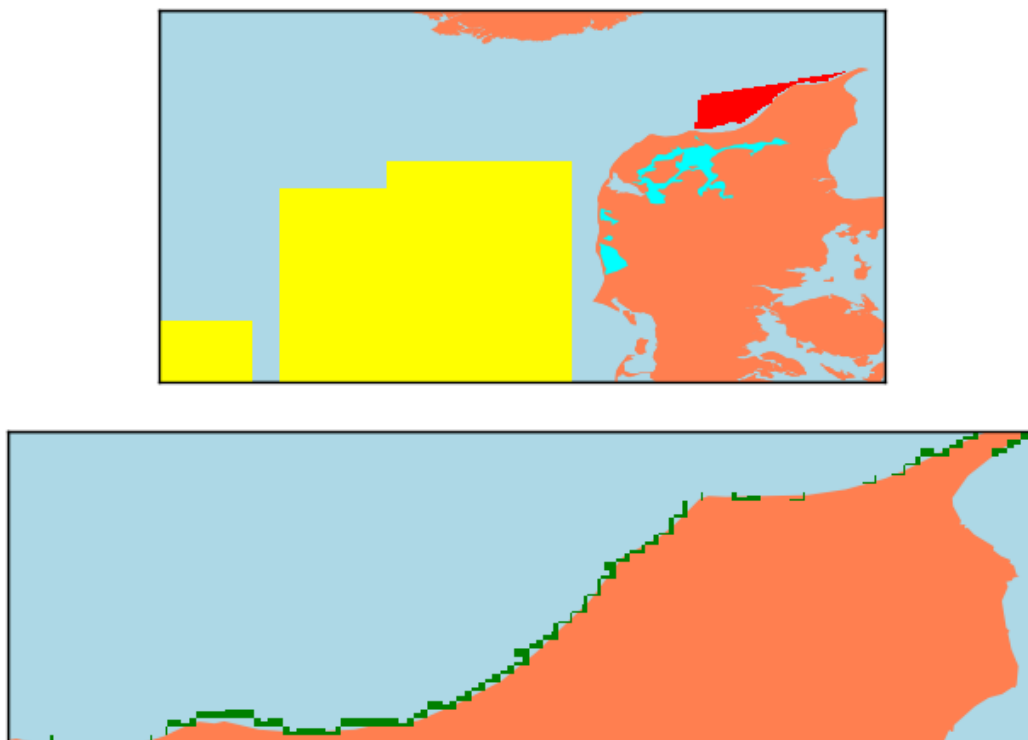
Figure 4.3a&b. Spawning and settlement areas for plaice. Upper figure (a) shows spawning areas. The Jammer Bay region spawning areas are indicated by red, whereas remote spawning grounds potentially contributing to the Jammer Bay recruitment are indicated by yellow. Lower figure (b) shows coastal cells (green) scaled perpendicular to the coast according to habitat suitability. The raggedness of the coastline reflects the 1 nm rasterization applied in the underlying hydrodynamic model. For the distribution of potential nursery habitats at <10 m, see Fig. 4.17.

4.2.4 Connectivity of habitat-forming invertebrate in the Jammer Bay

The local dispersal potential and connectivity will be assessed for habitat-forming invertebrate in the Jammer Bay, including the effect of egg and/or larvae release south of the Jammer Bay advected northward by the prevailing Jutland current. We consider the representative subset of ecologically interesting invertebrates listed in Table 4.2. The table lists the habitat requirement (in the classification of Vasquez M et al. (2021)) of each species along with the estimated pelagic period. As for plaice, propagule not settled by the end of the settling period are assumed lost to recruitment in the Jammer Bay. Propagules are released at the seabed, and considered to drift passively in the pelagic period, subject to vertical/horizontal turbulence in the water column.

Table 4.2. Habitat requirements of considered habitat-forming invertebrates. The last column is the pelagic period in hours(h), days(d) or weeks(w). The two values indicate considered start and end of settling period.

	Infralittoral mud	Circalittoral mud	Offshore circalittoral mud	Infralittoral sand	Circalittoral sand	Offshore circalittoral sand	Infralittoral coarse sediment	Circalittoral coarse sediment	Offshore circalittoral coarse sediment	Infralittoral mixed sediment	Circalittoral mixed sediment	Offshore circalittoral mixed sediment	Infralittoral rock and biogenic reef	Circalittoral rock and biogenic reef	Offshore circalittoral rock and biogenic reef	Upper bathyal sediment	Pelagic period
Alcyonium digitatum										x	x	x	x	x	x		24h;36h
Pennatula phosphorea (and *Virgularia mirabilis*)		x	x													x	24h;36h
Ostrea edulis										x	x		x	x			14d;21d
Modiolus modiolus							x	x	x	x	x	x	x	x	x		3w;7w
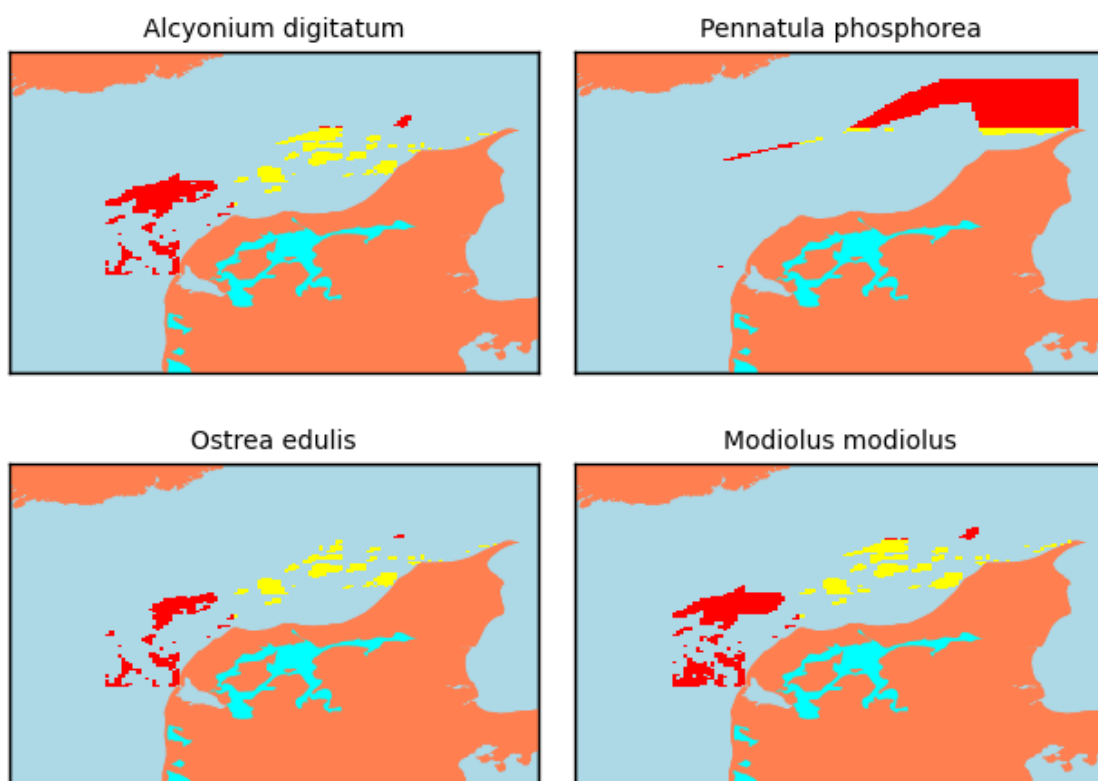
Figure 4.4. Suitable habitats for each invertebrate species in the Jammer Bay region, according to habitat requirements indicated in Table 4.2. Habitats in the study area are yellow, whereas additional included seeding habitats providing propagule to the study areas are indicated by red.

4.2.5 Potential impact of demersal bottom gear fishing on plaice recruitment

Assessment of the potential impact of demersal trawling and anchor/Danish seine fishing on plaice recruitment is associated with high uncertainty for several reasons:

- Even though the connectivity from given spawning sites to given nursery grounds can be assessed with some confidence level as driven by local, dynamic ocean currents, the spawning site loading (actual spawning per area) is unknown and addressing this requires a detailed spatial life cycle population model parameterized by observed egg distributions.
- The impact per fishing effort and gear type on newly settled plaice larva is poorly confined, and likely a complex, nonlinear function. Further the spatial and temporal development of a specific fishery is influenced by local target stock abundance and overall quotas.
- Increased mortality on newly settled plaice may be compensated by a negative self-regulation by population density-effects at this stage or later in the life cycle; therefore a net impact analysis requires better understanding and quantification of self-regulation in plaice stocks.

Therefore, first steps toward quantifying the potential impact envelope, taking uncertainties into account, map fishing effort distribution and variability together with early-stage nursery grounds,

weighted with their relative importance as quantified by connectivity metrics by settling location, and aligning this with the timing of the egg and larval development.

At low to moderate intensity of employing bottom contact gear, the impact (at a given larval and post-larval stage) is expected to be proportional to the swept bottom area with a gear specific scaling factor. This directly corresponds to a stage dependent mortality rate

$$\mu_i(x,t) = \sigma_i SAR(x,t) \tag{2}$$

where SAR(x,t) is the swept area ratio (i.e., trawled area per unit area per week) at position x and time t, and σ_i the stage-dependent and gear specific sensitivity. SAR(x,t) is mapped and discussed under Task 2.1, where data sampled on a weekly basis in the period 2015-2022, and averaged on a regular longitude-latitude mesh with 0.01 degree resolution in the Jammer Bay, corresponding to on average 850 m resolution, is presented. Fig. 4.5 shows a histogram of the data set containing 856062 data points. The data range is [0; 1.24], so that the seabed in a fraction of habitats is actually swept more than once per week.
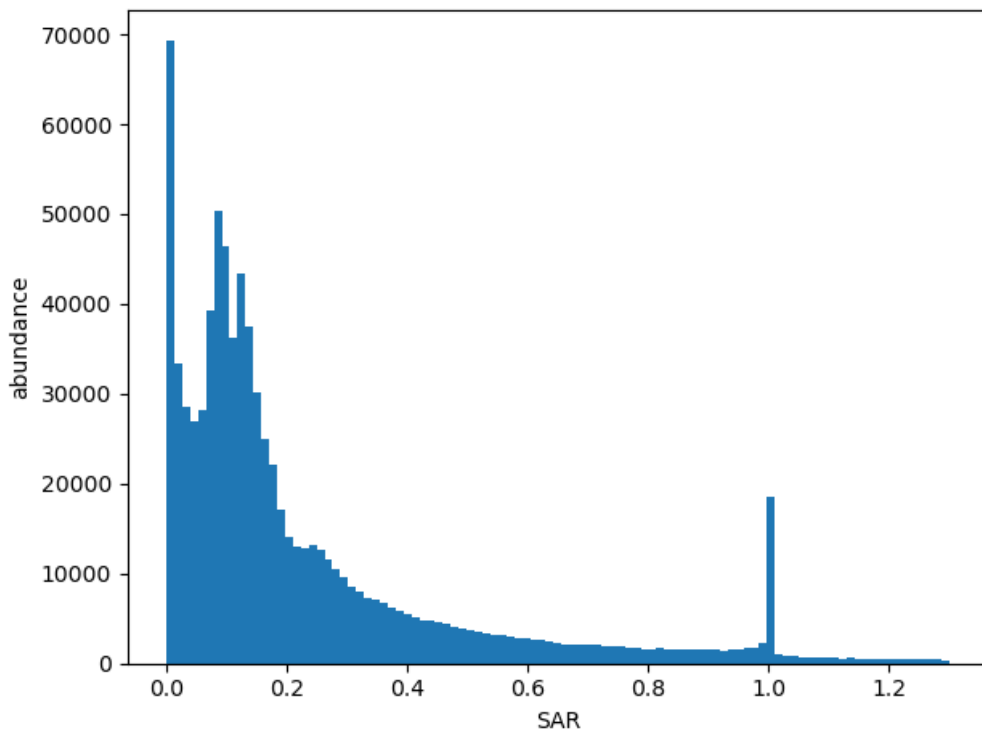
Figure 4.5. Histogram of SAR(x,t) in (swept area ratio, unit per week), sampled on a weekly basis in the period 2015-2022, and averaged on a regular long-lat mesh with 0.01 degree resolution in the Jammer Bay, corresponding to an approximately 0.60 km x 1.11 km resolution for the full study area. This area was subsampled for analysis of overlap with nursery areas.

We define a habitat disturbance rate index (which is a mortality proxy) called the nursery disturbance index (NUDI) like

$$NUDI(t) = \frac{1}{A_N} \int_{A_N} SAR(x,t)dA \qquad (3)$$

where A_N is the area of the set of nurseries in the Jammer Bay, shown in Fig. 4.2.3b. Technically we compute the integral for each time t (weekly resolution) by interpolating SAR(x,t) on a sub grid in each habitat bounding box, and summing over the sub grid. The sub grid is chosen regular, coherent with the habitat bounding box and zonal/meridional spacings as equal as possible. It is found that a sub grid resolution of 200 m is sufficient to ensure numerical convergence, and this is reasonable since the underlying SAR resolution is 850 m, whereas the hydrodynamic grid resolution is 1.8 km.

4.3   Results

4.3.1   Connectivity of plaice in the Jammer Bay
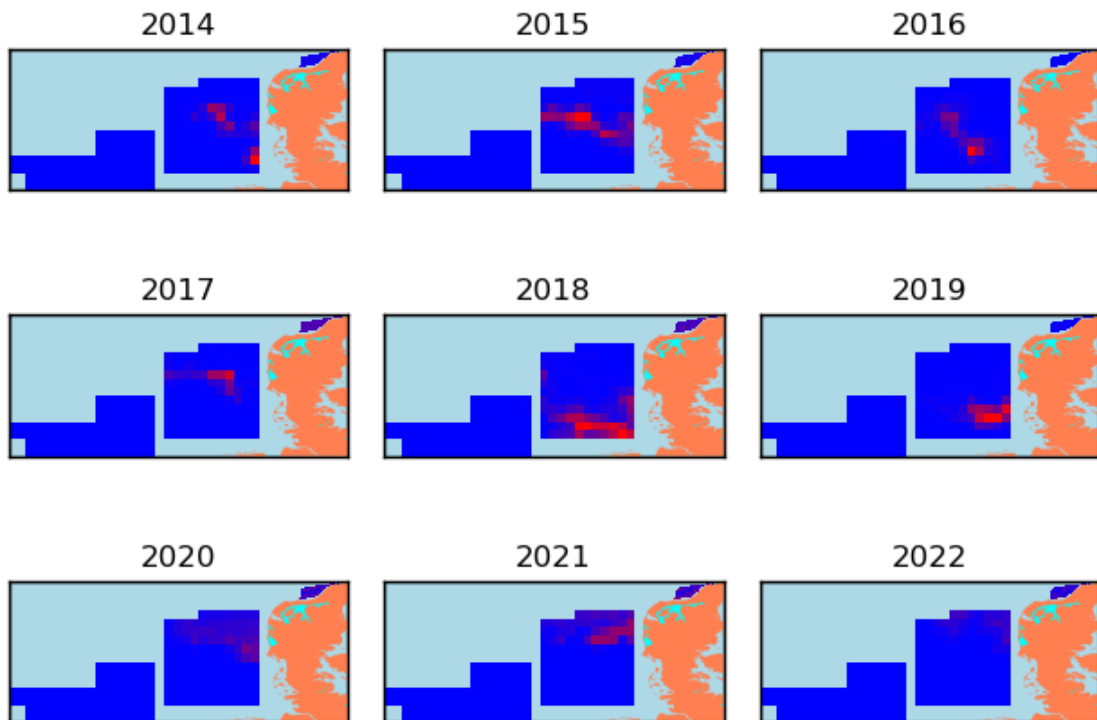
Figure 4.6. Spatial contrasts in annual relative survival chance of plaice recruits to the Jammer Bay, coloured by spawning ground. Colour scale is individual for years, so highest recruitment chance is coloured red each year, while low survival chance is toward blue.

Fig. 4.6 shows the spatial contrasts in the relative survival chance of plaice recruits to the Jammer Bay by year for the period 2014-2022, and coloured by spawning grounds in the North Sea at Dogger Bank and in the German Bight (Hufnagl et al. 2013). The average absolute recruiting chance to the Jammer Bay of plaice eggs is of order 0.25-0.5 10^{-4}, when stage-specific mortalities are applied according to the literature, as summarized in Table 4.1. The total pelagic phase

of plaice eggs and larvae is in the order of 80 days. Because the typical ocean circulation pattern in the North Sea is counter-clockwise, water masses arriving in the Jammer Bay area can be traced back to the more southerly located spawning areas in the North Sea 80 days prior. Therefore, eggs spawned in these areas are more likely to arrive to the Jammer Bay region, by a hydrographic, stage dependent match-mismatch mechanism. We see a large year-to-year variation in the location of most-favourable spawning site. We also see a slight tendency in most recent years for a Northward displacement of the optimal spawning site in the extended Southern and Central spawning areas. The displacement could be interpreted as a consequence of ocean warming, since growth is enhanced, and the duration of each early life stage is decreased by 13 % for each degree water temperature increases (Table 4.1). However, correlation with actual sea surface temperatures during egg and larval development is low within and to the north of the German Bight during the study period, and therefore explanations must be sought in regional variation in hydrographical conditions. However, with increasing sea temperatures the average optimal spawning location is likely to move closer to the Jammer Bay because the pelagic period and corresponding transport distances are shortened.
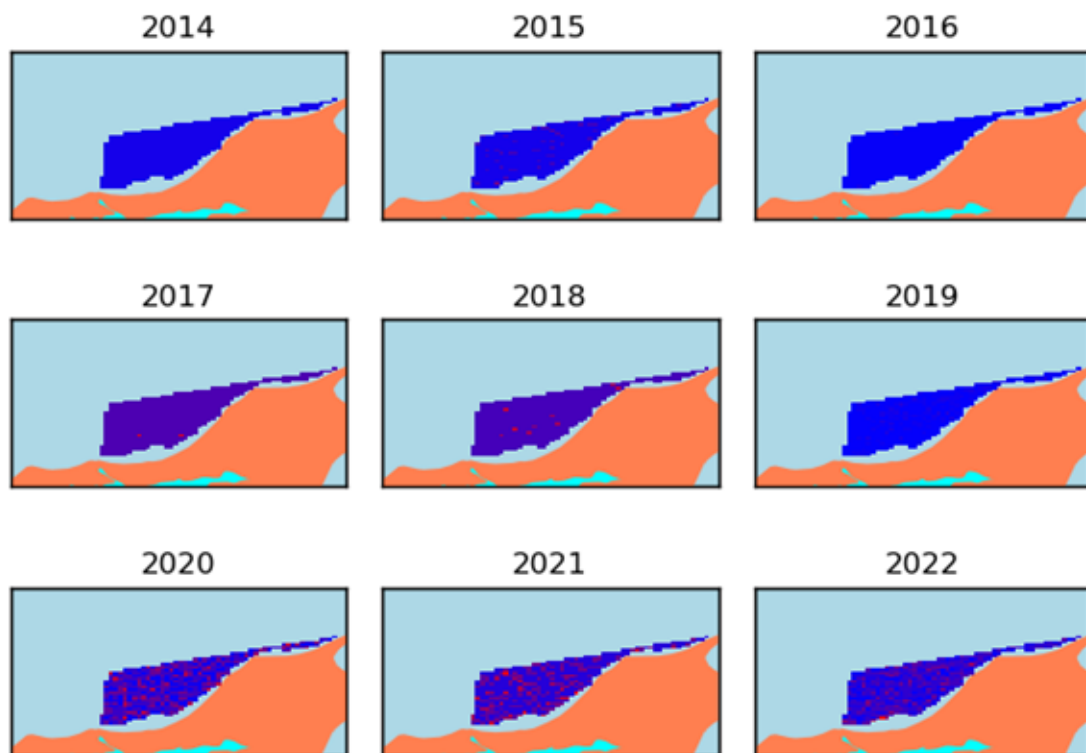
Figure 4.7. Relative survival potential by year to the Jammer Bay of plaice recruits, coloured by spawning ground. Same as Fig. 4.6 but zoomed into the Jammer Bay.

There is also a small retention of spawning in the Jammer Bay spawning, as displayed in Fig. 4.7. The retention is strongly dependent on local mixing processes, mesoscale eddies or other anomalies in the circulation pattern retaining larvae in the area. We also see that the retention contribution has a strong year-to-year variation, but especially in the last years retention has increased, which is consistent with the hypothesis of an ocean-warming effect. Interestingly, the retention does not spatially have a hot spot appearance (as Fig. 4.6), but is more dispersed over the Jammer Bay, in years with good retention.

Fig. 4.8 displays the overall transport chance for North Sea plaice offspring to settle in the Jammer Bay, i.e., statistics over space.
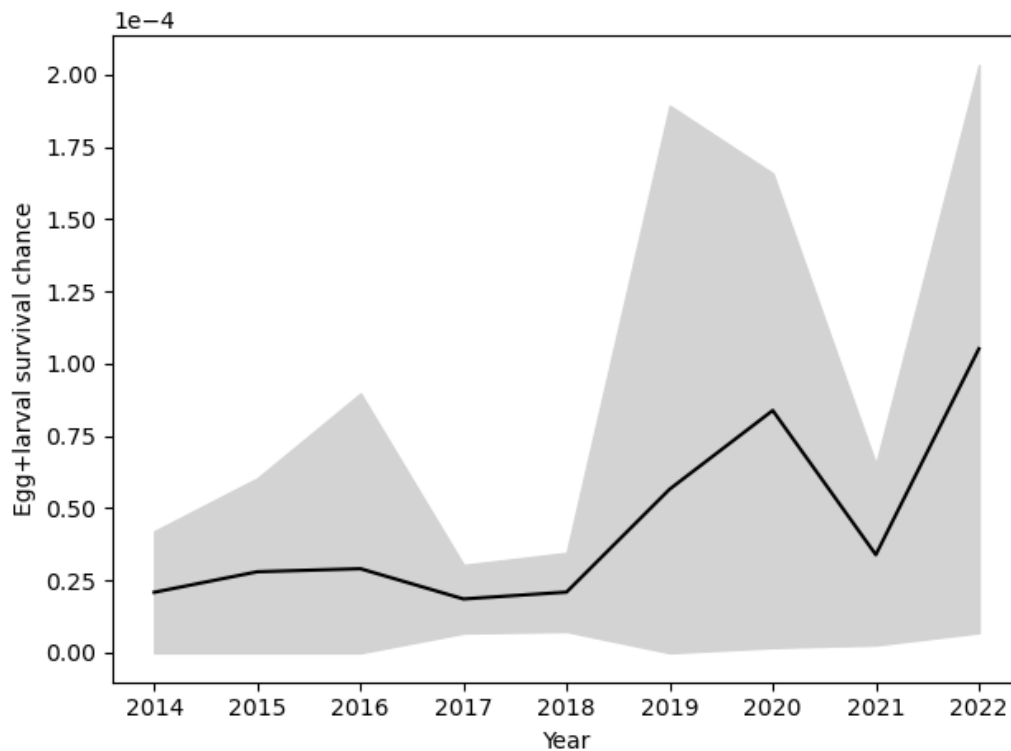
Figure 4.8. Average transport probability to the Jammer Bay of local and remotely spawned offspring. The grey zone indicates +/- 1 standard deviation, when statistics is over all spawning grounds, each year.

The overall level is relatively low, in the order of $0.25-0.5 \cdot 10^{-4}$. Of this, the impact of ecosystem processes (e.g., predation, starvation, sunlight degradation of eggs) accounts for of order $\exp(-\Sigma_i Z_i T_i) \sim 0.01$ using values in Table 4.1, where Z_i and T_i are corresponding stage mortality and completion times. In other words, physical transport processes (match-mismatch) and ecosystem processes impose similar reduction levels and sculpturing on the potential local recruitment. The grey zone (standard variation in Fig. 4.8) elucidates a significant spatial variation, where the upper limit corresponds to the hot spots in Figure 4.6. We also note a statistically significant year trend, in the direction of increased survival. This may potentially be a positive effect of ocean warming, since duration of pelagic stages decreases by 13 % per degree warming, and therefore less time is spent in high-mortality early life stages. In addition to this, temperature itself may change the levels of predation mortality, however, this is not addressed in this context, but similar overall size scaling of mortality is expected. This shows that ecosystem connectivity may change even if ocean currents are unaffected because time scales are changed by ocean warming. For small temperature changes ΔT the ecosystem survival chance increases as $S \sim S_0^{1-0.15\,\Delta T}$, so that low prior survival S_0 benefit most.

Fig. 4.9 shows the variation in receptiveness between two contrasting years (2020 and 2021) for the Jammer Bay nurseries. The two upper plots indicate western parts of the Jammer Bay

may be more receptive to settlement, from a connectivity perspective. The lower figure displays the year-to-year variability in local receptiveness, i.e., part of the local recruitment being driven by local spawning, if all spawning sites were used with equal intensity. This shows a significant small local component, fluctuating around 20 %.
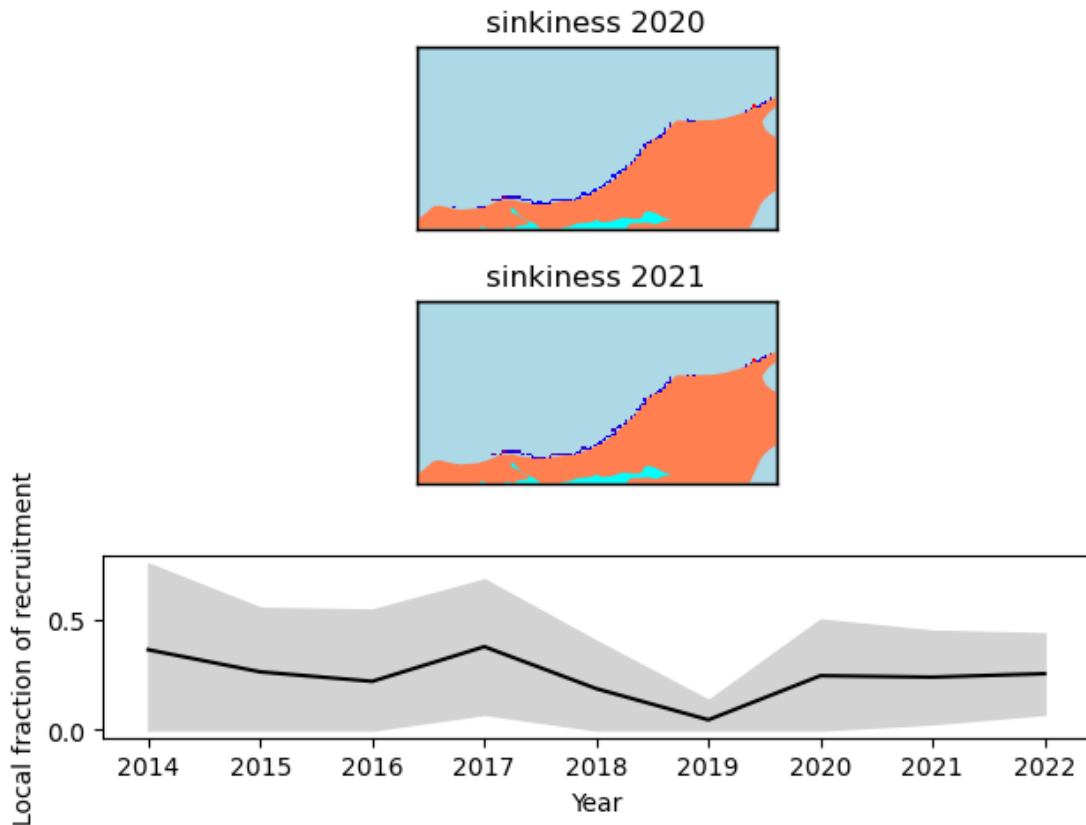
Figure 4.9. Upper two figures receptiveness for the Jammer Bay nurseries for 2020 and 2021, assuming equal per area spawning intensity at known spawning grounds. Lower figure is the average receptiveness over years, and the grey zone is +/- 1 standard deviation, when statistics is over all spawning grounds, each year.

4.3.2 Connectivity of habitat-forming invertebrates in the Jammer Bay

Fig. 4.10 shows the average transport probability (over 2014-2022) within the habitat network of each invertebrate species considered in this study. For the species with short pelagic duration [soft octocorals of the families Alcyoniidae, e.g., *Alcyonium digitatum* L., 1758 (trivial names in English and Danish: dead man's finger, dødningehånd) coupled to hard substrates, and Pennatulacea, e.g., *Pennatula phosphorea* L. 1758 (phosphorescent sea pen, søfjer) and *Virgularia mirabilis* (Müller, 1776) (slender sea pen, søstrå) on soft bottoms], the inner habitats are most important; spawning at the edges of the Jammer Bay are less likely to recruit in the Jammer Bay, but if a larger study area was considered, it would emerge that spawning at the edges of the Jammer Bay recruit elsewhere. For bivalve species with a longer pelagic duration, such as *Ostrea edulis* L., 1758 (European flat oyster, fladøster) and *Modiolus modiolus* (L. 1758) (northern horse mussel, hestemusling), we again see that southern spawning habitats are more likely to

contribute to northern recruitment habitats, due to the prevailing overall counter-clockwise circulation in the North Sea.
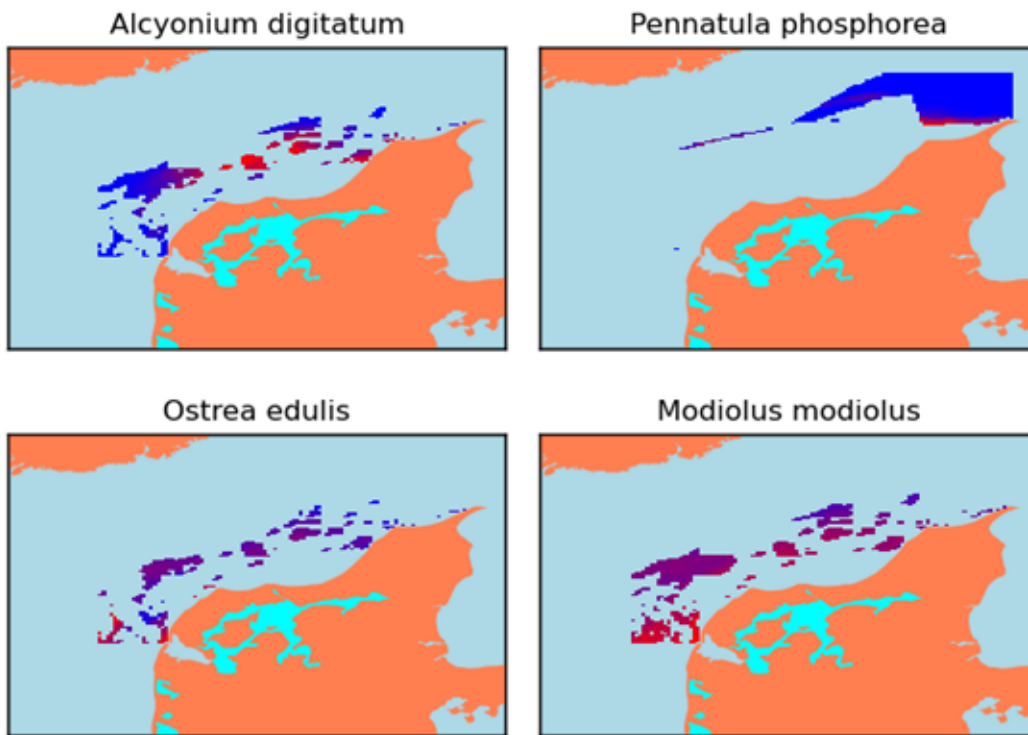
Figure 4.10. Average (over 2014-2022) of transport probability within the habitat network of each invertebrate species.

Fig. 4.11 shows year-to-year variation in average survival chance for habitats in the Jammer Bay, i.e., averaged over habitats, each year. Short pelagic duration species (*Alcyoniidae* and *Pennatulacea*) display fluctuations around an average level, whereas the long pelagic duration species appear to have an increasing time trend, in addition to strong interannual fluctuations. Since pelagic durations for these species are not temperature-corrected, this may point to a weaker qualitative change in local circulation patterns that needs to be investigated further. There appears to be no obvious covariation trend in time between these representative invertebrates.
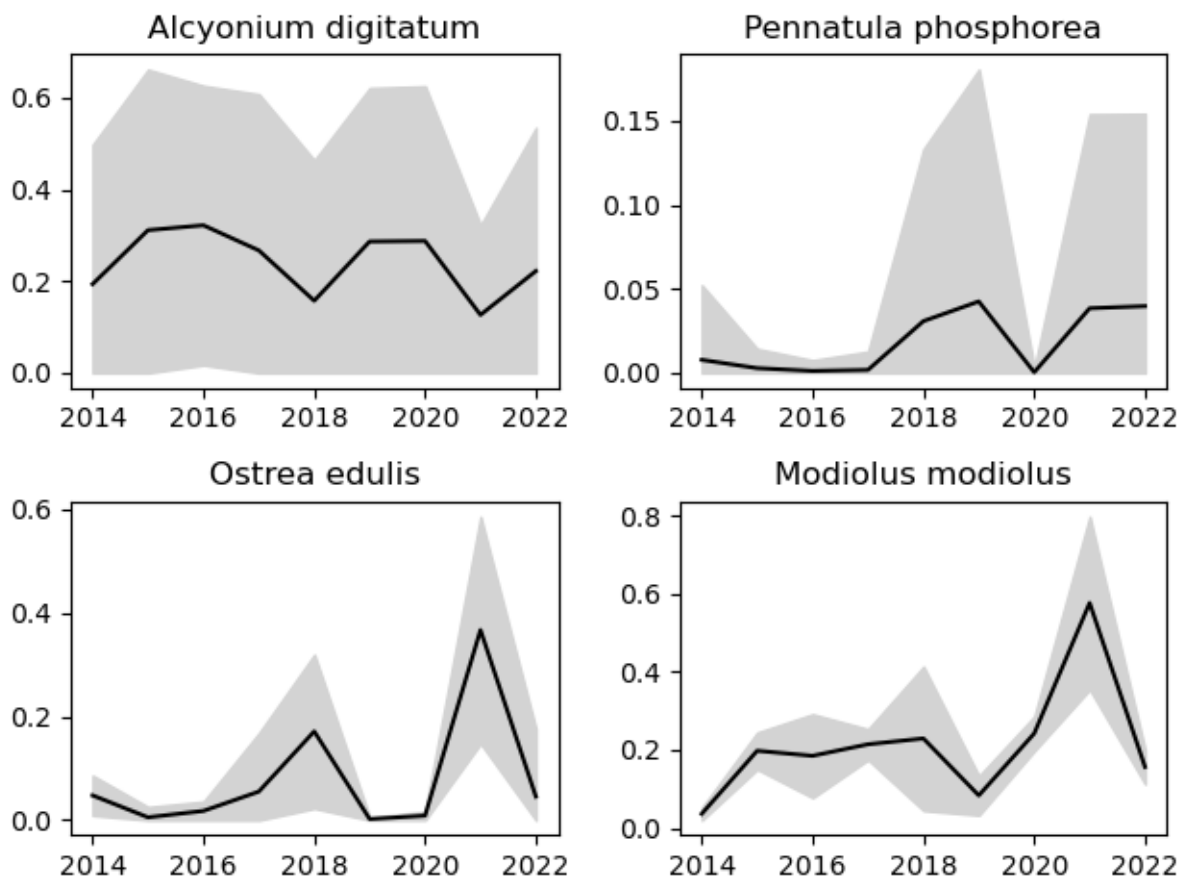
Figure 4.11. Average transport success (over each habitat) between different years. The grey zone indicates +/- 1 standard deviation, when statistics is over habitats, each year.

Fig. 4.12 shows the average (over 2014-2022) receptiveness within the habitat network of each invertebrate species. Somewhat surprisingly it indicates higher receptiveness for edge habitats in the network, especially for species with long pelagic period. This may be a door-step effect because a larger region of donor sites was considered for the Jammer Bay region. Thus, this figure indicates the range of local recruitment for these invertebrates.
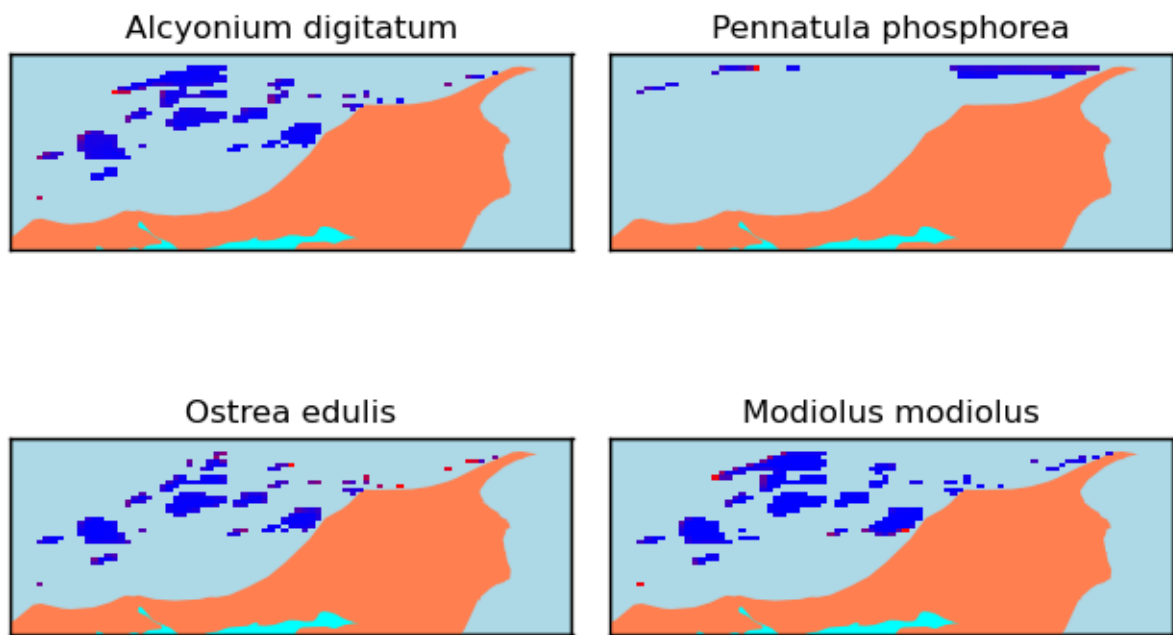
Figure 4.12. Average (over 2014-2022) receptiveness within the habitat network of each invertebrate species.

4.3.3 Potential impact of demersal bottom gear fishing on plaice recruitment

An interesting question is what drives the timing and ontogenetic diversity of newly settled plaice larvae. To address this question, we conducted a simulation of an ensemble of larvae experiencing a variable environment. Fig. 4.13a shows the average pelagic temperature in the Jammer Bay, averaged over the period 2014-2022, and plotted by Julian day. The grey zone in the upper figure also shows +/- 1 standard deviation range in ambient water temperatures. We use this annual cycle to expose the ensemble of larvae to temperature modulation of their growth rates, by drawing ambient temperatures from a normal distribution, with average and width corresponding to each day in Fig. 4.13b. Draws for each larva are assumed uncorrelated with its past thermal history. The simulation is based on spawning on March 1st, and we see that larva subject to thermal variability completes the demersal larval stage over a period of 10 days, in ultimo May. Thus, a larger ontogenetic variance must be explained by an extended spawning period (or cohort mixing), additional stochastic drivers of growth (e.g., abundance of small zooplankton) or time-correlation in environmental drivers.
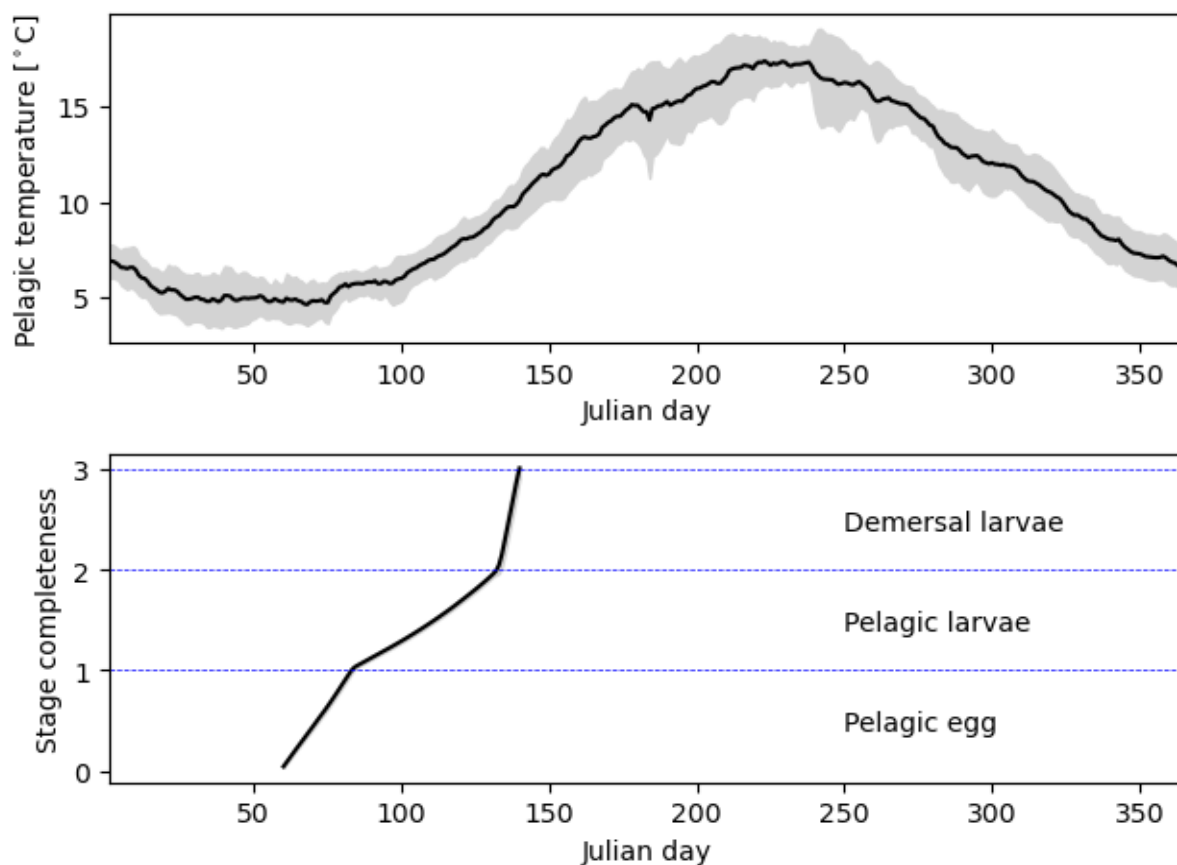
Figure 4.13. a) Upper plot: pelagic average (black curve) and standard deviation range (grey zone) temperature in the period 2014-2022, plotted by Julian day. b) Lower plot: ontogenetic progression simulation to plaice egg (stage 1) and larvae (stages 2,3), subject to temperature variability according to upper plot seasonal cycle.

Fig. 4.14 shows the nursery disturbance index (NUDI, Eq. 3) plotted by month for plaice nurseries in the Jammer Bay. We see that the overall disturbance level is quite high (a value of 1 would mean that all habitats on average are impacted once per week). Maximum levels are of order 0.5. Average levels display a seasonal cycle between 0 and 0.06, peaking twice, first in late spring and then early autumn. Unfortunately, as Fig. 4.13 indicated, the first peak coincides with the arrival and settling of demersal post-larvae. This first demersal stage is expected to be most sensitive to trawling disturbance, being less capable of orienting and fleeing due to metamorphosis and changed metabolic performance (Silva et al. 2015). The actual impact requires estimation of the stage-dependent sensitivity σ_i.
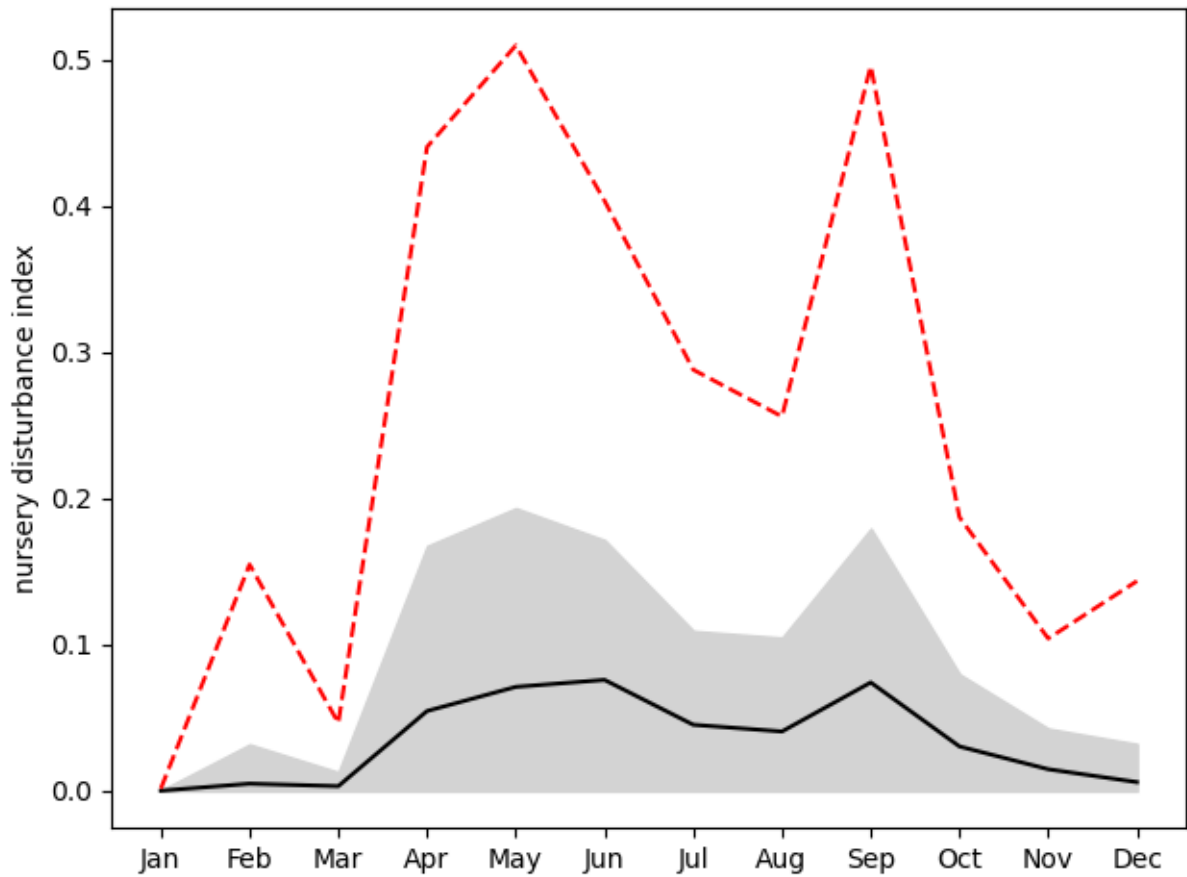
Figure 4.14. Nursery disturbance index (NUDI) plotted by month for plaice nurseries in the Jammer Bay. Black curve is average level, grey zone +/- 1 standard deviation, and dashed line is the observed maximum for that month in the period 2014-2022.

The annual impact is related to the Danish/anchor seine fishing intensity in the coastal sandy parts of the southern the Jammer Bay area where a low relatively stable number of vessels (at around 5 in the modelling period) between 15 and 24 m, primarily located in Hirtshals and Hanstholm have been conducting a directed fishery for plaice (Fig. 4.15).
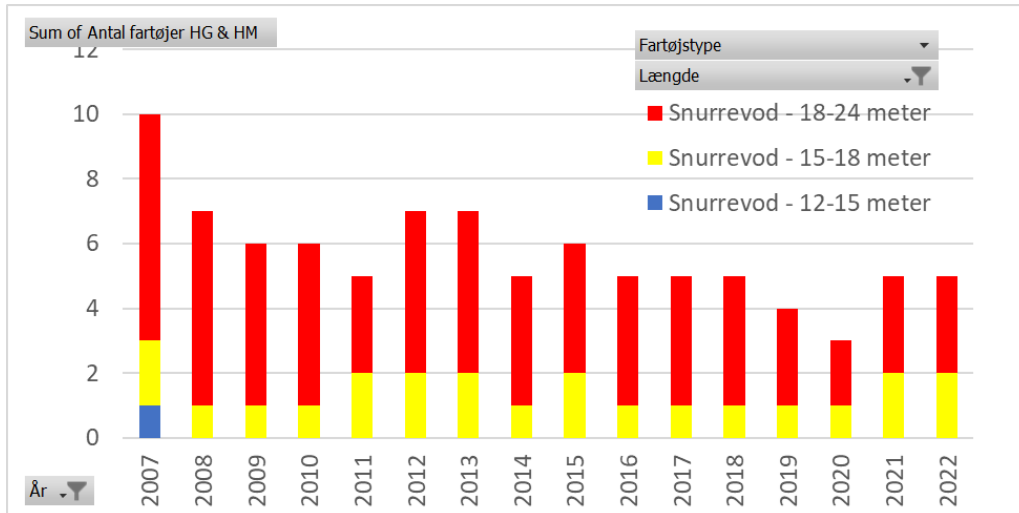
Figure 4.15. Number of Danish/anchor seine fishing vessels operating from Hanstholm and Hirtshals in the period 2007-2022.

Therefore, an indication of the temporal pattern is probably reflected in the landings of plaice, by far most the important species from the coast near parts of this fishery. Monthly landings of plaice from the Skagerrak over the years 2013-2023 (Fig. 4.16) show somewhat the same pattern of two seasonal peaks as in Fig. 4.14, but also a declining trend in recent years' landings.
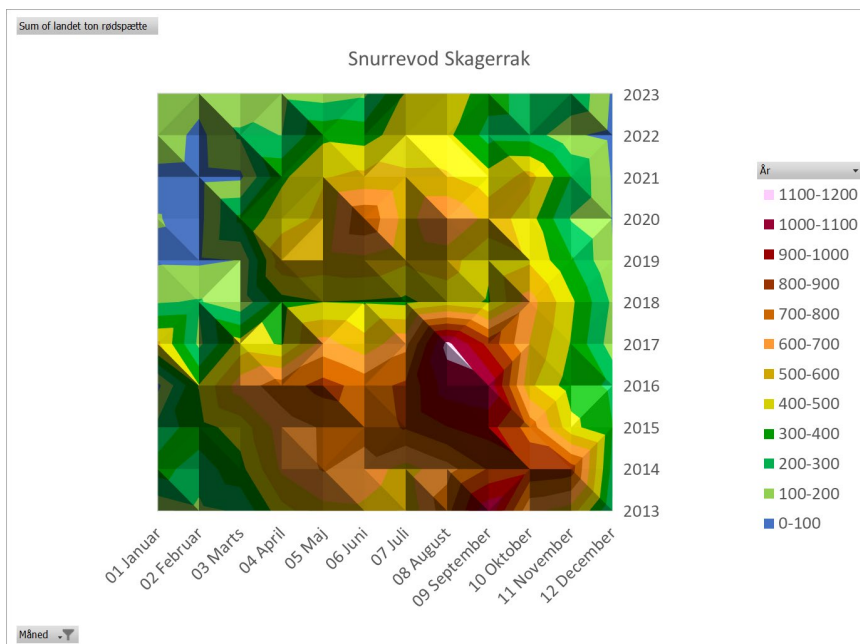
Figure 4.16. Landings of plaice from the Danish/anchor seine fishery in the Skagerrak, in tons per month for the period 2013-2023.
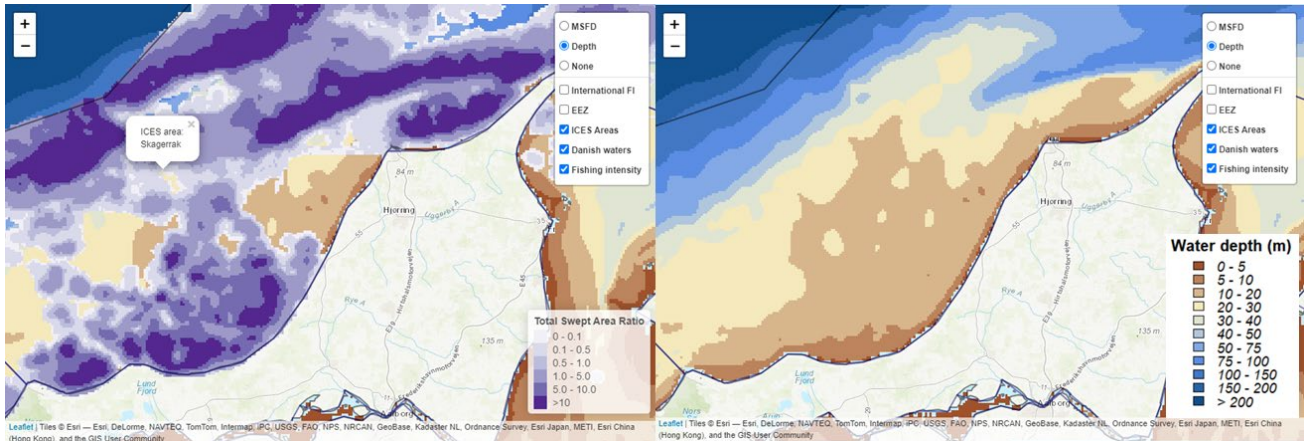
Figure 4.17. Average annual SAR (swept area ratio) of anchor/Danish seine fishery (left panel) overlain depth contours (right panel) in the Jammer Bay area. (Maps reproduced from:" The seafloor footprint of Danish fishing" https://ono.dtuaqua.dk/DDFAM/)

4.4   Discussion & perspectives

The simulation results indicate strong inter-annual variability in recruitment potential for both plaice and invertebrates, driven by climatic variability. This is in significant contrast to simplistic stock-recruitment relationships with random variation around the recruit/spawner curve of the stock often applied in stock-assessment and simplified ecosystem models. Climatic variability by physical processes may be important to consider in stock recovery processes at low spawning biomass when population density effects does not control stock dynamics, but also in local recruitment dynamics where small-scale hydrographical processes lead to variation in local settling density with subsequent density dependent effects on both growth and survival (Pihl et al. 2000). The timeliness of ocean state data products soon allows the possibility to forecast local recruitment and refine stock-recruitment relationships used for advice, and to distinguish whether physical or ecosystem processes shape population dynamics. For plaice recruiting to the Jammer Bay, it was indicated that these controls were at the same level.

Temperature history and region, southern North Sea, Irish Sea and west of Ireland explained 73% of variability in individual larval growth (Comerford et al. 2013) and, in combination with different spawning periods, leading to quite distinct settling times for the different populations. The spatial aspect was covered in a modelling study in the Irish Sea where the majority of plaice larvae exhibiting circa tidal vertical swimming and settling behaviour ended up in shallow waters in good agreement with observations (Fox et al. 2006). Our work demonstrated the possibility of a global warming effect in the plaice connectivity pattern, but indirect ecosystem effects have not been considered, and these needs to be investigated in future studies. Similarly, the temperature sensitivity of invertebrates needs to be assessed to increase realism and consolidate the potential for assessing the impact of ocean warming in comparison to other physical and anthropogenic drivers.

Another key finding of our study is that the first seasonal fishery peak coincides with the arrival and settling of plaice larvae that have been shown to be vulnerable due to metabolic demands from the metamorphosis processes (Geffen et al. 2007, Silva et al. 2015) and therefore must be considered most sensitive to physical disturbance. The detailed spatial overlap of the Danish

anchor seine fishery with the occupied habitats by early post-larval plaice is of crucial importance for estimating the potential mortality of the early juvenile stages. It has earlier been found that newly settled post-larvae and young juvenile 0-group plaice occupy shallow waters of < 1 m depth even at exposed costs with gradually sloping bottoms and no vegetation (Wennhage and Pihl 2001). The size of the of the involved vessels (Fig. 4.15) indicates that fishing at these depths is unlikely. However not all larvae may settle close to the beach, the detailed settling pattern of plaice leaves room for early exposure to fishing gear if larvae settle at deeper waters and gradually move towards the shore. Early larvae less than 7 mm are passive drifters unable to swim against a minimal current of <0.5 cm s^{-1}, thereafter they increase their swimming capacity up till > 3 mm s^{-1} until metamorphosis at >12 mm (Silva et al. 2015). In the late larval stage (12-15 mm), buoyancy increases, and the metamorphosing plaice spends most of its time near the bottom where habitat selection depends on food availability and/or lack of predators e.g., brown shrimp (*Crangon crangon*) (Wennhage and Gibson 1998). Fig. 4.17 indicates the annual spatial intensity of the of the anchor/Danish seine fishery at different depth zones in the Jammer Bay area. The absence of a brown shrimp fishery north of Thyborøn indicates that even deeper waters, with a suitable substrate in the Jammer Bay area, may be chosen as settling habitat, leaving the metamorphosed post-larvae vulnerable to the seine fishery (Fig. 4.17). Adding to risk scenarios of newly metamorphosed plaice, more recent studies have shown a shift in habitat selection of 0-group plaice in the western Dutch Wadden Sea between 1986 and 2009, so that although settlement still occurred in the intertidal zone, juveniles shortly thereafter (at sizes >15 mm and before May) moved to deeper waters (Freitas et al. 2016). The question is if the same behavioural pattern exists in the Jammer Bay area.

A study on ecological effects of the Danish anchor seine showed limited seabed disturbance in relation to otter board trawling. However, it also showed non-catch contact with large parts of the gear for different invertebrate groups (Noack et al. 2017). Collection of the escaped organisms showed relatively low levels of visual damage probably due to the robust exoskeleton of the organisms, but the experimental design was limited to collection of larger individuals with no chance of observing organisms at the settling stage. Therefore, to evaluate the impact level, more detailed studies are needed to quantify the mortality per effort, in relation to developmental stage, especially for demersal post-larvae and post-settled juveniles.

Current work has focused on early life stages of plaice and invertebrates, where transport patterns can more reliably be simulated. This is a first step toward life cycle models, where conservation and management questions can be addressed directly.

4.5   Acknowledgements

4.6   References

Bolle LJ, Dickey-Collas M, Van Beek JKL, Erftemeijer PLA, Witte JI, Van Der Veer HW, Rijnsdorp AD. 2009. Variability in transport of fish eggs and larvae. III. Effects of hydrodynamics and larval behaviour on recruitment in plaice. Marine Ecology Progress Series, 390, 195–211.

Cardinale M, Bartolino V, Llope M, Maiorano L, Sköld M, Hagberg J. 2011. Historical spatial baselines in conservation and management of marine resources. Fish and Fisheries, 12(3), 289–298.

Christensen A, Butenschön M, Gürkan Z, Allen IJ. 2013. Towards an integrated forecasting system for fisheries on habitat-bound stocks. *Ocean Science*, *9*(2), 261-279.

Christensen A, Mariani P, Payne MR. 2018. A generic framework for individual-based modelling and physical-biological interaction. https://doi.org/10.1371/journal.pone.0189956

Christensen A, Murawski J, She J, John MS. 2023. Simulating transport and distribution of marine macro-plastic in the Baltic Sea. *PLOS ONE*, *18*(1), Article e0280644.

Coombs SH, Nichols JH, Fosh CA. 1990. Plaice eggs (*Pleuronectes Platessa*) in the Southern North Sea - Abundance, spawning area vertical distribution, and buoyancy. Journal Du Conseil, 47(2), 133–139.

Comerford S, Brophy D, Fox CJ, Taylor N, van der Veer HW, Nash RDM; Geffen AJ. 2013. Temperature effect on growth and larval duration of plaice, *Pleuronectes platessa,* in three regions of the Northeast Atlantic. Mar. Ecol. Prog. Ser. 476:215-226.

Fox CJ, McCloughrie P, Young EF, Nash RDM. 2006. The importance of individual behaviour for successful settlement of juvenile plaice (*Pleuronectes platessa* L.): a modelling and field study in the eastern Irish Sea. Fish Oceanogr. 15: 301−313

Geffen AJ, van der Veer HW, Nash RDM. 2007. The cost of metamorphosis in flatfishes. JOURNAL OF SEA RESEARCH 58 (1) 35-45

GEUS (1999): Seabed Sediments around Denmark Digital Map 1:500.000.
Hansen, F. T., & Christensen, A. 2018. *Same Risk Area Case-study for Kattegat and Øresund. Final report*. DTU Aqua Report No. 335-2018.

Hufnagl M, Peck M A, Nash RDM, Pohlmann T, Rijnsdorp AD. 2013. Changes in potential North Sea spawning grounds of plaice (*Pleuronectes platessa* L.) based on early life stage connectivity to nursery habitats. Journal of Sea Research, 84(Sp. Iss. SI), 26–39.

Höffle H, Van Damme CJG, Lelièvre S; Loots C; Nash RDM, Vaz S, Wright PJ; Munk P. 2018. Linking spawning ground extent to environmental factors - patterns and dispersal during the egg phase of four North Sea fishes. Can. J. Fish. Aquat. Sci. 75 (3) 357-374.

NEMO4-ERGOM 2023. https://doi.org/10.48670/moi-00012 and https://doi.org/10.48670/moi-00013

Neumann T, Siegel H, Gerth M. 2015. A new radiation model for Baltic Sea ecosystem modelling. Journal of Marine Systems 152, 83-91.

Nielsen E, Støttrup J, Heilmann J, MacKenzie B. 2004. The spawning of plaice *Pleuronectes platessa* in the Kattegat. Journal of Sea Research, 51(3-4), 219–228.

Noack T, Madsen N, Mieske B, Frandsen RP, Wieland K, Krag LA. 2019. Estimating escapement of fish and invertebrates in a Danish anchor seine. ICES Journal of Marine Science, 74: 2480–2488.

Pereira Gabellini A, Mariani P, Christensen A. 2023. Population connectivity and dynamics in early-life stages of Atlantic fish communities. *Frontiers in Marine Science*, *10*, Article 1141726. https://doi.org/10.3389/fmars.2023.1141726.

Petereit C, Hinrichsen H-H, Franke A, Köster F. 2014. Floating along buoyancy levels: dispersal and survival of western Baltic fish eggs. Progress in Oceanography, 122, 131–152.

Petitgas P, Magri S, Lazure P. 2006. One-dimensional biophysical modelling of fish egg vertical distributions in shelf seas. Fisheries Oceanography, 15(5), 413–428.

Pihl L, Modin J, Wennhage H. 2000. Spatial distribution patterns of newly settled plaice (*Pleuronectes platessa* L.) along the Swedish Skagerrak archipelago. Journal of Sea Research 44: 65-80.

Ryland JS. 1963. The Swimming Speeds of Plaice Larvae. Journal of Experimental Biology, 40(2), 285–299.

Silva L, Moyano M, Illing B, Faria AM, Garrido S, Peck MA. 2015. Ontogeny of swimming capacity in plaice (*Pleuronectes platessa*) larvae. Mar Biol., 162, 753–761

Taylor DL. 2003. Size-dependent predation on post-settlement winter flounder *Pseudopleuronectes americanus* by sand shrimp *Crangon septemspinosa*. Mar Ecol Prog Ser 263:197-215

Ulrich C, Hansen JH, Boje J, Christensen A, Hüssy K, Sun H, Worsøe Clausen L. 2016. Variability and connectivity of plaice populations from the Eastern North Sea to the Baltic Sea, part II. Biological evidence of population mixing. Journal of Sea Research, 120, 13-23.

Vasquez M, Allen H, Manca E, Castle L, Lillis H, Agnesi S, et al. 2021. EUSeaMap 2021. A European broad-scale seabed habitat map. D1.13 EASME/EMFF/2018/1.3.1.8/Lot2/SI2.810241 – Seabed Habitats EUSeaMap 2021 - Technical Report. https://doi.org/10.13155/83528.

Visser A. 1997. Using random walk models to simulate the vertical distribution of particles in a turbulent water column. Marine Ecology - Progress Series, 158(1), 275–281.

Wennhage H. 1999. Recruitment processes in the flatfish *Pleuronectes platessa* (L.): larval supply, habitat selection and predator-prey interactions at settlement. PhD thesis, Göteborg University

Wennhage H, Gibson RN. 1998. Influence of food supply and a potential predator (*Crangon crangon*) on settling behaviour of plaice (*Pleuronectes platessa*). J Sea Res 39:103–111.

Wennhage H, Pihl L. 1994. Substratum selection by juvenile plaice (*Pleuronectes platessa* L.): impact of benthic microalgae and filamentous macroalgae. Neth. J. Sea Res. 32, 343-351.

Williams PJ, Brown JA. 1992. Developmental changes in the escape response of larval winter flounder *Pleuronectes americanus* from hatch through metamorphosis. Mar Ecol Prog Ser 88, 185–193.

5. Source-sink dynamics of sandeel recruitment to seabed habitats (Task 2.4)

Ole Henriksen, Marie Villefrance, Henrik Mosegaard, Mikael van Deurs

5.1 Introduction and aim

Sandeels, small elongated fish, belonging to the family Ammodytidae, are a critical component of marine ecosystems, particularly in the North Sea. They play a pivotal role in the marine food web, serving as a primary food source for numerous fish, birds, and mammals. Their importance is underscored by their influence on the larger fisheries industry, as their population fluctuations can significantly affect the availability of other commercially important fish species. The life cycle of sandeels is unique and closely tied to their sandy habitats. Their preference for sandy substrates is well established (Wright et al. 2000). They are known to burrow into sand, a behaviour that not only provides protection, but also enables them to sustain oxygen requirements through the advection of oxygen-rich water, which is facilitated by their gill ventilation (Behrens et al. 2007). After hatching from eggs that are attached to sand grains, they go through a larval phase drifting with ocean currents (Christensen et al. 2008). This is followed by a developmental period where they exhibit active swimming and juvenile schooling behaviour. Upon reaching a length of approximately 40 mm, they metamorphose and settle into sandy habitats in the North Sea, joining the adult population. As such, sandeels have a life strategy closely associated to sandy habitats having a remarkable adaptation for burying in the sand, which they start immediately after settling. Maturation occurs around 1-3 years of age, and their annual cycle is divided into feeding and overwintering phases (Henriksen et al. 2021). During the colder months, they bury themselves in the sand and survive on stored energy reserves for 6-8 months (van Deurs et al. 2010). This overwintering is briefly interrupted for spawning, typically in January. As spring arrives, they emerge to forage during the day, returning to the sand at night.

In the context of the Jammer Bay area, sandbanks in the focus area stretching from Hanstholm to Hirtshals, form crucial habitats for sandeels. These areas have potentially high significance as a fisheries resource, particularly for smaller fishing boats, but the variability in population sizes of sandeel highly affect the fishing opportunities in any given place. The aim of Task 2.4 is to explore several key aspects of sandeel ecology and distribution in this region. The primary focus is to understand the "source-sink dynamics" of sandeel larvae in the Jammer Bay region and its connectivity with adjacent areas like the north-eastern North Sea and western Skagerrak. This involves exploring whether the aggregations found in certain areas and the yearly recruitment success (also termed year-class strength) are a result of e.g., local reproduction, larvae drifting from neighbouring areas, or juveniles aggregating due to rich feeding opportunities.

A previous project (PELA, van Deurs et al. 2022) conducted by DTU Aqua in the North Sea addressed this by examining sandeel larvae and using drift modelling and statistical analysis. However, the unique hydrography of the Eastern parts of the North Sea and their connection with the Skagerrak region remained unresolved, primarily due to limitations in available oceanographic data. The current project aims to overcome these limitations by utilizing high-quality oceanographic data recently acquired in the Jammer Bay project. The previous project on

sandeels must acknowledge a critical aspect, which highlighted the challenges of measurement errors in larvae size determination. Initially, larvae sizes were measured without a consistent scale, leading to potential inaccuracies. This issue was compounded by conversions between measurement units, which could introduce further errors. To address these concerns, a meticulous process of remeasuring larvae was undertaken in this work package. This involved the use of a standard scale in all measurements and recalibration of previous data. By calculating a correction factor, we aim to rectify any discrepancies and ensure a high quality, reliable dataset for sandeel larvae lengths. This step is vital for the integrity of our research, as precise measurement is fundamental to understanding the life cycle and distribution of sandeels.

The specific objectives of this task included:
- Deliver a protocol for measuring larvae using image processing tools, such as *ImageJ*
- Provide high quality data sets for larvae abundances and lengths.
- Visualisation and reporting on the local sandeel recruitment in the Jammer Bay and North Sea area overall.
- Developing a spatial model for the source-sink dynamics of sandeel larvae in the Jammer Bay, integrating this with the North Sea model.
- Providing a comprehensive description and visualization of the dynamics of marine connectivity to enhance understanding of sandeel population fluctuations and movements.

The Task 2.4 is significant, as it will offer valuable insights into the life cycle and recruitment patterns such as spawning and settlement of sandeels, which are crucial for effective fisheries management and conservation efforts in these marine environments.

5.2 Materials and methods

5.2.1 Collection of sandeel larvae

Sandeel larvae samples were obtained using a specialized netting method during the first quarter of the International Bottom Trawl Survey (IBTS Q1) coordinated by the International Council for the Exploration of the Sea (ICES). The sampling tool employed was the MIKey M net, a compact ring net featuring a 20 cm diameter and a 335 µm mesh size. This net was affixed to the larger MIK net, typically used for annual herring larvae surveys conducted at night during the Q1 IBTS. Originally introduced by the ICES Working Group on Eggs and Larval Surveys (WGEGGS2) to gather data on cod and plaice eggs, the MIKey M net was found to also capture small, newly hatched sandeel larvae, thus inspiring the first project, abbreviated PELA. The net was used in double oblique hauls, extending from the ocean surface to about 5 m above the seabed. Each MIKey M net was fitted with a flowmeter to ascertain the volume of water filtered, aiding in estimating larval abundances.

The collected samples of larvae, spanning six years from 2015 to 2020, were initially analysed and explored in the PELA project (van Deurs et al. 2022). This period included years of varying recruitments (e.g., low in 2015 and 2017 and high in 2016). The analysis encompassed samples from different countries that undertake and coordinate the IBTS-survey in different areas of the North Sea. The countries included Denmark, Germany, Norway, and the Netherlands, covering major sandeel habitats during the IBTS Q1. Larvae from these countries were sorted, counted, and measured using an image analysis software called *ImageJ*. Subsequently sam-

ples from France have been added in order to expand the range of the survey, routinely processed by French institute of IFREMER using *ZooSCAN*. Larval abundance was estimated as numbers m^{-2}, that is, numbers in catch divided by volume filtered (numbers m^{-3}) multiplied by water depth (m).

Following the collection and measurement of larvae, a crucial step was undertaken to enhance the accuracy of the measurements. This involved the development of a detailed protocol for measuring larvae using image-processing tool. The initial measurements encountered some inconsistencies, particularly in the scaling and unit conversions. To address this, a comprehensive remeasurement of larvae was conducted, ensuring each image included a proper scale and documenting each step meticulously. This remeasurement allowed us to develop a correction factor to adjust any discrepancies for the samples that where not remeasured.

5.2.2 Larval drift simulations

An agent-based modelling framework (IBMlib, see also task T2.3) have been developed at DTU Aqua and will be used for the drift simulations (Christensen et al. 2018). Different versions of the agent-based modelling framework have previously consistently been applied in relation to sandeel. The model will be enhanced by integrating the most recent biological knowledge, alongside a newly acquired hydrographic dataset from the Danish Meteorological Institute (DMI). This dataset, characterized by its high spatial and temporal precision, covers the Skagerrak, North Sea, Kattegat, and the Western Baltic Sea, and will be a vital component in refining the accuracy and relevance of the model.

In order to model the average drift of sandeel larvae, the mean size of the larvae for each haul was calculated, adjusted for a 10% shrinkage post-capture due to storage (a common procedure as per existing literature). The relationship between size at hatching and temperature, as outlined in Régnier et al. (2018), has also been considered. Larvae were tracked backward to determine the time and location of hatching. In addition, a forward drift simulation until they reached metamorphosis at 40 mm determines the time and location for settlement. Settlement likelihood is determined by the presence of sandeel habitat, as identified by polygons from Jensen et al. (2011), within the trajectory of drift location upon reaching 40 mm. If within a 10 x 10 km grid cell a suitable habitat is present, the larvae would settle. Otherwise, they will continue to drift for up to 14 days. Failure to encounter a suitable habitat within this period results in the death of a larvae. The hatching and settlement locations derived from these simulations are represented as probability distributions, simplified mathematically as ellipses (excluding those that did not reach suitable habitat). The results are based on the centroids of these ellipses and include the proportion of fish that successfully settled.

5.2.3 Statistical modelling of spatial distribution

The process of statistical modelling of spatial distribution in this study employs the capabilities of Generalized Additive Models (GAMs). These models are exceptionally adept at estimating the abundances of fish populations, effectively adjusting for various factors that could influence the data, such as the location of the haul, depth, time of day, and swept area. GAMs are particularly useful for defining non-linear smooth relationships between the observed outcome (like fish abundance) and various predictors including year, season, haul position, depth, and larvae length. By incorporating spatial and spatio-temporal smooth functions, these models facilitate the prediction of fish abundances across different locations and times. This methodology is an

extension of the approach detailed by Berg et al. (2014) and ongoing work developing a more generic tool and package in the statistical software of *R* open for other scientists.

This comprehensive modelling framework needs to be specially tailored and further developed to suit the unique behavioural patterns and ecological needs of the sandeel. Such customization is vital to ensure that the model delivers precise and actionable insights, enabling a deeper understanding of sandeel population dynamics and aiding in their effective management and conservation. The prospect of refining and adapting these advanced modelling techniques to the specificities of the sandeel represents a promising avenue in marine ecological research.

5.3   Results

In this work package, we successfully developed and delivered a comprehensive protocol for measuring sandeel larvae using image processing tools (Appendix 5.1). This significant achievement enabled us to effectively address the issues related to larvae length and measurement inconsistencies. The remeasurement of sandeel larvae samples was a critical component and the process involved revisiting previously collected samples to ensure accurate and consistent length measurements. This work has also been documented (Appendix 5.2). Consequently, we have produced two valuable datasets: one detailing larvae abundance and the other focusing on larvae lengths. Here, we provide a detailed overview of the collected and processed data. The data cover the majority of the North Sea collected by the annual IBTS-survey in Q1 coordinated by different countries and institutes (Fig. 5.1).
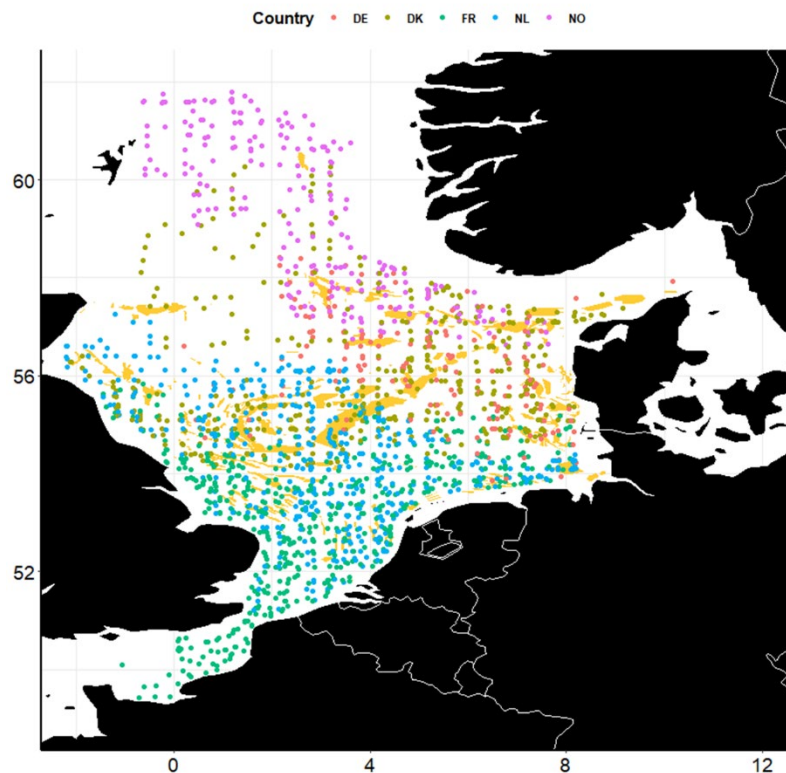
Figure 5.1. Overview over coverage and station locations collected by IBTS Q1 between 2015 and 2020 coordinated by different countries (colour of dots).

While we achieved a comprehensive coverage of the North Sea, the survey coverage was incomplete. Some years in our study period are missing data, and not all stations were consistently available, e.g., 2016 Germany or 2017 Norway (Table 5.3.1). This was due to various reasons, including the non-submission of data from some countries, the lack of laboratory workup on collected samples, or vessel and sampling issues in a given year. In total, 1863 stations were included, where 1469 stations had no recorded sandeel larvae, also termed zero stations.

Table 5.1. Overview over the dataset of larvae abundances showing the number of samples collected at each station for each year and each country that coordinated IBTS sampling in a given region in that year. The number of zero stations is given in parenthesis. Please see Figs. 5.1 and 5.2 for more detailed information on coverage by country and abundances of each sample.

Year	Germany	Denmark	France	Netherlands	Norway	Sum
2015	12 (12)	74 (37)	97 (88)	85 (71)	24 (22)	292 (230)
2016	0 (0)	78 (35)	116 (105)	56 (23)	24 (22)	274 (185)
2017	28 (25)	77 (62)	106 (101)	74 (65)	0 (0)	285 (253)
2018	26 (23)	81 (35)	97 (88)	92 (79)	73 (63)	369 (288)
2019	40 (40)	82 (70)	68 (64)	90 (66)	79 (70)	359 (310)
2020	57 (46)	56 (27)	62 (60)	54 (43)	28 (27)	257 (203)
Total	163 (146)	448 (266)	546 (506)	451 (347)	228 (204)	1836 (1469)

The number of samples for measurement varied with availability and year, and thus not all samples were measured. In total 6448 individual fish larvae were measured, and a full overview has been given in Table 5.2.

Table 5.2: Overview over the dataset of larvae lengths showing the number of individual larvae measured for each year and each country that coordinated IBTS sampling in a given region in that year. The number of stations for measured larvae is given in parenthesis. Please see Figs. 5.3 and 5.4 for more detailed information on distributions of lengths in space and time.

Year	Germany	Denmark	France	Netherlands	Norway	Sum
2015	0 (0)	693 (37)	105 (9)	190 (13)	15 (2)	1003 (61)
2016	0 (0)	850 (43)	172 (11)	500 (32)	2 (2)	1524 (88)
2017	45 (3)	180 (15)	23 (5)	141 (9)	0 (0)	389 (32)
2018	43 (3)	1287 (45)	128 (9)	322 (13)	95 (10)	1875 (80)
2019	0 (0)	124 (11)	36 (4)	294 (24)	55 (8)	509 (47)
2020	172 (10)	613 (29)	22 (2)	360 (11)	1 (1)	1168 (53)
Total	260 (16)	3747 (180)	486 (40)	1807 (102)	168 (23)	6448 (361)

The larvae sampling was comprehensive across the North Sea, effectively covering known sandeel habitats. The capture of larvae was predominantly observed over or near these sandy habitats and high capture rates were mainly confined to the Dogger Bank area and along the Danish coastline (Fig. 5.2). Larvae found near habitats in the central parts of the North Sea and near the UK coastline were minimal. Data revealed a distinct pattern in sandeel larvae abundance over time. Specifically, there was a noticeable increase in the number of larvae in February compared to January across all surveyed years. Additionally, the data highlighted variations

in both the coverage and availability of samples from the surveys on a monthly and annual basis, (Fig. 5.3).
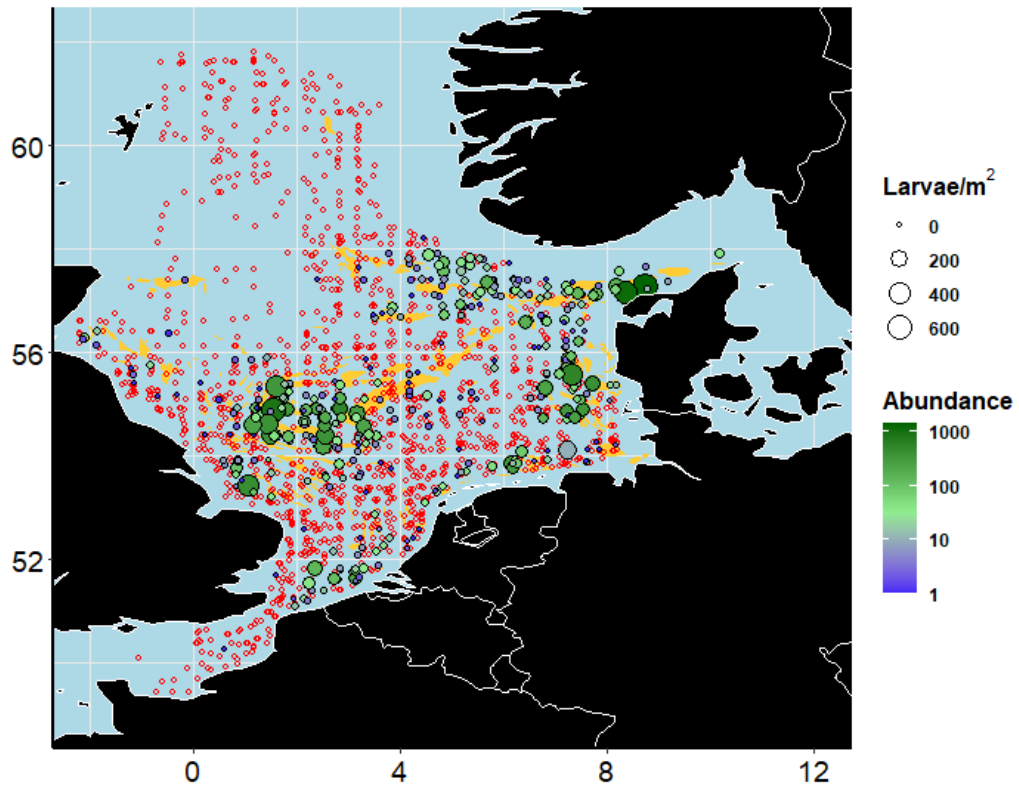
Figure 5.2. All station locations with samples collected by IBTS Q1 between 2015 and 2020. The bubbles show sandeel larvae abundances in number (colour of dots) and in number per m² (size of dots). Stations with samples of zero larvae are also shown (open red dots). The yellow contours are the mapped sandeel habitat in the North Sea.
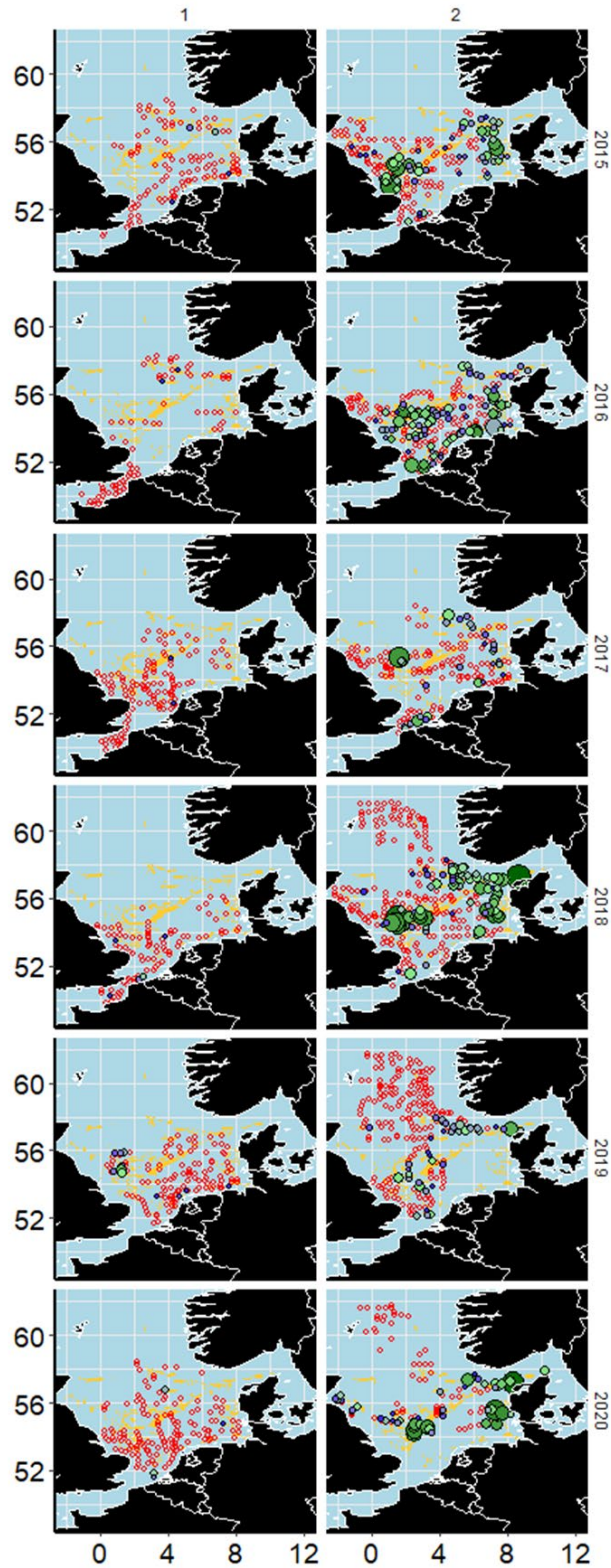
Figure 5.3. All station locations with samples collected by IBTS Q1 shown for each month (1 is January and 2 is February) for each year, 2015-2020. The bubbles show sandeel larvae abundances in number (colour of dots) and in number per m² (size of dots). Stations with samples of zero larvae are also shown (open red dots). The yellow contours are the mapped sandeel habitat in the North Sea.

The sandeel larvae collected were generally small, with an average size of 4.7 mm (Fig. 5.4, median size of 4.6 mm). The majority of samples displayed average sizes that were comparable to the sample mean. However, larger larvae were predominantly found in the central regions of Dogger Bank and in the north-eastern areas near the Norwegian coast (Fig. 5.4). The annual distribution of lengths where very similar across years, where the main difference seems to be the numbers of larvae sampled (Fig. 5.5).
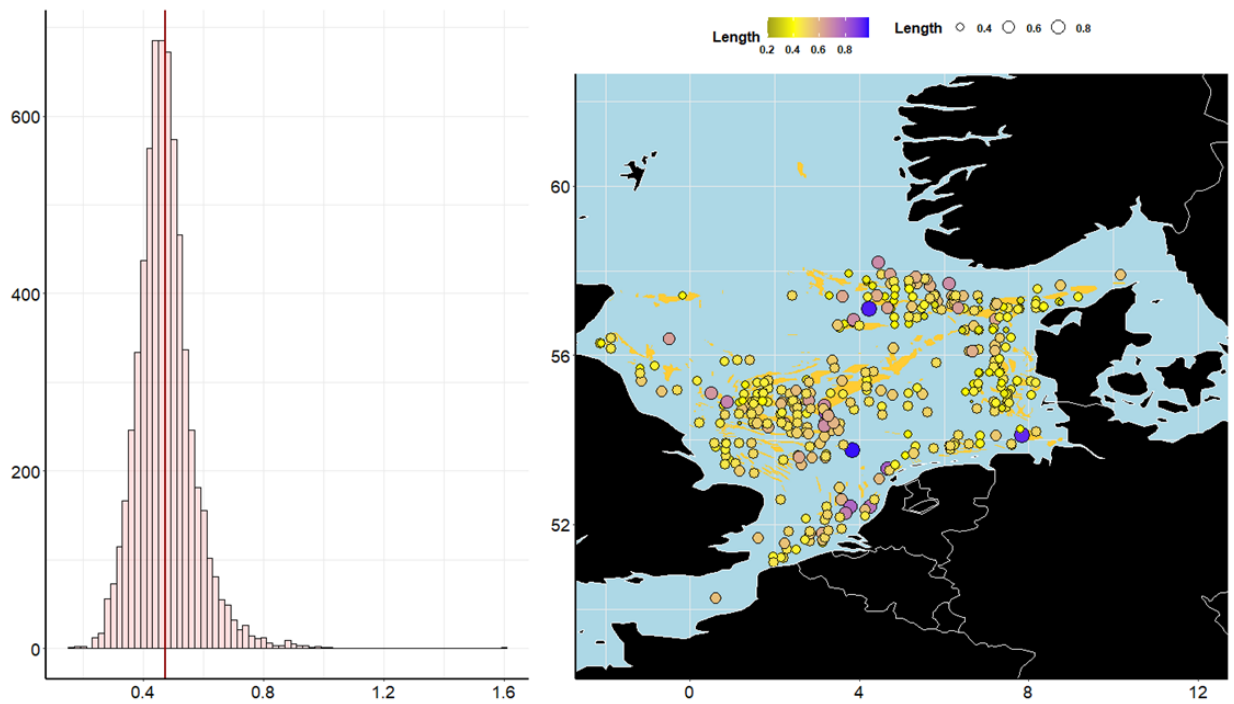
Figure 5.4. The length distribution of all measured sandeel larvae (left panel) and the spatial distribution of lengths in the North Sea (right panel). The mean length of all samples is shown (vertical red line, left panel). The circles on the map show the average length of each station sample (colour and size of circles, right panel).
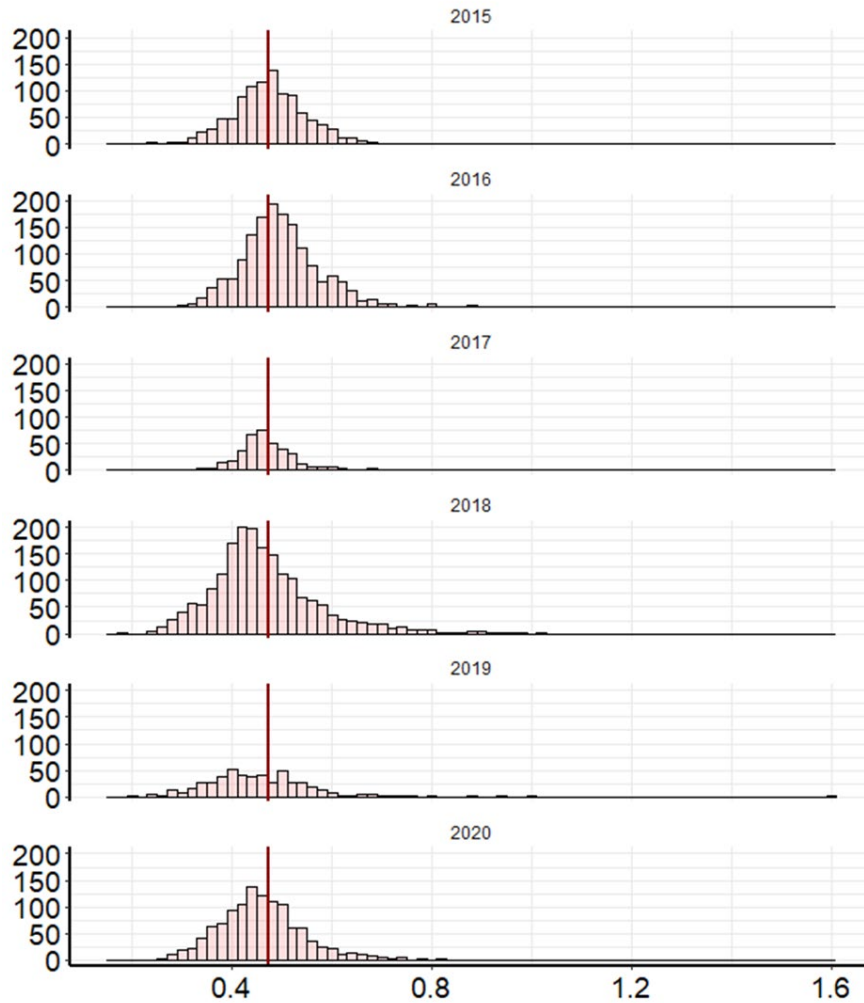
Figure 5.5. The length distributions of all recalibrated or measured sandeel larvae for each year, 2015-2020. The mean length of all samples for all years is shown (vertical red line).

5.4 Discussion and perspectives

One of the key achievements of Task 2.4 has been the creation and provision of two new valuable datasets: one detailing larvae abundance and the other focusing on larvae lengths. These datasets represent a significant advancement for future research, particularly in the study of sandeel populations. Their value lies not only in enhancing our current understanding of sandeel recruitment patterns such as hatching and settlement, but also in their potential application in broader ecological studies.

The remeasurement and recalibration of sandeel larvae samples using a detailed protocol and image processing tools was a pivotal component of this work package. It significantly improved the accuracy of larvae length measurements, contributing to the creation of high-quality datasets for larvae abundances and lengths. However, despite these successes, we faced challenges in completing the analyses on larval drift and statistical modelling as initially planned. Due to time constraints and data readiness issues, we were unable to conduct these analyses within the project timeline. As a result, our focus shifted towards thoroughly documenting the data collection and processing methods. We provide a detailed overview of the collected and

processed data, emphasizing the methodologies and protocols employed. This documentation serves as a vital resource for future research and offers insights into the potential improvements and adjustments needed for subsequent studies in this field.

Despite these challenges, the findings provide valuable insights into the recruitment patterns of sandeels and their affinity to specific seabed habitats. The variations in larvae populations observed over different years illustrate the dynamic nature of marine ecosystems. These insights are crucial for effective fisheries management and conservation efforts, particularly in understanding the ecological role of sandeels as a key species in marine food webs.

Looking forward, this work package lays the groundwork for more in-depth future studies. It emphasizes the need for enhanced data collection methods, consistency in survey execution, and the development of more sophisticated modelling techniques tailored to the unique behaviours of marine species like the sandeel. The integration of high-quality oceanographic data, as seen in this work package, is a step towards more accurate and predictive models that can inform sustainable fisheries management and conservation strategies.

In conclusion, while Task 2.4 faced limitations, its contributions to the understanding of sandeel recruitment dynamics are invaluable. It highlights the interplay between biological, environmental, and methodological factors in marine research and underscores the ongoing need for adaptive and comprehensive study approaches in marine ecology.

5.5   Acknowledgements

5.6   References

Behrens JW, Steffensen JF. 2007. The effect of hypoxia on behavioural and physiological aspects of lesser sandeel, *Ammodytes tobianus* (Linnaeus, 1785). Marine Biology, 150(6), 1365-1377.

Berg CW, Nielsen A, Kristensen K. 2014. Evaluation of alternative age-based methods for estimating relative abundance from survey data in relation to assessment models. Fisheries research, 151, 91-99.

Christensen A, Jensen H, Mosegaard H, St. John M, Schrum C. 2008. Sandeel (*Ammodytes marinus*) larval transport patterns in the North Sea from an individual-based hydrodynamic egg and larval model. Canadian Journal of Fisheries and Aquatic Sciences, 65(7), 1498-1511.

Christensen A, Mariani P, Payne MR. 2018. A generic framework for individual-based modelling and physical-biological interaction. Plos One, 13(1), e0189956.

Henriksen O, Rindorf A, Mosegaard H, Payne MR, van Deurs M. 2021. Get up early: Revealing behavioral responses of sandeel to ocean warming using commercial catch data. Ecology and Evolution, 11(23), 16786-16805.

Jensen H, Rindorf A, Wright PJ, Mosegaard H. 2011. Inferring the location and scale of mixing between habitat areas of lesser sandeel through information from the fishery. ICES Journal of Marine Science, 68(1), 43-51.

Régnier T, Gibb FM, Wright PJ. 2018. Temperature effects on egg development and larval condition in the lesser sandeel, *Ammodytes marinus*. Journal of Sea Research, 134, 34-41.

van Deurs M, Christensen A, Frisk C, Mosegaard H. 2010. Overwintering strategy of sandeel ecotypes from an energy/predation trade-off perspective. Marine Ecology Progress Series, 416, 201-214.

van Deurs M, Bekkevold D, Huwer B, Henriksen O, Albertsen CM, Munk P, Storr-Paulsen M, Makri M, Davies JO, Mildenberger T, Jensen GH. 2022. Pelagic species – A contribution to the preservation of sustainable pelagic fisheries in the North Sea (PELA). DTU Aqua. DTU Aqua-rapport No. 403-2022.

Wright PJ, Jensen H, Tuck I. 2000. The influence of sediment type on the distribution of the lesser sandeel, *Ammodytes marinus*. Journal of Sea Research, 44(3-4), 243-256.
.

Appendix 5.1: Protocol for measuring and documenting sandeel larvae using *ImageJ*

Step 1: Open your photo in *ImageJ*
Open *ImageJ* and press **"Open…"** under the **"File"** tab.
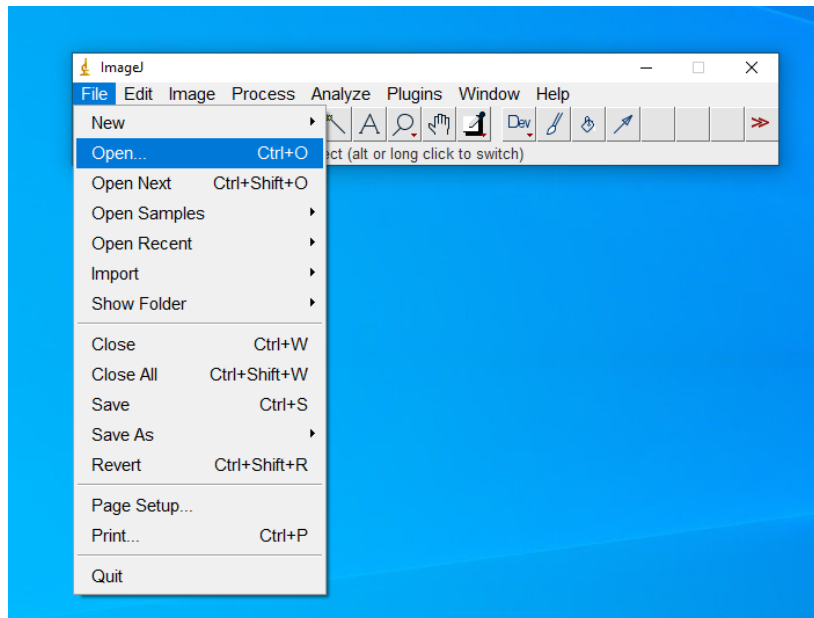
Select your photo by either double clicking on the file or clicking on it and then press **"Open"**.
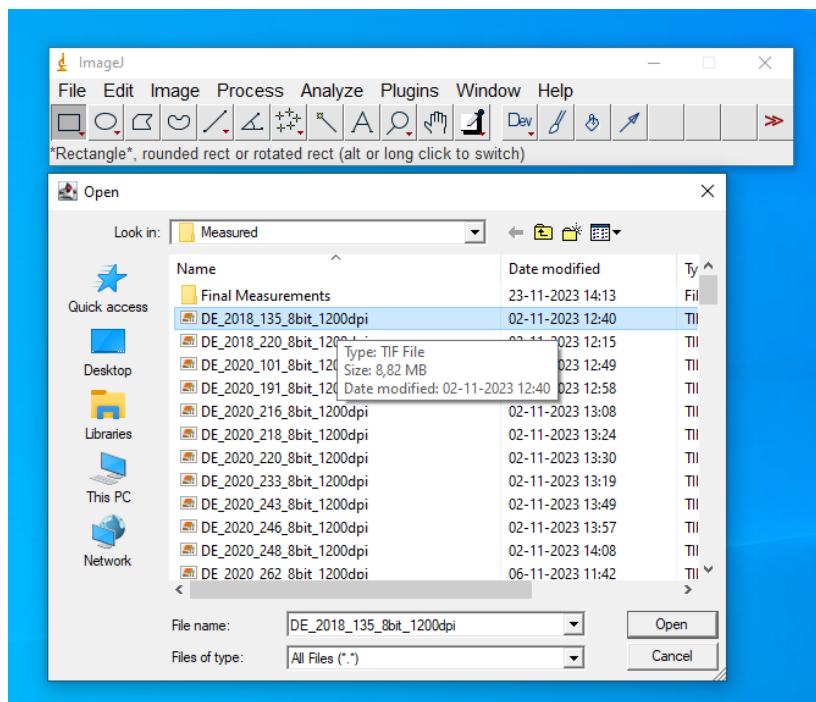
Step 2: Set measurements
Press **"Set Measurements"** under the **"Analyze"** tab.
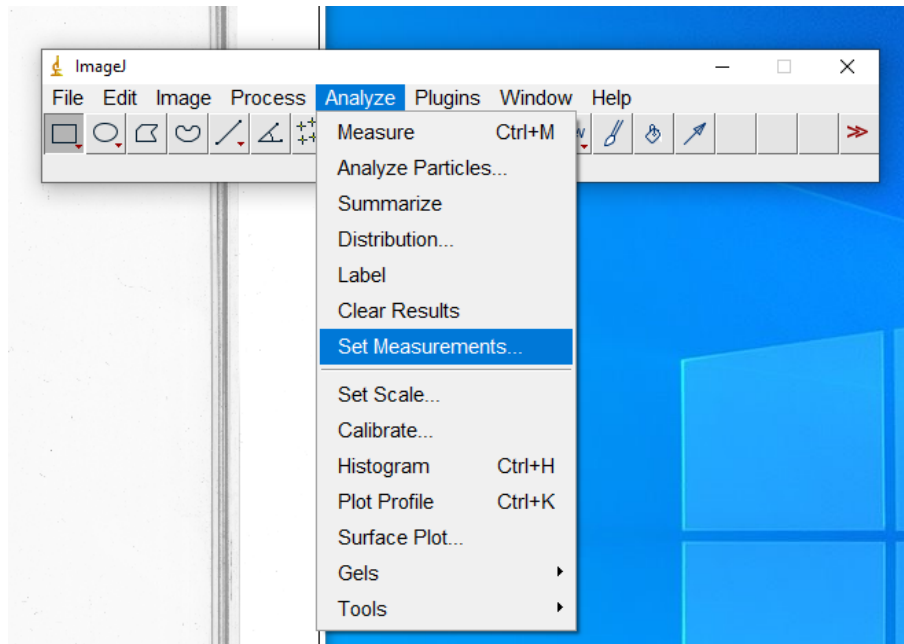
Make sure the measurements are set as shown below. Most importantly, make sure that **"Add to overlay"** and **"Display label"** is activated. Then press **"OK"**.
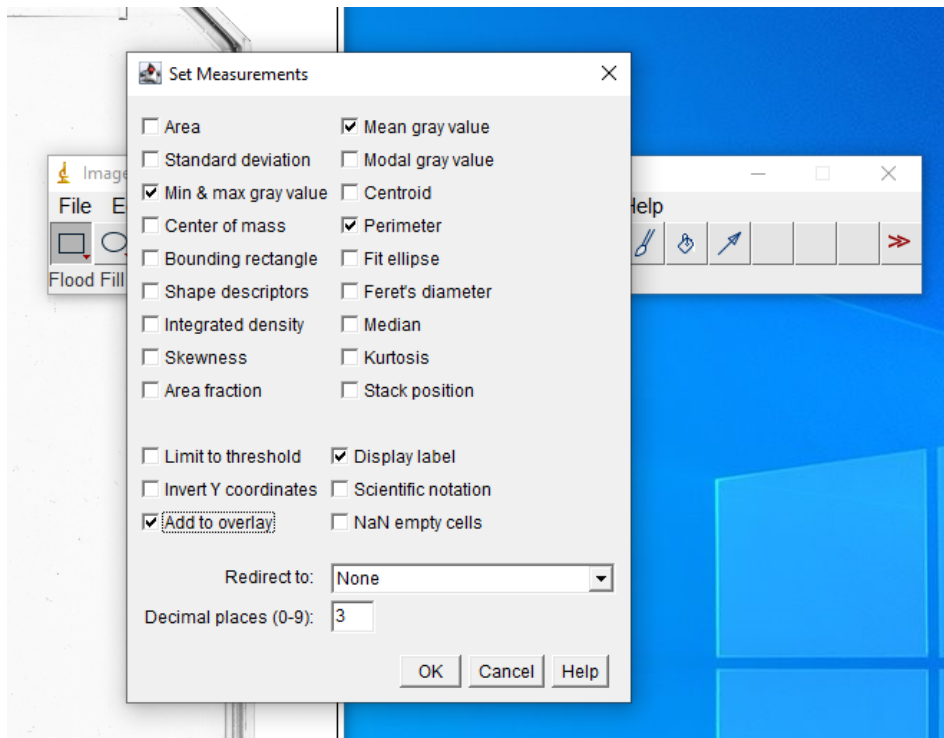
Step 3: Set scale
Right-click the Line tool and press **"Straight Line"**.
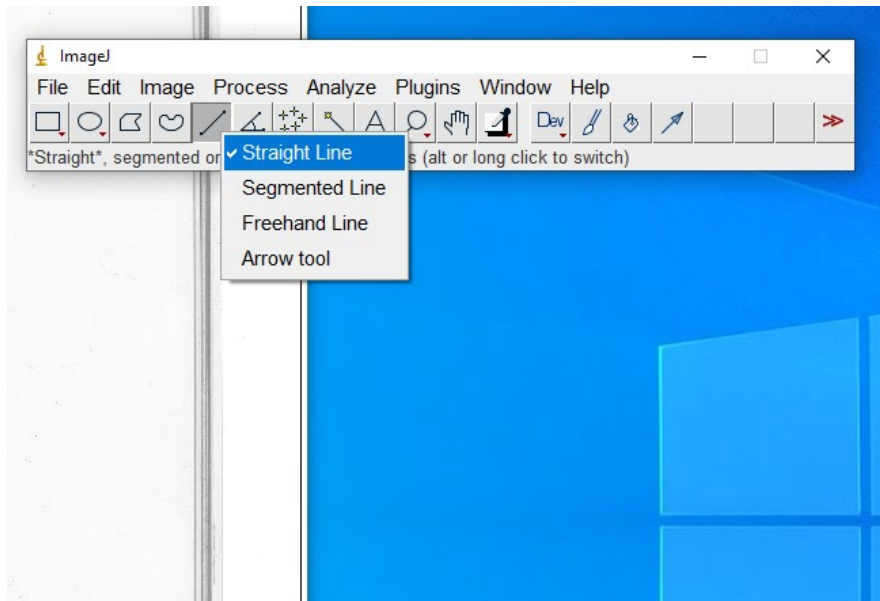
Now zoom-in on the scale in the bottom part of the picture by pointing the mouse at the area and pressing **"+"** on your keyboard. Now draw a 1 cm line along the scale by holding down left-click on your mouse and release when you are done. It should now look something like the yellow line on the screenshot below.
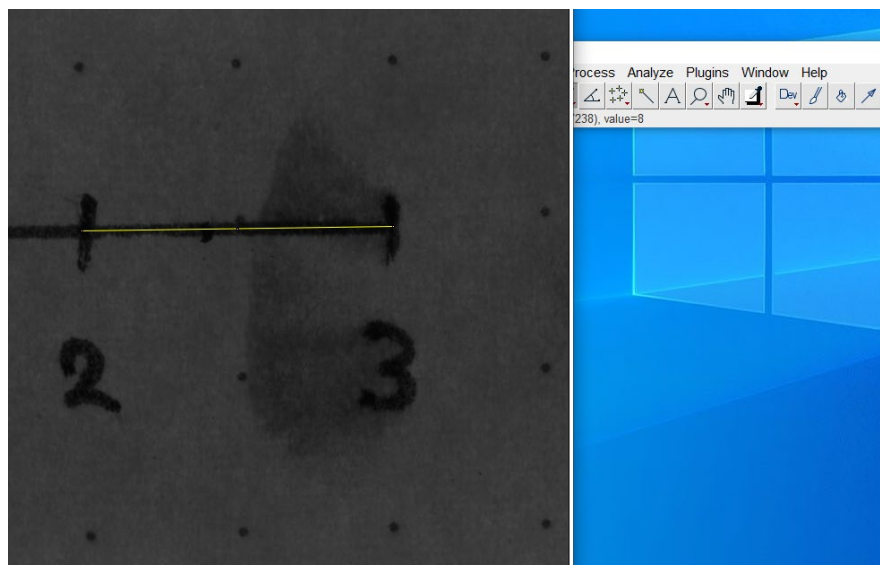
Click **"Set Scale…"** under the **"Analyze"** tab.
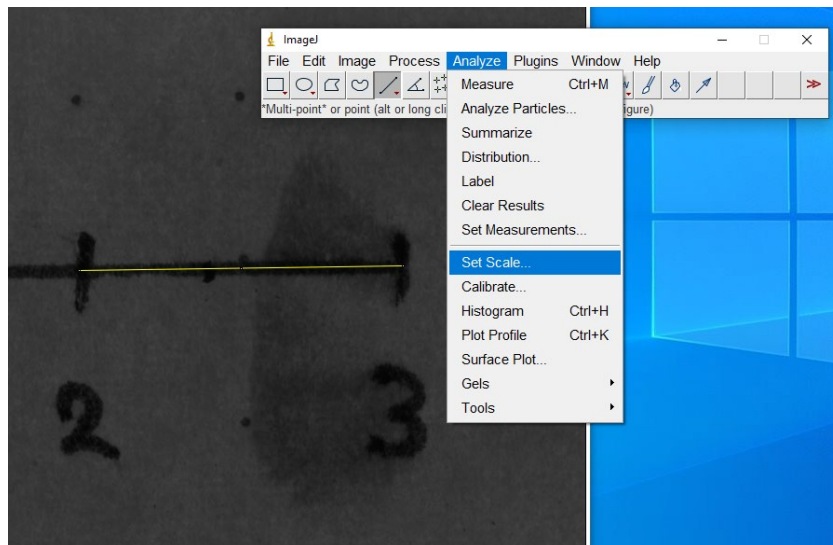
Change the **"Known distance"** to **1**, and **"Unit of length"** to **cm**. Then press **"OK"**. Now the scale is set.
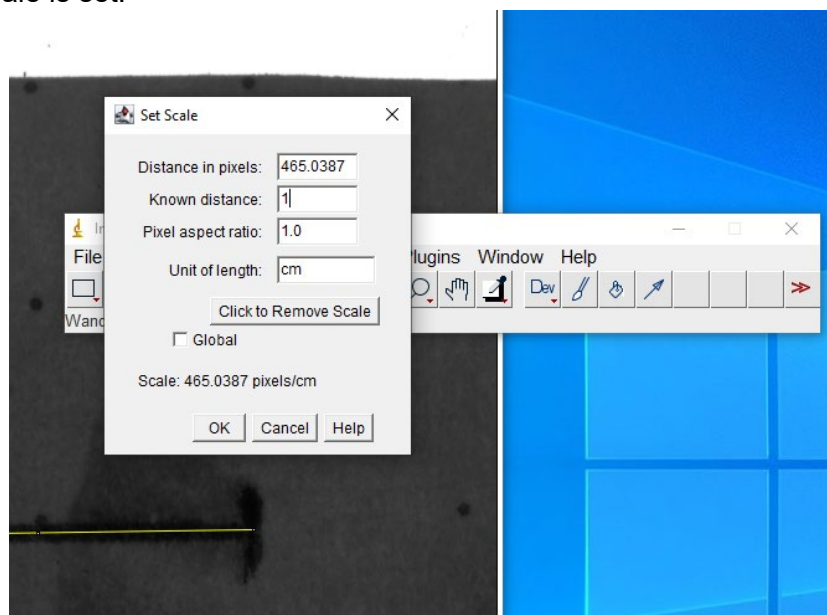
Step 4: Measuring the sandeel larvae

Right click the line tool and press **"Segmented Line"**.
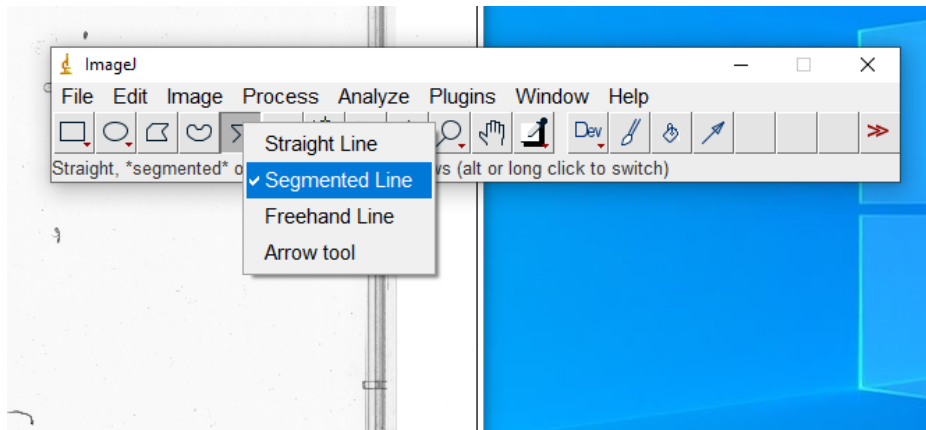
Now zoom-in on one of the larvae in order to measure it. Measure from head to tail. You start measuring in segments by pressing left click on your mouse (pressing left click once every time you need to do a new segment/change direction of the line) and then dragging the line along the centre of the body of the larvae. When you finish measuring the larvae, press double left-click on your mouse in order to finish the line. You will end up with a larvae measurement as the one shown left in the screenshot below.
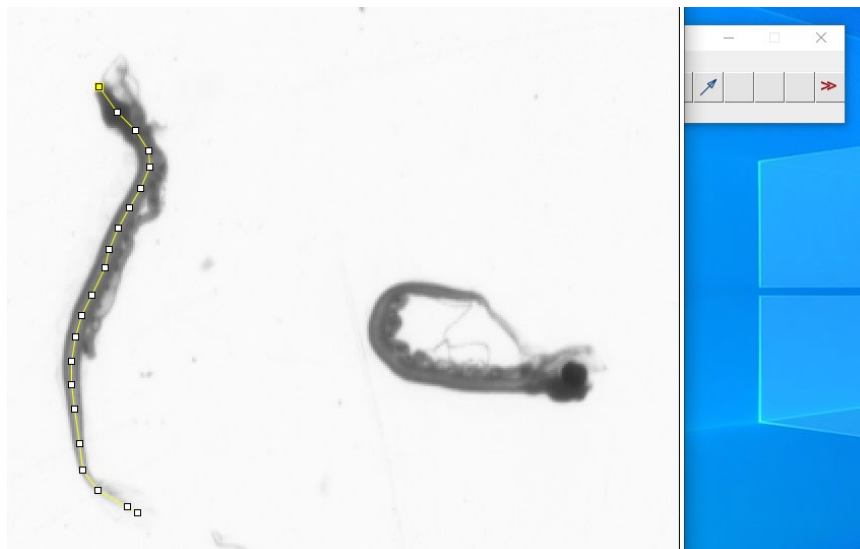
Now press **"CTRL" + "M"** on your keyboard in order to measure the length of the line drawn. A **"Results"** window with a table will now pop-up with the known length and label of the larvae, as well as a label next to the larvae.
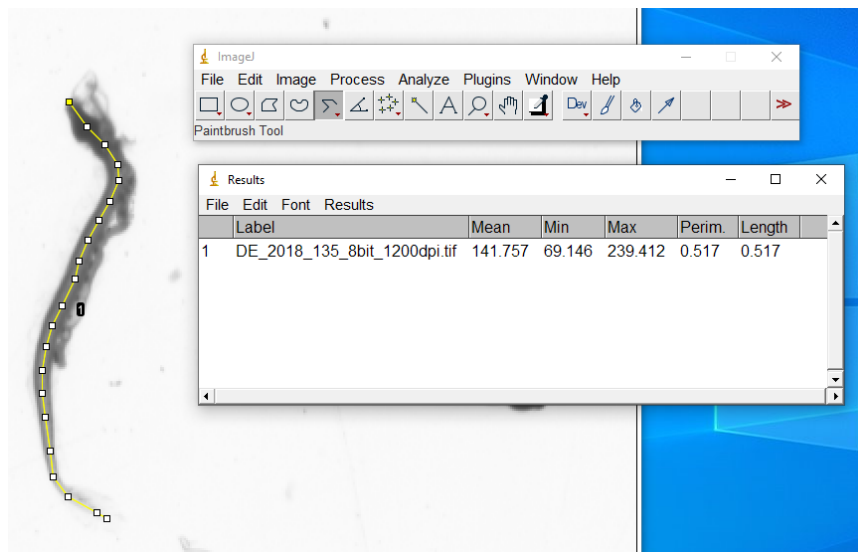
You can now move on to the next larvae, draw the segmented line, press **"CTRL" + "M"** and so on until all the larvae (or 50) have been measured and labelled.
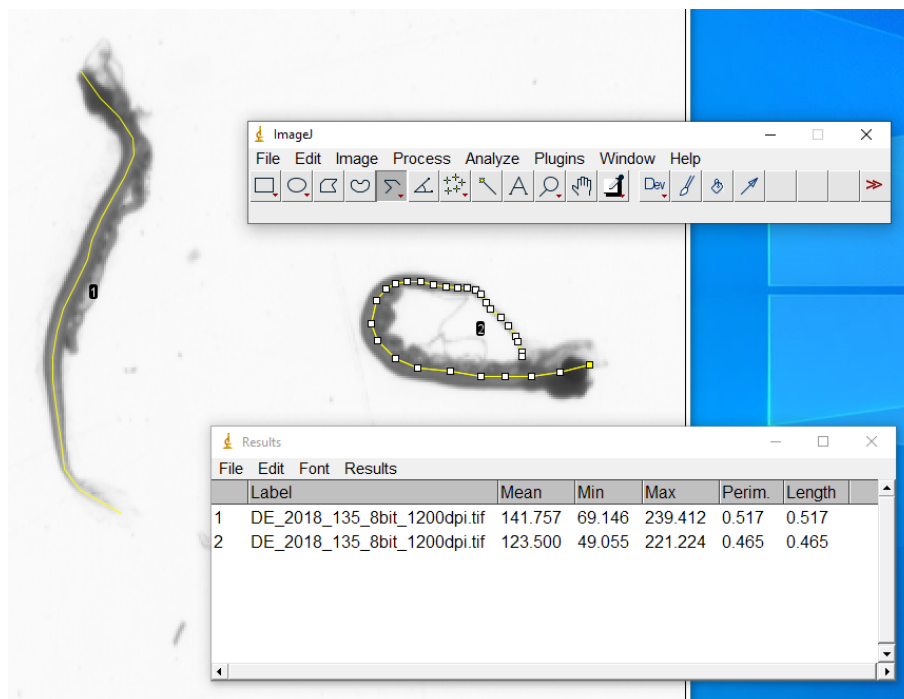
Step 5: save Results and Image
When all larvae have been measured, press **"Save as…"** under the **"File"** tab in the **"Results"** window.
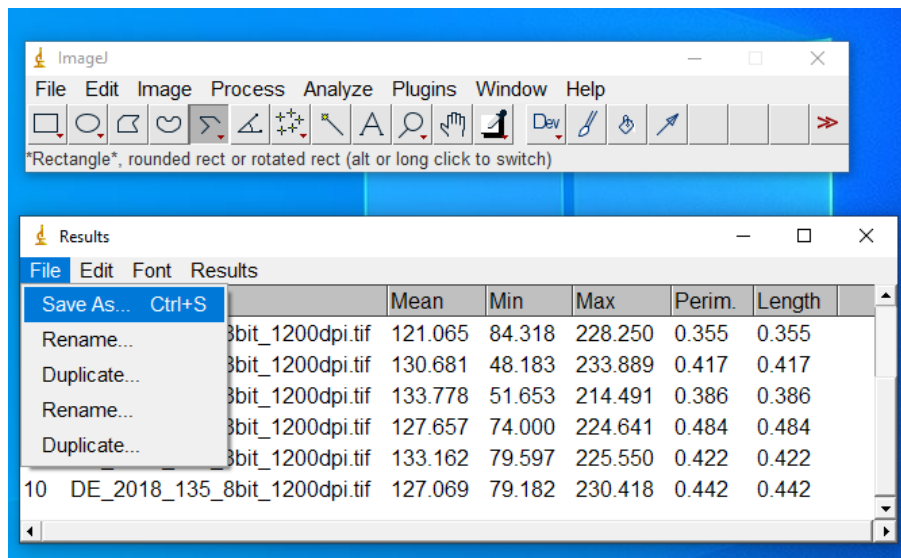
Save the results file as a **.CSV file** with the name of the picture under **"Final Measurements"**. In this case the picture is "DE_2018_135_8bit_1200dpi" and the results file is saved as "DE_2018_135.csv" as shown below. Press **"Save"**.
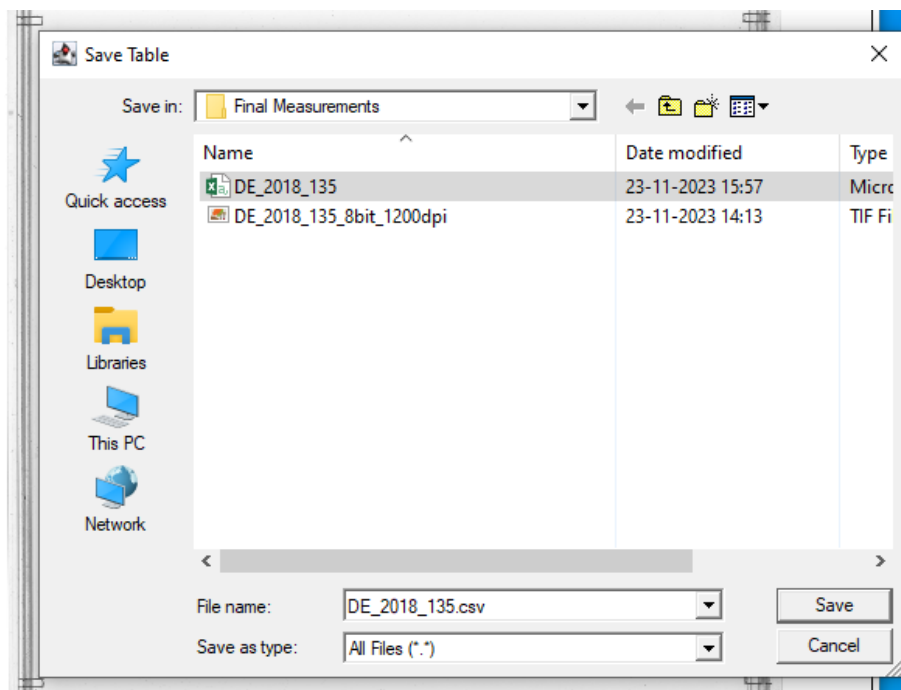
Now save the image as a **Tiff** file by pressing **"File -> Save As -> Tiff…"**.
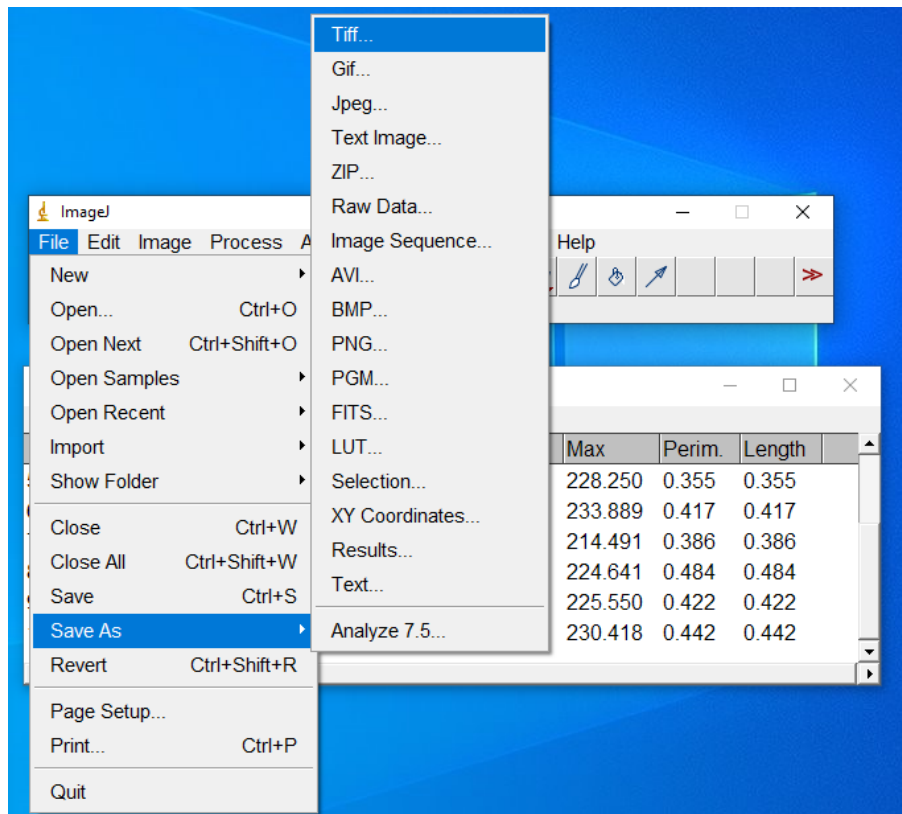
Save the file with under **"Final Measurements"** with the same name as the original picture.
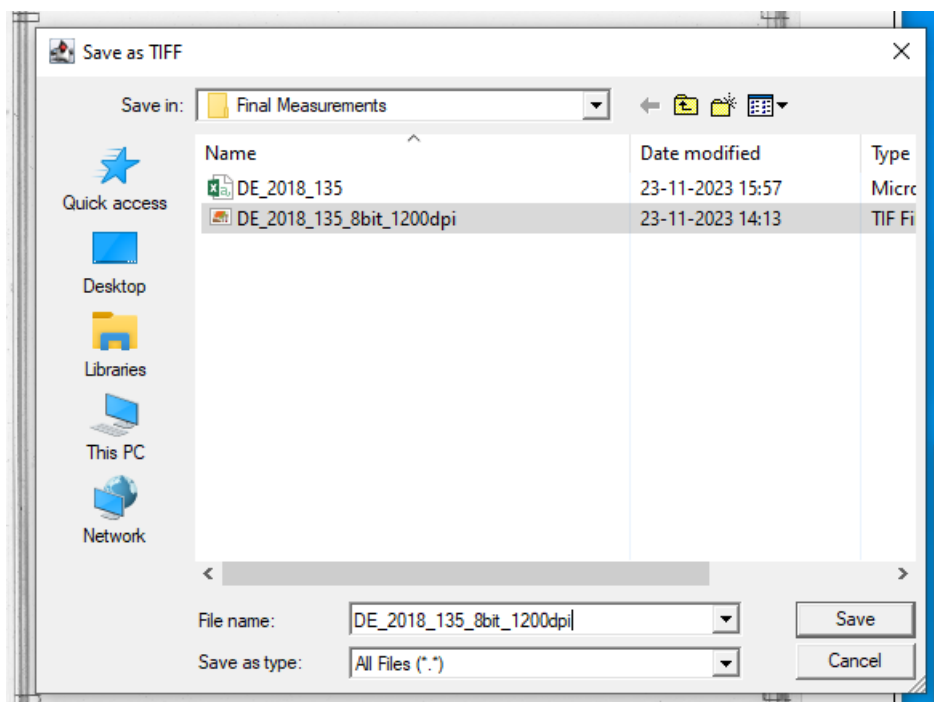
Step 6: Edit the CSV file in Excel (to fit R)
Open the .csv file in Excel by double-clicking the .csv file you saved. You will now be met by an Excel sheet looking like the picture below.
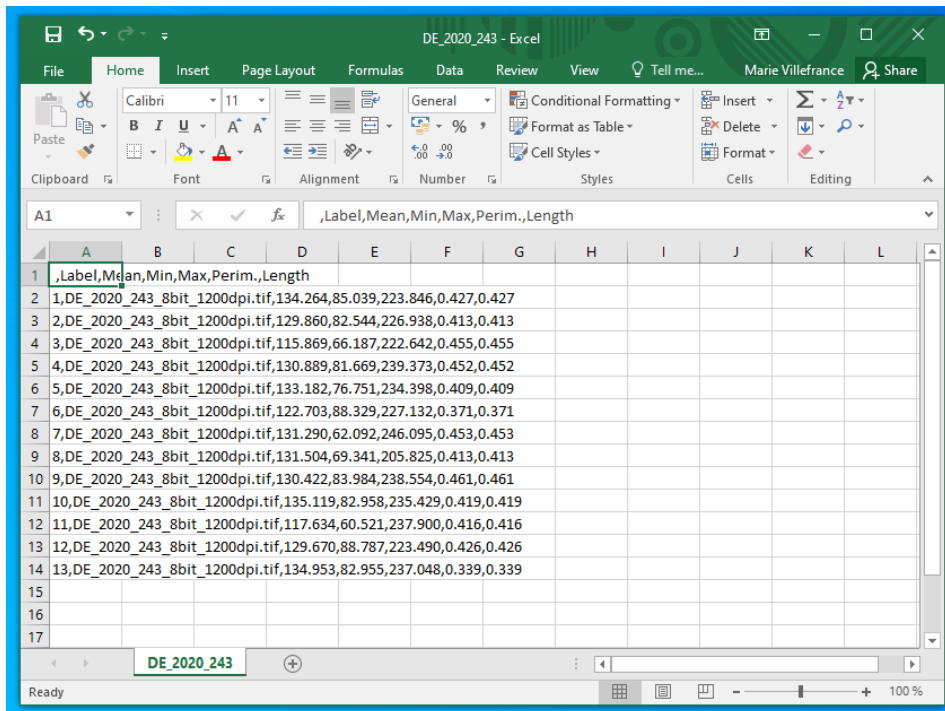
Right click on the first column "**A**". Then press "**Data**" in the top and press "Text to columns".
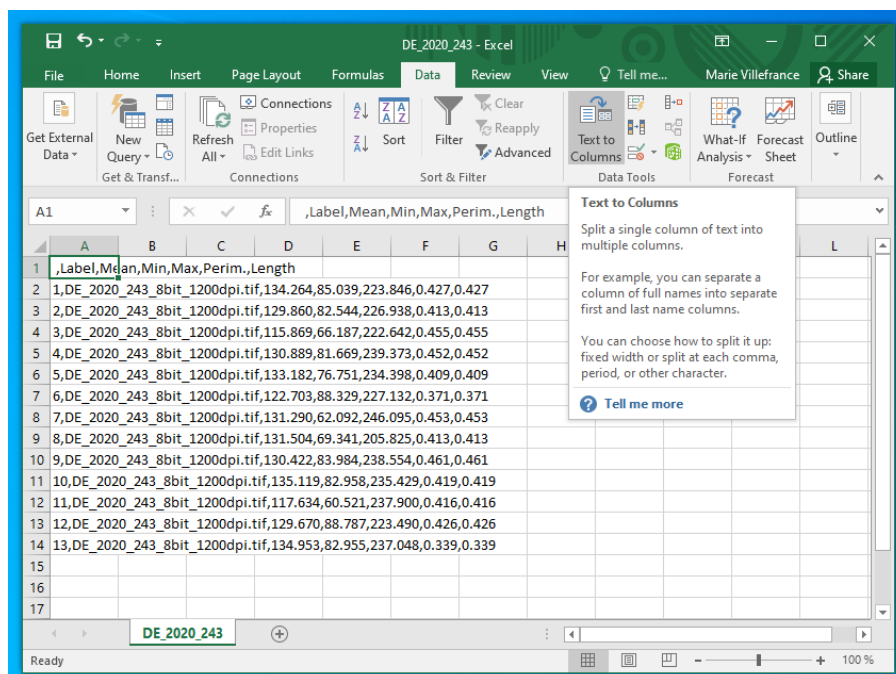
Set the original data type to "**Delimited**" and press "**Next**".
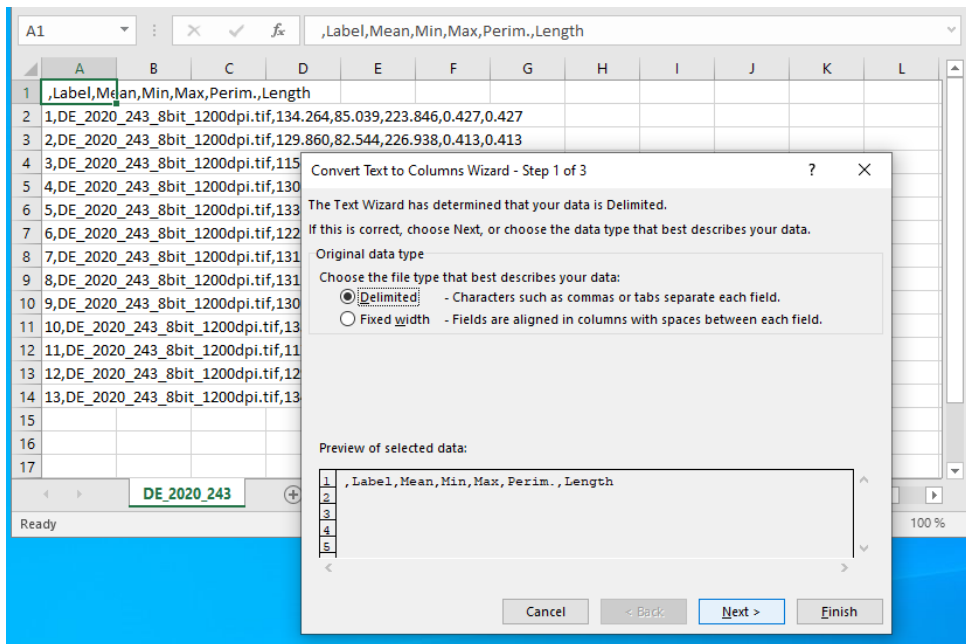
Set the delimiters to "**Comma**" only, and press "**Next**".
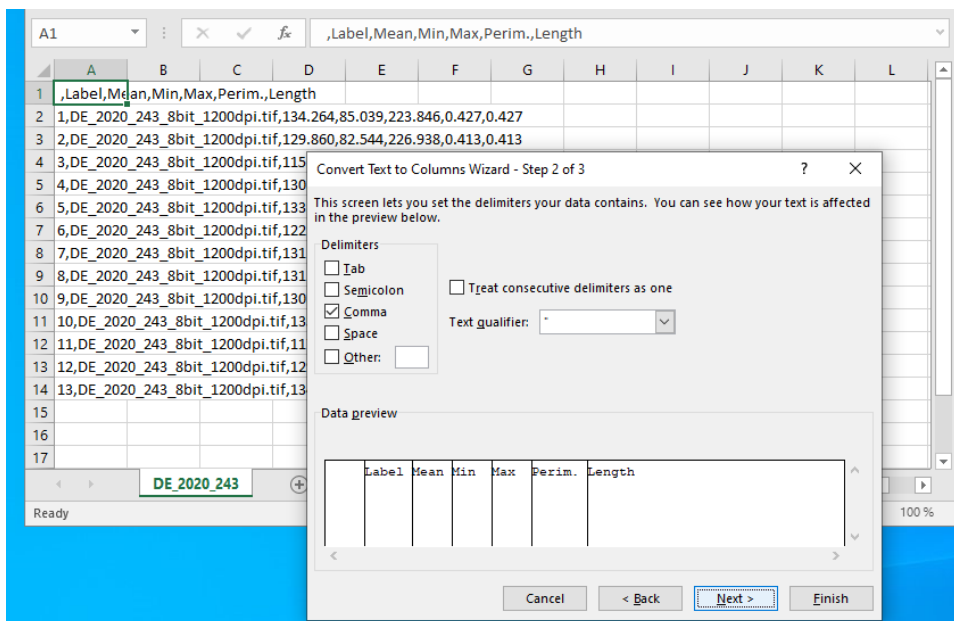
Make sure that "**Column data format**" is set to "**General**" and then press Finish.
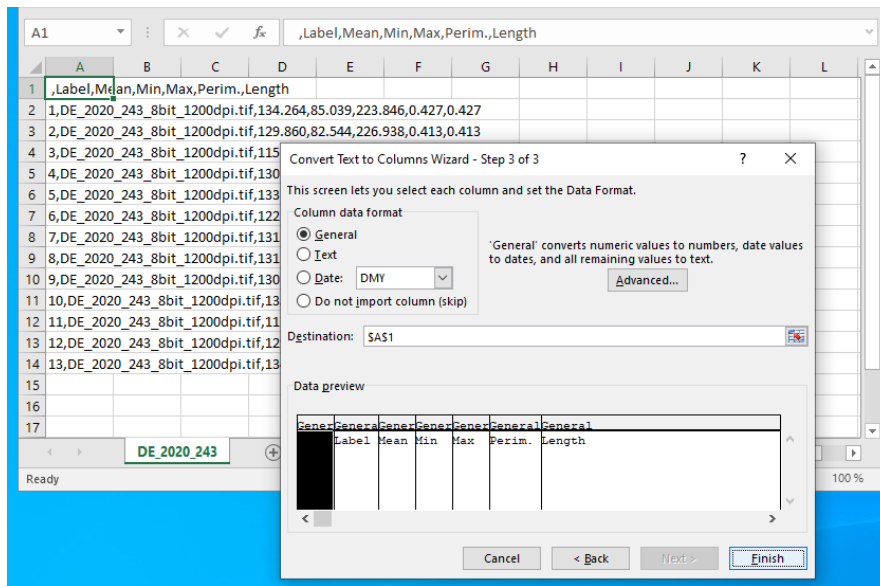
Your Excel ark should now look something like the picture below.
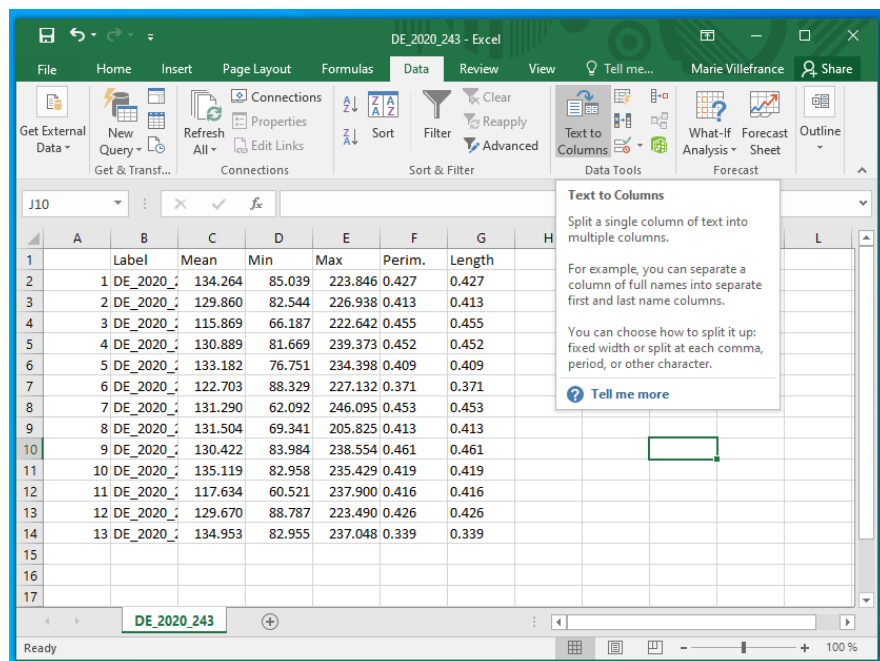
Now enter Country, Year, Station and HaulID in new columns to the right as shown on the picture below.

It is important that the order of which you enter Country, Year, Station and HaulID is the same in every csv file you edit. You can now save and close the csv file. Make sure to keep track of which csv files you have edited and which you have not!

Appendix 5.2: Measurement error and remeasuring larvae

One of the aims of the PELA-project was to map essential spawning and nursery grounds for sandeels in the North Sea. This included measuring sizes of sandeel larvae collected on the IBTS Q1 survey. Although, issues with the measurement of larvae were unfortunately detected, the processing initial of samples is referred to as "MM". The first detection of a potential error in measurements were detected 27-03-2023, where there was detected some odd sizes > 2.5 cm among measured larvae, which did not really fit the expectations of hatch time and month and the assumption that most larvae were newly hatched from spawning grounds. The primary sources of error appear to be related to measurement and conversion errors due to neglect of the established protocol for microscope image acquisition in the lab. The lack of any inclusion of scale in images when measuring larvae, (i.e., method for "setting scale" in *ImageJ*) meant that there was no reference for the size measured, which is essential for accurate measurements. Also, MM measured all larvae in inches and then converted the length measurements into cm, which may course confusion and conversion errors, and possibly have hindered MM in catching any mistakes or doubtful measurements. Unfortunately, the recording of image acquisition and measurement in *ImageJ* was poorly documented.

In scrutinizing erroneous calibration, incorrect image handling or measurement errors, it was found that many images were taken at 1200 DPI (1200 pixels per inch) and that this resolution was employed to determine the size of objects within an image. The standard setting was 1200 DPI, which could indicate that most measurements using images at 1200 DPI may be ok. However, cropping was frequently used before image saving and measuring and documentation of this was lacking, therefore the actual DPI of many images could have been different from the assumed 1200, leading to biased measurements.

To address the problem, a plan was developed to cross-check images with their actual scale and isolate those with a different scale in a folder called "to remeasure", images that have other DPI than 1200. This would help identify images with potential measurement errors due to the incorrect scale assumptions and convert them into accurate measurements.

This action would however only help for images taken with the specified resolution, and not help identify images acquired with a different not declared microscope/camera magnification. Therefore, reanalysis of a number of selected samples was performed.

DPI is a measure of the resolution of an image, representing the number of dots or pixels per inch in a digital image, but can only be used a reference providing measurements in the specified unit of measurement, such as having a scale in the picture. Therefore, it was deemed unlikely that only images having other DPI than 1200 were wrongly measured, but hopefully a correction factor could be obtained to correct other images.

Detection of difference in measurements in subsamples

The first series of measurements conducted by MM was scrutinised for deviations from the standard resolution of 1200 DPI as well containing outliers in individual lengths. Based on such criteria a large number of samples were selected for acquisition of new photos and reanalysis.

The main difference was that new images included a scale in the picture, whereas MM either set the scale without a real scale using "global scale" settings or had a scale in a separate picture. Furthermore, MM measured all pictures in inches, whereas OH measured in cm. MM converted all measurements from inches to cm by a conversion factor (1 inch = 2.54 cm). Below we explore the measurement difference and potential error/bias.

First example (see picture below, Fig. 1) showing a fully documented measurement by Ole Henriksen (OH) in *ImageJ*. The sample is from 2016 with 102 sandeel larvae. MM and OH each measure a subsample of 50 larvae each as a subsample.
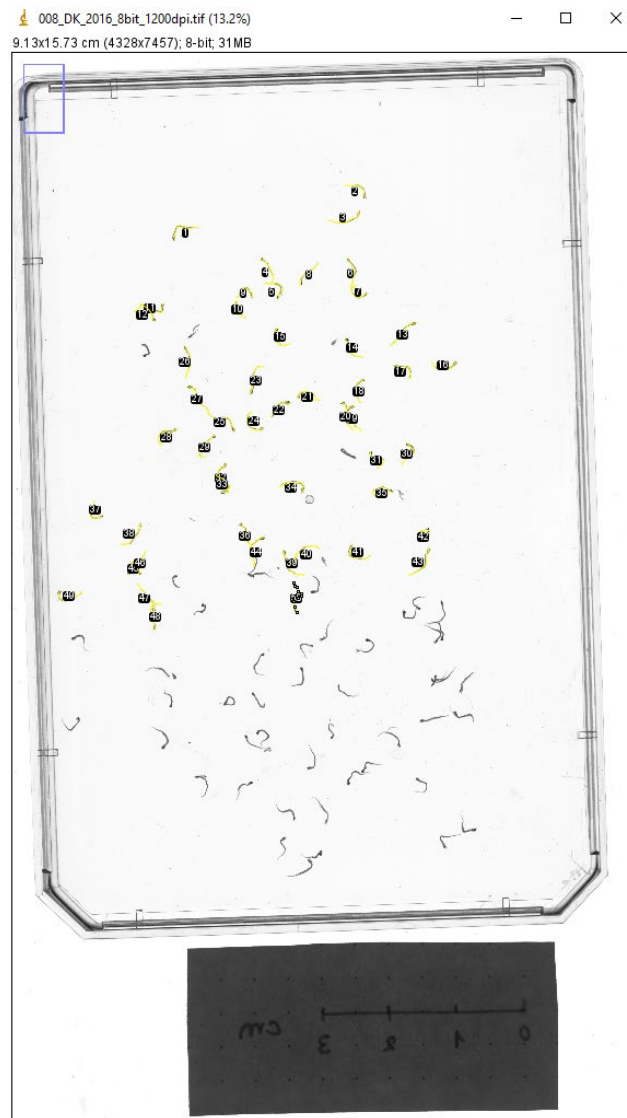
Figure 1. Image showing the full documentation of a sample measurement in *ImageJ*, where a scale, measured lines and larvae labels (1 to 50) are shown.

OH (blue) measured larvae that on average were smaller compared to MM (red), where OH measurements were 12.8% smaller than MM measurements (0.473 mm vs 0.537 mm, Fig. 2). The subsample measurement of 50 larvae makes it uncertain whether the difference in measurements is because of measuring different individuals or an error.
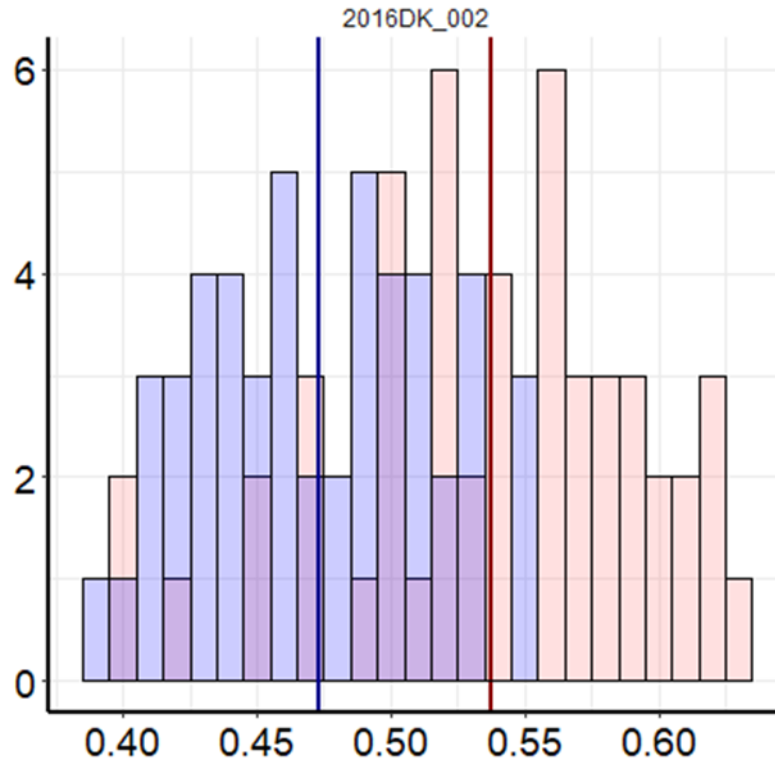
Figure 2. Length distributions of 50 larvae measured by OH (blue) and MM (red) and the average lengths of each distribution (vertical lines). Picture of measured sample by OH shown in Fig.1.

Therefore, we compared five samples having less than 15 larvae per sample, ensuring that they measured the same larvae. These investigations confirmed that OH (blue) measures of larvae on average were 12.5% smaller than MM measures over all five samples (Fig. 3). The specific difference between average measurements for each sample were 10.1%, 10.1%, 6.9%, 18.4% and 8.2%, respectively, were all average measurements by OH were smaller than average measurements by MM.
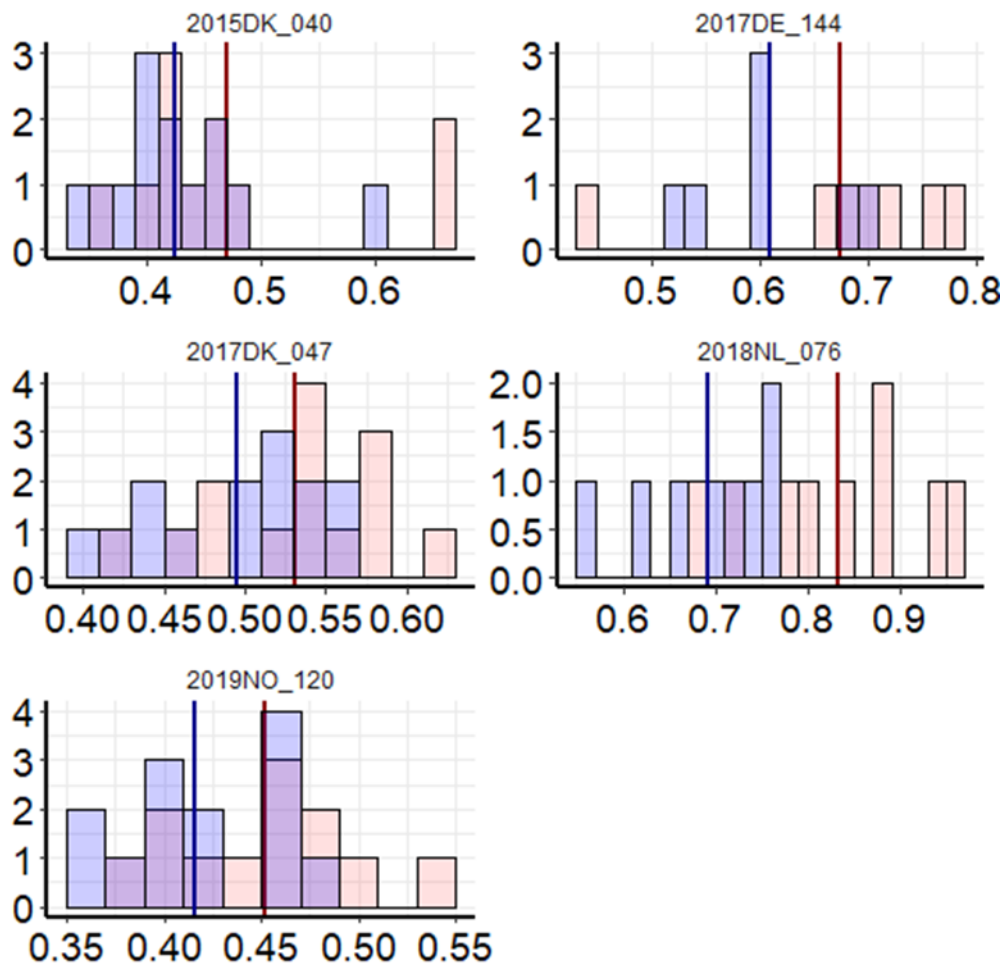
Figure 3. Length distributions of five samples measured by OH (blue) and MM (red) and the average lengths of each distribution (vertical lines).

Measurements of samples that had images ≠ 1200 DPI

Marie Villefrance (MV) was hired as a student assistant to remeasure under the JAMBAY-project. MV measured all images from folder called "to remeasure" that included all images that have other DPI than 1200. She took new pictures with a scale without cropping, saving them as images and then measuring them in ImageJ, providing full documentation for the work (please also see protocol). These investigations confirmed the above tendency of smaller measurements compared to MM. Larvae measured by MV (blue) were on average 34.5% smaller than larvae measured by MM (red) over all 113 samples (Fig. 4). As such, it was concluded that the measurement error was indeed present, possibly from scaling and/or conversion issues. Therefore, the new measurements should be used forward.
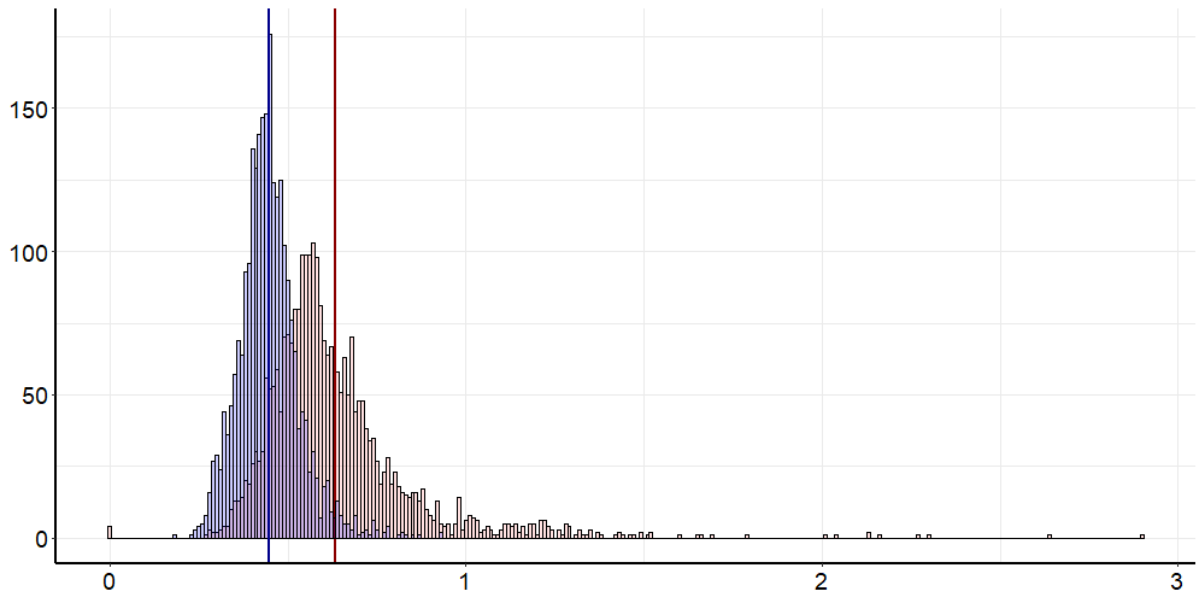
Figure 4. Length distributions of 113 samples measured by MV (blue) and MM (red) and the average lengths of each distribution (vertical lines).

Measurements of samples that had larvae over 0.8 cm (images 1200 DPI)

Although, MV had remeasured all samples from folder "to remeasure" that included all images that had a DPI different from 1200, it was noticed that many samples that have not been measured still had measurements that seemed unrealistically large, > 2cm (Fig. 5).
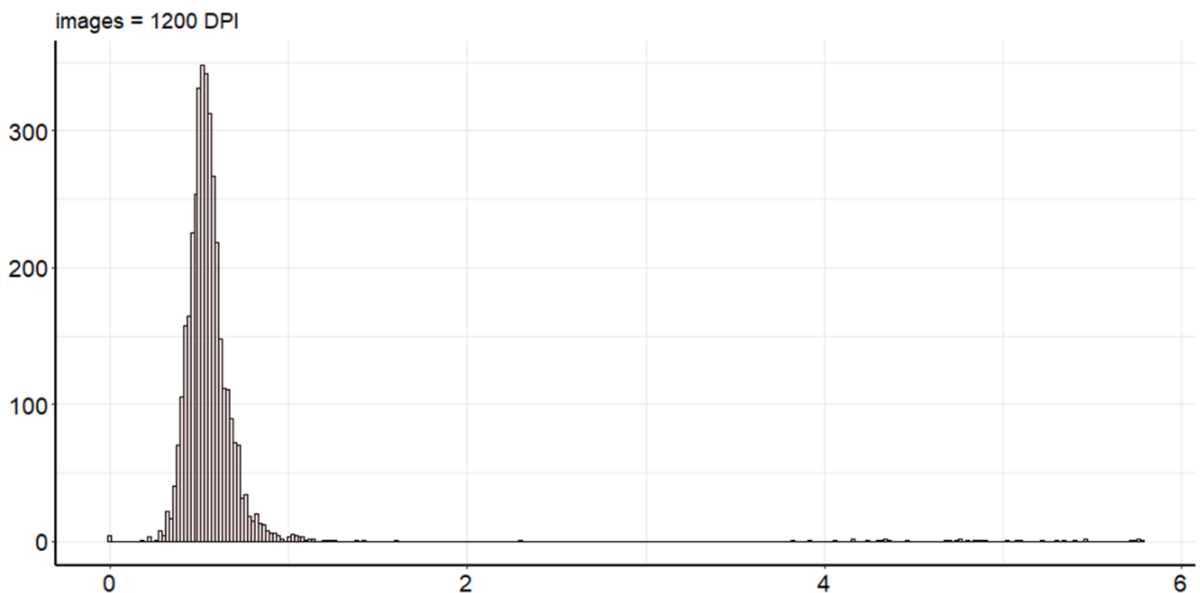
Figure 5. Length distribution of all samples that had pictures with 1200 DPI measured by MM (red). These samples were initially not remeasured by MV.

To check if measurement errors also were associated with samples measured by images with 1200 DPI, one sample was taken out to be remeasured by both OH and MV. Specifically, a

sample from 2016 containing 32 individuals that where over 3.5 cm. The measurements showed that OH (blue) and MV (green) matched closely, whereas MM (red) had measurements that were much larger differing by a factor of 8 or more (Fig. 6). Therefore, it was decided to take new pictures and remeasure with scale all samples that had individuals > 0.8 cm, even though images had 1200 DPI, in order to correct the tail of large individuals in samples.
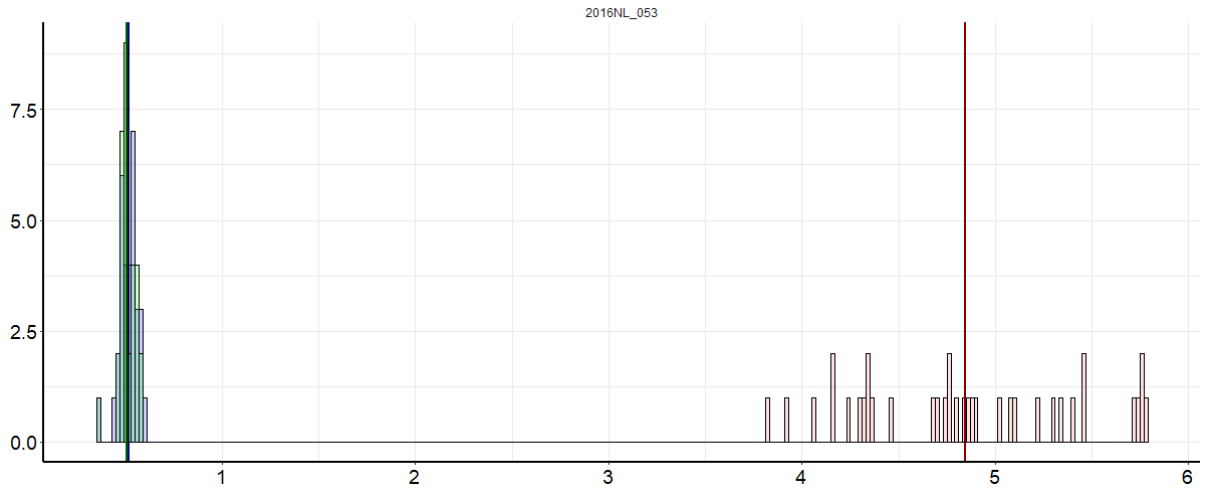
Figure 6. Length distributions of 1 sample remeasured by OH (blue), MV (green) and measured by MM (red) and the average lengths of each distribution (vertical lines).

The remeasurement of samples that had individuals > 0.8 cm (all having 1200 DPI) showed that the average length was 47.1% larger, when measured by MM (red) compared to MV (blue) over all 22 selected samples (Fig. 7). The remeasured larvae were considered corrected with the new measurements.
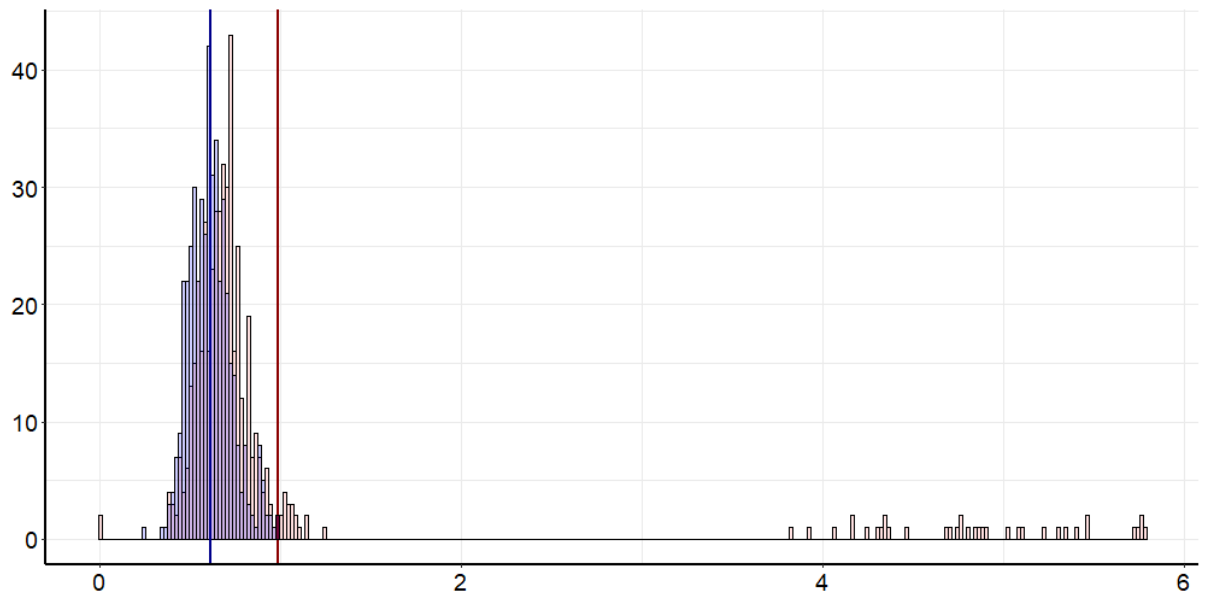
Figure 7. Length distributions of 22 samples measured by MV (blue) and MM (red) and the average lengths of each distribution (vertical lines).

Yet, there were still some measured larvae that seemed uncertain because of large sizes. Therefore, it was decided that all stations where more than 80% of all individuals being over 0.8 cm should be removed. As such, three stations were removed containing 1, 10 and 1 larvae. Furthermore, all individuals that where unrealistically small, e.g., 0 or below minimum size of the remeasured larvae by MV, where removed (2 individuals in total).

Remeasured samples versus remaining samples, and correction factor
Finally, the last question was how the length distributions of the remeasured samples (135 stations) compared with the remaining samples (190 stations) that were not remeasured. The comparison showed that the average difference was 11.3%, where the remeasured samples measured by MV (blue) were smaller than the remaining samples measured by MM (red) (Fig. 8 upper panel).

A correction factor can simply be stated as the ratio between the averages of remeasured samples by MV and the same samples measured by MM, which was 0.8925116. When the correction factor was applied then the distributions were very close. Thus, this was used to correct the remaining 189 stations containing 3045 larvae length measurements (Fig. 8).

Recommendations for microscopic image acquisition and samples
The following examples of risks are listed as information to inform lab personnel about potential error risks, and to improve specific protocol elements, all to heighten the quality of microscopic image acquisition and analysis.

There is a high risk of error if the procedure of microscope image acquisition does not include a calibration reference point for later image-based measurements (see the point "Set Scale" in *ImageJ*). Therefore, it is recommended to use a standard microscope scale for calibration.

For further documentation a picture of the scale photographed in connection with the uninterrupted image series at the same microscope and camera setting and time should be stored for later reference.

To spot erroneous measurements and avoid data confusion only one agreed unit of length for all calibrations should be used in the project.

Uttermost care should be taken if resampling of the image is needed, which artificially would alter the pixel dimensions in a photo editing program, e.g., by cropping where there is a risk that the conversion coefficient of pixels to physical scale may be changed.
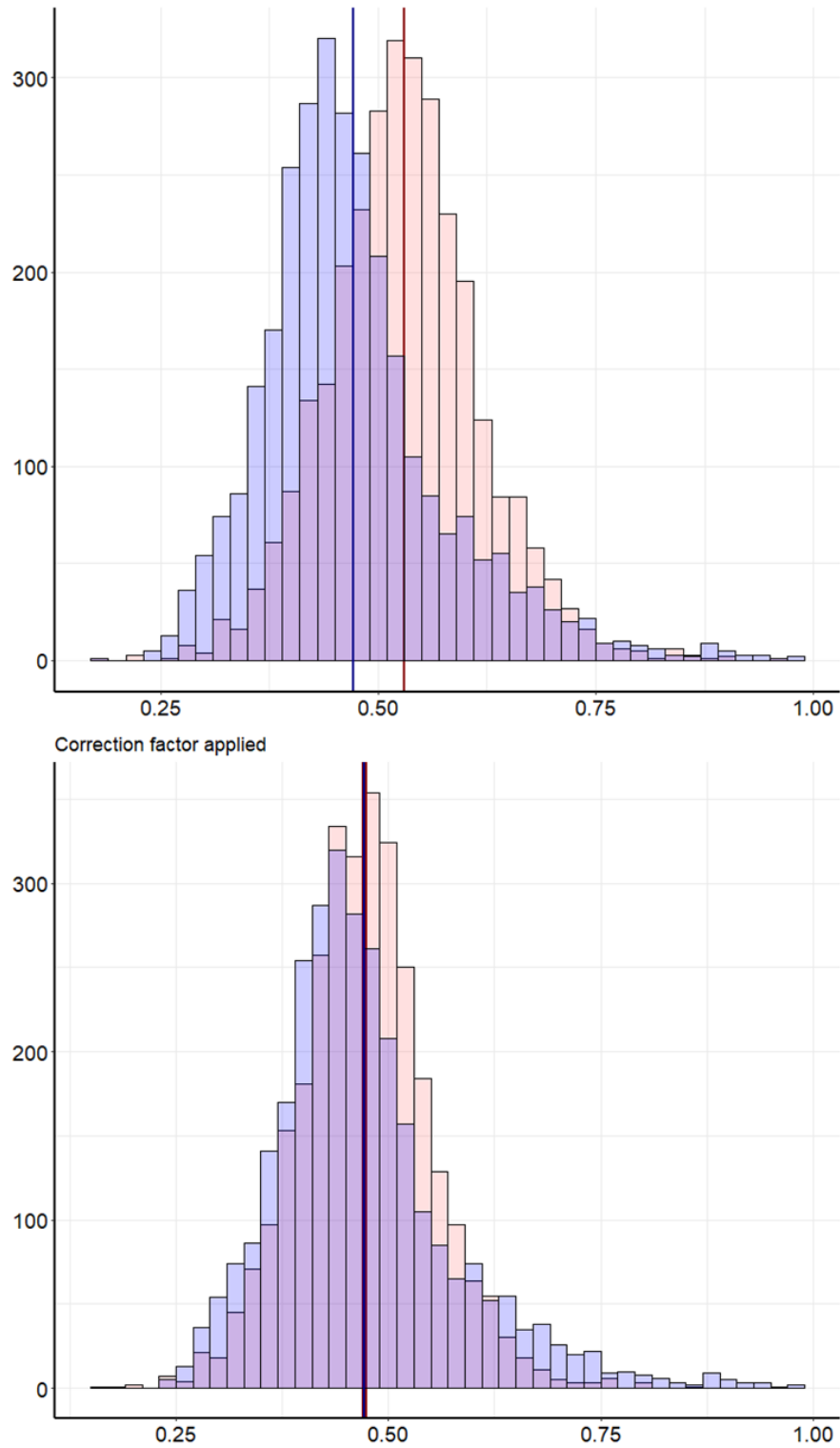
Figure 8. Length distributions of remeasured samples by MV (blue) and measured samples by MM (red) and the average lengths of each distribution (vertical lines). The measured samples by MV are seen without (upper panel) and with (lower panel) a correction factor.

6. Acknowledgements

European Union
European Maritime and Fisheries Fund